

**Omaha Public Power District**  
1623 Harney Omaha, Nebraska 68102-2247  
402/536-4000

August 28, 1986  
TS-FC-86-126P  
LIC-86-421

Mr. Ashok C. Thadani, Project Director  
PWR Project Directorate #8  
Division of PWR Licensing - B  
Office of Nuclear Reactor Regulation  
United States Nuclear Regulatory Commission  
Washington, D. C. 20555

- References:
1. Docket No. 50-285
  2. W. C. Jones to R. A. Clark, OPPD Letter LIC-84-090, April 4 1984.

Dear Mr. Thadani:

**Fort Calhoun Thermal Shield Support System Inspection Deferral**

In 1984, the Omaha Public Power District (OPPD) committed to an inspection of the Fort Calhoun Station reactor vessel thermal shield during the 1987 Outage. (Reference No.2) The purpose of this inspection was to assure that the thermal shield and thermal shield support system were not degrading as observed at other CE plants. Since that time, OPPD has performed a comprehensive research and analysis of the thermal shield degradation phenomena which has resulted in new information and monitoring techniques which were not available in 1984. Based upon the results of this new information, OPPD plans to replace the commitment for a 1987 inspection commitment to conduct an ongoing thermal shield monitoring program capable of detecting precursors to internal degradation. Further, should precursors to degradation be detected, OPPD will conduct an inspection and/or repairs as needed. However, at the latest, an inspection of the reactor internals will be conducted as required for the 10 year In-service Inspection during the Spring 1993 outage. OPPD seeks NRC concurrence with this commitment change.

OPPD's research and analysis of the degradation phenomena has included: 1) Thermal Shield design comparisons with other CE plants exhibiting thermal shield degradation; 2) Evaluation of the dynamic structural characteristics of the Fort Calhoun thermal shield support system; 3) Review and comparison of Fort Calhoun and other CE plants thermal shield operational data, inspections, and experience; and 4) Development of an internal vibration and loose parts monitoring program.

8609020158 860328  
PDR ADCK 05000285  
Q PDR

A047  
/

The failure mechanism at other plants has been analytically modeled, and when combined with analyses of thermal shield differences, indicates Fort Calhoun Station is less susceptible to the failure phenomena. The detailed results of these activities are presented in the attachment to this letter and are summarized as follows:

1. Vibration monitoring data taken through July, 1986 has not indicated any degradation of the thermal shield support system.
2. The visual inspection conducted at the 10 year in service inspection did not disclose any degradation of the thermal shield support system.
3. Monitoring and data evaluation on a planned basis allows for detection of degradation of the thermal shield support system before it becomes significant.
4. The hydraulic loads and the measured response obtained at the pre-critical vibration monitoring program indicate lower values for Fort Calhoun than the comparison plants and therefore, less potential for wear on the thermal shield support system.
5. The threaded locking collar used to secure the Fort Calhoun positioning pins, unlike the locking bar used at the other CE plants, maintains a preload between the positioning pin and the thermal shield threads. The preloaded pin does not wear in the thermal shield threaded holes due to buffeting from flow forces and thus is less susceptible to the deleterious effects of flow induced vibration.
6. The thermal shield support system stability analysis demonstrates Fort Calhoun has a significant stability margin. The stability margin is of the same order of magnitude as the comparison plants. This indicates that thermal shield support system degradation to the point of unstable behavior would be over a similarly long time period, comparable to the other plants.
7. No substantial safety hazard has been identified with a postulated thermal shield support system failure.

Mr. Ashok Thadani  
TS-FC-86-126P  
LIC-86-421  
Page 3

The Omaha Public Power District has thoroughly reviewed the thermal shield degradation phenomena over the last two years. We believe that the new information and results achieved to date, coupled with the continued use of a monitoring program, appropriately justify these changes in our commitment. These will assure OPPD's need to prevent degradation of the Fort Calhoun thermal shield and thermal shield support system. OPPD is prepared to discuss this topic with you at your earliest convenience. If you feel a meeting would be beneficial, please contact us.

Yours very truly,

*R. L. Andrews for*

R. L. Andrews  
Division Manager  
Nuclear Production

RLA/RLJ/TLP/jmo

Attachment

cc: LeBoeuf, Lamb, Leiby & MacRae  
1333 New Hampshire Avenue, N. W.  
Washington, D. C. 20036

Mr. D. E. Sells, Project Manager  
Mr. P. H. Harrell, Resident Inspector

ATTACHMENT

FORT CALHOUN THERMAL SHIELD SUPPORT SYSTEM  
INSPECTION DEFERRAL



## TABLE OF CONTENTS

- 1.0 INTRODUCTION AND HISTORY
- 2.0 SUMMARY OF RESULTS AND CONCLUSIONS
- 3.0 DESCRIPTION OF FORT CALHOUN REACTOR INTERNALS
  - 3.1 REACTOR INTERNALS ASSEMBLY DESCRIPTION
  - 3.2 COMPARISON OF FORT CALHOUN WITH OTHER CE PLANTS
- 4.0 THERMAL SHIELD OPERATING EXPERIENCE
  - 4.1 MAINE YANKEE
  - 4.2 ST. LUCIE UNIT ONE
  - 4.3 MILLSTONE UNIT TWO
  - 4.4 POSTULATED SEQUENCE OF EVENTS LEADING TO DEGRADATION
- 5.0 FORT CALHOUN THERMAL SHIELD SUPPORT SYSTEM STRUCTURAL CHARACTERISTICS
  - 5.1 DYNAMIC CHARACTERISTICS
  - 5.2 CONCLUSIONS
- 6.0 REVIEW OF FORT CALHOUN OPERATIONAL DATA
  - 6.1 PRECRITICAL VIBRATION MONITORING
  - 6.2 THERMAL SHIELD INSPECTIONS (VISUAL)
  - 6.3 INTERNALS VIBRATION MONITORING
- 7.0 SAFETY EVALUATION
  - 7.1 POTENTIAL FAILURE MODES
  - 7.2 CONSEQUENCES OF FAILURE
- 8.0 FORT CALHOUN THERMAL SHIELD STABILITY ANALYSIS

## 1.0 INTRODUCTION AND HISTORY

### 1.1 Introduction

Omaha Public Power District (OPPD) committed in Reference 1.1 to perform an inspection to determine the condition of Fort Calhoun's thermal shield support system no later than 1987. The inspection was to have been similar to that performed at Maine Yankee in that the preload in the positioning pins was to have been measured. Through continued participation in the investigation and analysis of the phenomena, OPPD believes that the additional information obtained since the date of our commitment justifies the conclusion that this inspection is not warranted at this time. Technical justification, contained herein strongly supports this conclusion. OPPD, therefore, has reached a decision not to perform the thermal shield inspection during the 1987 refueling outage at the Fort Calhoun Station.

### 1.2 History of the Thermal Shield Issue at Fort Calhoun

OPPD first became aware of the problems associated with the thermal shield support system as a result of the experiences of the other Combustion Engineering plants with installed thermal shields (see Section 4.0 for further discussion). Upon receipt of notification (CE ADP Infobulletin 82-12) from Combustion Engineering that a potential problem existed with the thermal shield support system, OPPD expanded its Ten Year Inservice Inspection (ISI) program, performed in January 1983, to include a thorough visual inspection of all accessible portions of the thermal shield positioning pins. Fort Calhoun's thermal shield was found to be in excellent condition. The ISI results supported our justification for continued operation (Reference 1.2), which was submitted to the Commission on April 26, 1983.

OPPD pursued the thermal shield issue by contracting with CE to perform an additional safety analysis to evaluate the impact of a postulated thermal shield failure at the Fort Calhoun Station. The results, transmitted to the Commission on August 2, 1983 (Reference 1.3), concluded that failure of the thermal shield support system was not a safety concern.

In a telephone conversation on February 14, 1984, the Commission concurred with OPPD that a dropped thermal shield was not a safety concern. However, the Commission recommended to OPPD that an appropriate time for the next thermal shield inspection would be in 1987. This recommendation was based on the limitation that the Loose Parts Monitoring System would not provide information that would identify a thermal shield problem prior to a failure and the Commission's concern about the future operation and performance of the thermal shield. OPPD, on April 4, 1984, committed in Reference 1.1 to inspect the thermal shield during the 1987 refueling outage.

The final report for St. Lucie 1 Thermal Shield Failure was received by OPPD in April, 1984. This report identified the initiating event leading to deterioration of the thermal shield support system as being the loss of preload in the positioning pins. Subsequent to receipt of this report and through additional evaluations by CE, it was learned that the Internal Vibrations Monitoring (IVM) System could be used to detect a loss of effectiveness of the positioning pins prior to any significant damage occurring. The use of our monitoring systems is discussed in more detail in Section 2 and 6 of this report.

REFERENCES

- 1.1 Letter (LIC-84-090) to R. A. Clark from W. C. Jones dated April 4, 1984.
- 1.2 Letter (LIC-83-103) to R. A. Clark from W. C. Jones dated April 26, 1983.
- 1.3 Letter (LIC-83-189) to R. A. Clark from W. C. Jones dated August 2, 1983.

## 2.0 SUMMARY OF RESULTS AND CONCLUSIONS

### 2.1 Discussion of Failure Mechanism

The failure of the thermal shield support systems at other Combustion Engineering NSSS facilities has been analyzed extensively. As mentioned above, the initiating event was the loss of preload in the positioning pins. Several factors have been identified as potential mechanisms for reducing the preload in the positioning pins, but the exact cause has not been ascertained. Regardless of the cause for loss of preload, it has been established that degradation to the thermal shield support system is a slow process that has the gradual loss of the positioning pins' effectiveness as its precursor.

The process begins with a gradual loss of preload in the positioning pins. Some of the factors identified as potential contributors to the loss of preload are radiation induced stress relaxation, fluctuating hydraulic loads, deformation of the core support barrel during assembly as the weight of the thermal shield is transferred to the support lugs, and possible installation errors. A combination of these factors seems to be the best explanation available. Plastic deformation of the positioning pins has also been postulated as a possible contributor to the problem, but this seems unlikely, since such deformation would be expected to take place early in the operating life of the station. The fact that our thermal shield is still intact and properly supported refutes this mechanism as a possibility at the Fort Calhoun Station.

The plants that have experienced failures have locking bars installed to keep the pins in place; once contact was lost between the pin and the CSB, movement between the pin and thermal shield was possible. This movement resulted in wear between the threads of the pin and the thermal shield, thereby further reducing the effectiveness of the pins and allowing the amplitude of relative

motion to increase. This motion, induced by fluctuating hydraulic loads as discussed in Section 5.0, also causes wear to initiate in the thermal shield support lug region. These support lugs provide the primary component of the stiffness coefficient in the upper region of the thermal shield ( $k-1$  in figures 8-1, 8-2, and 8-3. Once the thermal shield support lugs begin to wear, the value of  $k-1$  declines and the support system begins to approach an unstable condition. Once the support system becomes unstable, severe damage can occur.

Initially, loss of preload will only cause wear to occur at low power (near zero) conditions when thermal loading of the pins is lowest. Operation at low power conditions will then continue the degradation process through wear. If not corrected, the positioning pins will eventually lose their effectiveness at full power conditions as well. The reason for this is that at full power conditions the differential expansion of the core support barrel relative to the thermal shield (the CSB being at a higher temperature) increases the loading in positioning pins, thus providing effective support to a thermal shield that could have lost some of its initial preload. At low power the thermal shield is near isothermal conditions and the additional loads are absent. Thus, a loss of preload should be detectable at low power long before it will be seen at full power conditions.

## 2.2 Detection of Thermal Shield Support Degradation

As part of their analysis of the St. Lucie 1 thermal shield failure, Combustion Engineering has determined that the Internals Vibration Monitoring System (IVM) is an effective indicator of the adequacy of the support of the thermal shield. The IVM system is used to monitor the core support barrel (CSB) vibration frequency which will remain the same value as long as the thermal shield is adequately supported. A shift in certain well defined frequencies of CSB vibration is indicative of a change in the relative motion of the thermal shield to the core support barrel.

Since the loss of effectiveness of the positioning pins will first be detectable during isothermal conditions, analysis of the IVM data taken at low power will give the first indication of this effect taking place. This analysis will provide a sufficiently early indication of the problem to enable OPPD to schedule examination and/or corrective action during a normally planned refueling outage.

As shown in Figure 4-1 the loss of effectiveness of the positioning pins at the St. Lucie 1 Station was first indicated (by IVM analysis subsequent to failure) near the beginning of operating Cycle 4. The continuing reduction in the IVM CSB frequency leading up to the onset of unstable motion 28 months later shows that this is a gradual process. It is important to note that the IVM data used in the St. Lucie analysis was all taken at full power and, as such, would not identify the loss of effectiveness of the positioning pins until significant degradation had already taken place. Still, the thermal shield did not exhibit unstable motion, leading to eventual failure, until some 28 months after the first full power IVM data identified the precursor. Had low power data been taken, it would have shown a loss of effectiveness of the positioning pins even earlier than the beginning of Cycle 4.

On July 3, 1986, OPPD recorded IVM data at low power, near isothermal conditions. This data was analyzed and showed no indication of loss of positioning pin effectiveness. It is concluded that the thermal shield is adequately supported.

### 2.3 Monitoring Program

There are three separate elements of the Fort Calhoun Loose Parts Monitoring Program that are currently in place. The first element consists of recording the eight accelerometer channels onto magnetic tape on a monthly basis. This data is kept for historical reference purposes. Audio monitoring by the Shift Technical



Advisors (STAs) is the second element of the program. The STAs listen to each channel once per eight hour shift for any impacting sounds occurring in the primary system.

The third and new element of the program will be to perform a modified amplitude probability distribution (MAPD) function on the eight recorded accelerometer channels. The MAPD is the Amplitude Probability Density function with the probability density plotted on a semi log scale versus the amplitude of the signal. The MAPD is used to quantify changes in the Loose Parts Monitoring signals.

The plots can be used to give an indication of the RMS "g" value of the impacts as well as the rate of impact. The magnetic taping of the accelerometers will continue on a monthly interval with the MAPD plots being generated on a quarterly basis. The STA monitoring will continue on a once per shift cycle.

The Internals Vibration Monitoring Program at Fort Calhoun utilizes the excore detectors located around the reactor vessel. Presently, a magnetic tape recording is made of the excore detectors' signals on a monthly basis. At the same time that the tape recording is made, a power spectral density plot is made of the excore detectors. On a "need for analysis" basis, over the last few years, a complete evaluation of the signals have been performed by plotting power spectral densities, cross power spectral densities, coherence, phase and phase separated cross power spectral densities for the four excore channels. An explanation of these signal processing techniques and how they are used is given in Reference 2.1. A low power data collection, reduction, and evaluation will be performed once per fuel cycle to determine any change in the isothermal condition of the reactor internals.

The Omaha Public Power District will evaluate the excore signals on a quarterly basis to monitor for early signs of any reactor internals degradation. The monthly taping and power spectral densities



will continue at the same rate along with collecting, reducing, and evaluating low power data at least once per fuel cycle.

#### 2.4 Design Differences at Fort Calhoun

A description of the Fort Calhoun reactor internals and a comparison with other Combustion Engineering plants is presented in Section 3.0. As stated in the above reference, the most significant design differences are (1) the location of the lower positioning pins relative to the active core region, (2) the use of a locking collar to secure the positioning pin instead of a locking bar.

The lower positioning pins are located at an elevation below the active core region, lower than at the other CE plants. This location makes the pins less susceptible to the effects of radiation induced stress relaxation, which is one of the factors identified as contributing to a loss of preload.

With the locking bar mechanism, once contact is lost between the pin and the CSB, movement between the pin and thermal shield is possible. The use of a locking collar instead of a locking bar adds significantly to the integrity of the support system. At Fort Calhoun the locking collars were threaded onto the pins after the preload was established, torqued to 50 ft-lbs, and then welded around their entire 360 degree circumference both to the pins and the thermal shield. This procedure thoroughly secures the pin to the thermal shield and ensures that there can be no relative motion between their threads. Hence, no wear can take place even if the initial preload is lost, as long as the welds remain intact. The results of the 10 year ISI have shown that these welds have remained intact. The net effect is to maintain the structural integrity of the pins within the thermal shield, thereby not allowing the amplitude of the relative motion between the thermal shield and core support barrel to increase beyond that allowed by the unloaded

pins. This in turn helps limit the rate of wear in the support lug region and provides additional time to allow for planning and executing a timely program of inspection and/or corrective action.

## 2.5 Safety Analysis

An analysis was performed by Combustion Engineering to determine the impact of a failed thermal shield support system upon the safety parameters of reactor operation. The method used involved determining the possible failure modes of the thermal shield, and evaluating their effect upon the parameters important to safety. The mechanisms that could result in core damage were evaluated for each failure mode. These mechanisms include increased core bypass flow, creation of debris, reduction in core flow rate due to tilting of the thermal shield, and core shroud jetting. The effect of these mechanisms on coolant activity levels and reduced DNB over-power margin were analyzed and the results documented in Section 7.0. The results demonstrate that the potential failure of the thermal shield is not a safety concern. OPPD considers this issue to be a commercial concern only.

## 2.6 Conclusion

In support of OPPD's position, the following facts are reiterated.

- 1) OPPD strongly feels that the failure mechanism is now sufficiently understood.
- 2) The failure mechanism is a slow process with a gradual loss of preload in the positioning pins as its precursor.
- 3) The IVM system, in conjunction with the loose part monitoring system, is capable, through analysis of its signals, of detecting initial loss of effectiveness of support system in

sufficient time to allow for a planned inspection and repair program to be implemented before significant damage is incurred, thus precluding any commercial concern for this eventuality.

- 4) Design differences of the Fort Calhoun thermal shield support system, primarily the locking collar design and lower hydraulic loads, make it less susceptible to the identified failure mechanism.
- 5) Failure of the thermal shield is not a safety concern.
- 6) Recent IVM data analyses, from both full power and at near zero power, have indicated no degradation of the thermal shield support system. This information verifies that the thermal shield is currently not in a degraded condition.

OPPD will continue monitoring the condition of the thermal shield on a monthly basis and evaluating the data at least on a quarterly basis. Low power IVM data will continue to be taken and evaluated once per fuel cycle. If it is determined that the thermal shield support system has initiated the slow degradation process, OPPD will develop and implement a timely program of inspection and/or corrective action prior to incurring any significant damage.

REFERENCES

- 2.1 ANSI/ASME Standard OM-5-1981.

### 3.0 DESCRIPTION OF FT. CALHOUN REACTOR INTERNALS

#### 3.1 Reactor Internals Assembly Description

The major support member of the reactor internals is the core support barrel (CSB) assembly (Figure 3-1). This structure consists of the core support barrel, the core support plate and support columns, the core shroud, the thermal shield and the core support barrel to pressure vessel snubbers. The major material of construction for the assembly is Type 304 stainless steel.

##### 3.1.1 Core Support Barrel

The core support barrel (CSB) (Figure 3-1) is a right circular cylinder with a nominal inside diameter of 120 5/8 inches. The CSB is supported by a 4-inch thick ring flange from a ledge on the reactor pressure vessel. The core support barrel in turn supports the core support plate upon which the fuel assemblies rest. The core support plate transmits the weight of the core to the core support barrel by means of vertical columns and a beam structure. Four alignment pins, located 90 degrees apart, are press fitted into the flange of the core support barrel (Figure 3-1). The reactor vessel, closure head and upper guide structure assembly flanges are slotted in locations corresponding to the alignment pin locations to provide proper alignment between these components in the vessel flange region.

An internal boss is located around each of the two 32-inch reactor vessel coolant outlet nozzles on the inside diameter of the reactor pressure vessel wall. The internal boss provides a mating surface for the core support barrel 32-inch outlet nozzles. The reactor vessel nozzle boss and core support barrel nozzles are closely machined to a common contour separated by a small gap. The gap permits

differential axial and radial expansion of the core support barrel and reactor vessel shell while minimizing bypass leakage.

Since the core support barrel is 26 feet long and is supported only at its upper end, snubbers (Figure 3-2) are installed near the bottom outside surface of the core support barrel to prevent large amplitude motion. The snubbers consist of six equally spaced lugs around the circumference and are the grooves of the "tongue-and-groove" assembly; the reactor vessel lugs are the tongues. Minimizing the clearance between the two mating pieces limits the amplitude of any vibration. During assembly as the CSB is lowered the reactor vessel tongues engage the core support barrel groves. Radial and axial expansions of the core support barrel are accommodated, but lateral movement is restricted. The reactor vessel tongues have bolted and lock welded Inconel X shims and the core support barrel grooves are hardfaced with Stellite to minimize wear.

### 3.1.2 Core Support Plate and Support Columns

The core support plate is a 120-inch diameter, 2-inch thick, Type 304 stainless steel plate into which the necessary flow distributor holes for the fuel assemblies have been machined. Fuel assembly locating holes are also machined into this plate. Columns and support beams are placed between this plate and the bottom of the core support barrel in order to provide stiffness to this plate and transmit the core load to the bottom of the core support barrel.

### 3.1.3 Core Shroud Assembly

The core shroud assembly (Figure 3-1) consists of rectangular plates 5/8-inch thick, 142-3/8 inches long and of varying widths. The bottom edges of these plates are fastened to the core support plate by use of anchor blocks.

The core shroud provides an envelope for the perimeter of the core and limits the amount of coolant bypass flow. The gap between the outside of the peripheral fuel assemblies and the vertical shroud plates is maintained by eight tiers of horizontal centering plates attached to the vertical shroud plates and core support barrel. The plates are positioned to establish the core envelope during shop assembly by adjusting bushings located in the core support barrel. The vertical shroud plate edges are butted together minimizing the vertical joint gap. The overall core shroud assembly, including the vertical shroud plates, the centering plates, and the anchor blocks, is a bolted and lock welded assembly. All bolts and pins are lock welded. In addition, all bolts (bodies and heads) are designed to be captured in the event of fracture; the bolt heads are trapped by lock bars or lock welds, and the bodies are trapped by the use of incomplete tapping of through holes. Holes are provided in the core support plate to allow coolant to flow upward between the core shroud and the core support barrel, thereby minimizing thermal stresses in the shroud plates and eliminating stagnant pockets.

### 3.1.4 Thermal Shield and Thermal Shield Support System

The thermal shield is a 3-inch thick, 304 stainless steel cylindrical structure with an inside diameter of 127 inches and a height of 154 inches (see Figure 3-1). The thermal shield is supported at the top by eight equally spaced support lugs welded to the outer periphery of the core support barrel.

Thermal shield support pins are fitted during assembly to position the thermal shield on the support lugs. This is shown in Figure 3-3. The support pins are welded to the thermal shield. There is a .001 to .002 inch clearance on the sides between the support pins and the support lug to permit relative thermal expansion between the core support barrel and the thermal shield. The thermal shield is positioned radially by a total of twenty-four positioning pins. Eight of the pins are located approximately 23.5 inches below the top of the support lugs and the remaining sixteen positioning pins are located approximately 10 inches from the bottom of the thermal shield. The positioning pins thread into the thermal shield and are preloaded against the core support barrel.

A locking collar is threaded on the positioning pin and torqued to the outside diameter of the thermal shield thereby preloading the locking collar and positioning pin to the thermal shield (see Figure 3-3). The locking collar is lockwelded to the positioning pin and the thermal shield to prevent rotation and provide a means of capture.

### 3.1.5 Upper Guide Structure Assembly

The upper guide structure assembly (UGS) (Figure 3-4) consists of an instrument support plate, 41 control element assembly shrouds, a fuel assembly alignment plate and a holddown ring. The upper end of the assembly is a flanged grid structure consisting of an array of 24-inch deep beams. The grid is encircled by a 24-inch deep cylinder with a 3-inch thick plate welded to the cylinder. The periphery of the plate contains four accurately machined and located alignment keyways, spaced at 90-degree intervals, which engage the core barrel alignment keys. This system of keys and slots provides an accurate means of aligning the core support barrel with the UGS.



The control element assembly shrouds extend from the fuel alignment plate to an elevation about 8 inches above the support plate. There are 29 single-type shrouds. These consist of centrifugally cast cylindrical upper sections welded to cast bottom sections, which are shaped to provide flow passages for the coolant passing through the alignment plate while shrouding the CEA's from crossflow. There are also 12 dual-type shrouds which consist of two single-type shrouds connected by a rectangular section shaped to accommodate the dual control element assemblies. The shrouds are bolted to the fuel assembly alignment plate. At the upper guide structure support plate, the single shrouds are connected to the plate by the spanner nuts. The spanner nuts are torqued in place and lockwelded. The dual shrouds are attached to the UGS support plate by welding.

The upper guide structure assembly also supports the in-core instrument guide tubes. The tubes are conduits which protect the in-core detectors and guide them during insertion and removal operations.

#### 3.1.6 Holddown Ring

A holddown ring is set between the reactor vessel head flange and the upper guide structure to resist upward movement of the core support assembly. This arrangement permits differential axial thermal expansion of the reactor vessel flange and the core support barrel and UGS flanges while providing a net downward force.

#### 3.1.7 Flow Skirt

The flow skirt (see Figure 3-1) is a right circular perforated cylinder that is attached to the reactor vessel by welding. The flow skirt material is Inconel.

### 3.1.8 Core Stops

Nine equally spaced core stop lugs are welded to the reactor vessel and are located at the periphery, but below the core support barrel lower flange. The core stops limit the vertical drop of the core support barrel assembly to approximately one inch in the event of a postulated failure.

## 3.2 Comparison of Ft. Calhoun With Other C-E Plants

### 3.2.1 Thermal and Hydraulic Design Data Comparison

Table 3-1 provides a comparison of thermal hydraulic characteristics for the thermal shield for Ft. Calhoun, Maine Yankee, St. Lucie Unit 1 and Millstone Unit 2. The table shows that the average coolant velocity in the Ft. Calhoun downcomer is approximately 8% lower than for the three other plants. The hydraulic loads per unit area on the thermal shield are, therefore, smaller for Ft. Calhoun. This conclusion is supported by the values in the table for the radial pressure differential across the thermal shield wall. Hydraulically induced pressure differentials across the core support barrel at the elevations of the thermal shield support pins are also smaller for Ft. Calhoun. All of these factors indicate that the radial hydraulic loadings on the thermal shield and core support barrel walls are lower, and more favorable, for Ft. Calhoun relative to the other plants.

Radial temperature differences between the CSB and thermal shield have been estimated for Ft. Calhoun by extrapolating from Maine Yankee values. It is expected that the temperature difference across the upper thermal shield support pins is comparable to the other three plants. The temperature difference across the lower pins, because of their axial position relative to the active core, will be approximately equal to or less than the Maine Yankee value and will definitely be smaller than for St. Lucie Unit 1 and Millstone Unit 2.

### 3.2.2

#### MECHANICAL DESIGN COMPARISON OF THE THERMAL SHIELD SUPPORT SYSTEM

The thermal shield support system design for Fort Calhoun is similar to the design employed on other CE plants. The physical description of the Fort Calhoun thermal shield support system is given in section 3.1.4. Table 3-2 provides a comparison of the physical details of the CE plants that had a thermal shield as part of the reactor internals assembly original design.

The Core Support Barrel (CSB) for Fort Calhoun supports 133 fuel assemblies whereas the other CE plants with a thermal shield design have 217 fuel assemblies, therefore, the CSB for Fort Calhoun is smaller in diameter.

The thermal shield for Fort Calhoun is designed to be compatible in diameter with the smaller core support barrel while maintaining the same 3 inch thickness. The number of supports (see Figure 3-3) on Fort Calhoun is less (eight vs. nine) than on other CE plants, however, due to the variation in weight of the thermal shields, the load per support lug is comparable for all four plants. In addition, the azimuthal distance between each of the supports and each of the top and bottom positioning pins is slightly closer than on the other plants. These differences indicate no major departure from the thermal shield support system design from other CE plants. The more significant differences, as it relates to maintaining a thermal shield support system that is less susceptible to wear of the positioning pins, is the location of the lower positioning pins relative to the active core and the incorporation of a locking collar instead of locking bars. The locking collar maintains a positioning pin preload relative to the thermal shield independent of the preload developed by the contact of the positioning pin with the core

support barrel. The location of the lower positioning pins being in excess of 11 inches from the active core, in comparison to Maine Yankee which is approximately 6 inches and St. Lucie Unit 1 and Millstone Unit that were within the active core, makes Fort Calhoun less susceptible to the effects of irradiation and thermal gradients. The combination of these features, i.e., pin location and locking collar, has a net positive effect.

The differential thermal effects at the lower elevation, being small, provides less additional loading to the installation preload mitigating stress relaxation. The locking collar prevents wear of the positioning pin threads from flow induced vibration of the pins if one postulates that under isothermal conditions, the lower pins have lost their effectiveness. In summary, although Fort Calhoun thermal shield support system design is not a major departure from designs employed on other CE plants, it does incorporate features that make loss of positioning pin effectiveness less likely and, therefore, less susceptible to eventual thermal shield support system degradation.

TABLE 3-1

Comparison of Thermal-Hydraulic  
Characteristics for Thermal  
Shield Region for C-E Plants

<u>Parameter</u>	<u>Plant Value</u>			
	<u>Ft. Calhoun</u>	<u>Maine Yankee</u>	<u>St. Lucie 1</u>	<u>Millstone 2</u>
Design Flow Rate, $Q_D$ -GPM	190,000	324,000	324,800	324,800
B.E. Flow Rate-% of $Q_D$	110.4	120.4	122.8	121.3
Average Velocity in Downcomer, FPS	27.5	30.1	30.3	29.9
Average Velocity in Inner Annulus, FPS	22.7	24.6	25.2	24.9
Average Velocity in Outer Annulus, FPS	29.4	32.3	32.5	32.1
Average Radial $\Delta P$ Across Thermal Shield, PSI	1.8	2.2	2.1	2.0
Average Radial $\Delta P$ Across Core Barrel at Elevation of Top Pins, PSI	17.1	23.9	19.6	19.1
Average Radial $\Delta P$ Across Core Barrel at Elevation of Bottom Pins, PSI	13.7	19.1	18.5	18.1
Average Metal $\Delta T$ Between T/S and CSB at Elevation of Top Pins, °F	39°F*	39°F	40°F	40°F
Average Metal $\Delta T$ Between T/S and CSB at Elevation of Bottom Pins, °F	5°F*	5°F	25°F	25°F

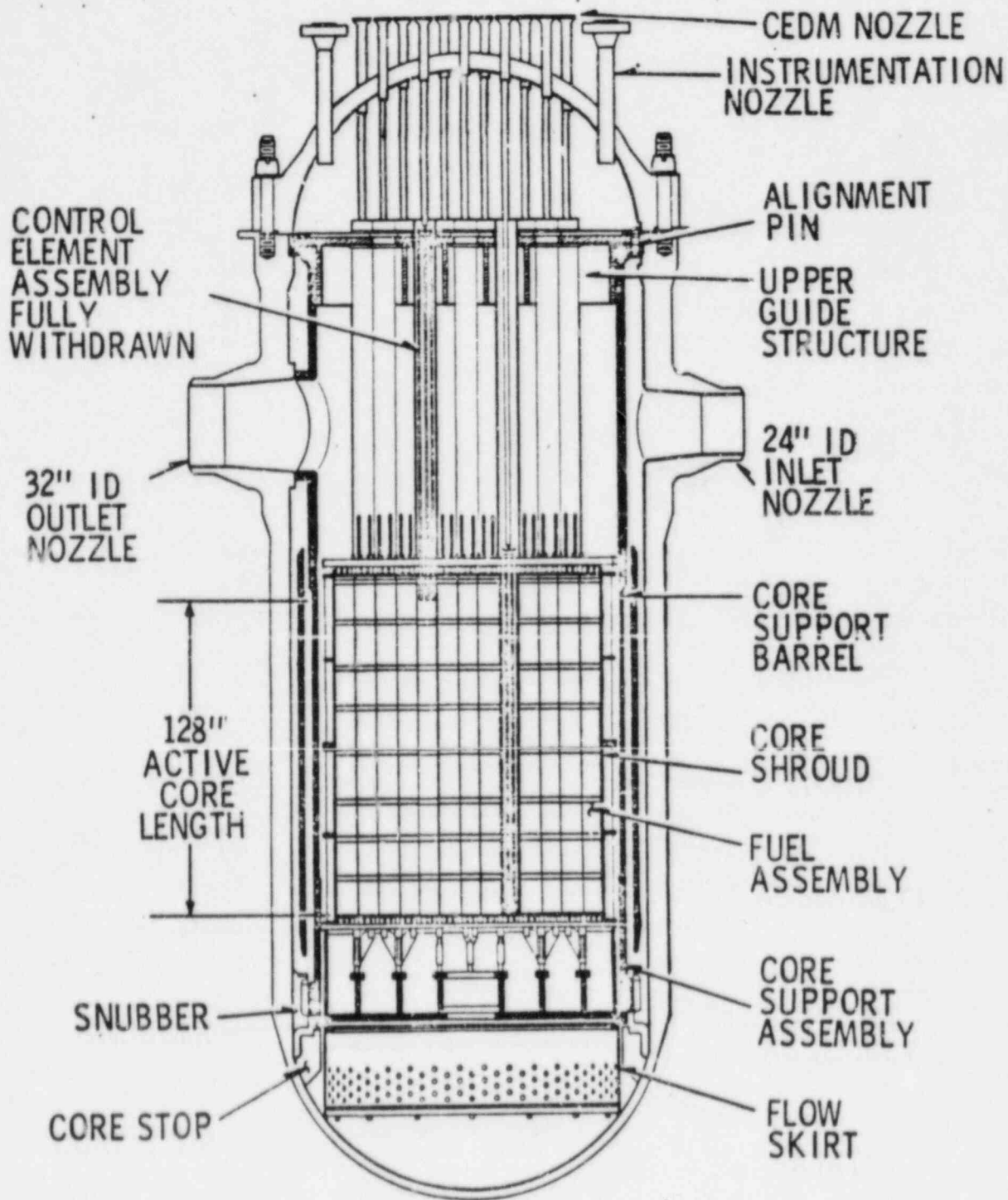
\*Ft. Calhoun values are approximate and are extrapolated from Maine Yankee values.

TABLE 3-2

PHYSICAL CHARACTERISTICS OF PLANTS HAVING THERMAL SHIELDS

	ST. LUCIE UNIT 1	MILLSTONE UNIT 2	MAINE YANKEE	FT. CALHOUN
<u>THERMAL SHIELD</u>				
THERMAL SHIELD CROSS SECTION				
OUTSIDE DIAMETER	162-3/4 IN.	162-3/4 IN.	162-3/4 IN.	133 IN.
INSIDE DIAMETER	156-3/4 IN.	156-3/4 IN.	156-3/4 IN.	127 IN.
OVERALL LENGTH	137-3/4 IN.	137-3/4 IN.	152 IN.	164 IN.
APPROXIMATE WEIGHT DRY	59,000 LBS.	59,000 LBS.	65,000 LBS.	57,000 LBS.
QUANTITY OF UPPER POSITIONING PIN	9 PINS	9 PINS	9 PINS	8 PINS
QUANTITY OF LOWER POSITIONING PIN	17 PINS	17 PINS	17 PINS	16 PINS
<u>CORE SUPPORT BARREL</u>				
OUTSIDE DIAMETER	151-1/2 IN.	151-1/2 IN.	151-1/2 IN.	123-5/8 IN.
QUANTITY OF THERMAL SHIELD SUPPORT LUGS	9 LUGS	9 LUGS	9 LUGS	8 LUGS
OVERALL LENGTH	328-1/2 IN.	328-1/2 IN.	328-1/2 IN.	311-1/4 IN.
<u>POSITIONING PIN</u>				
OVERALL LENGTH	5-5/8 IN.	5-5/8 IN.	5-5/8 IN.	4-7/16 IN.
DIAMETER	2 IN.	2 IN.	2 IN.	2 IN.
THREAD SIZE	2-1/4-16UN	2-1/4-16UN	2-1/4-16UN	2-1/4-12UN
PRELOAD TORQUE	250 FT-LBS	250 FT-LBS	250 FT-LBS	250 FT-LBS
<u>THERMAL SHIELD SUPPORT LUG</u>				
OVERALL WIDTH	2 IN.	2 IN.	2 IN.	2 IN.
OVERALL HEIGHT	10 IN.	10 IN.	10 IN.	10 IN.
POSITIONING PIN LOCKING DEVICE	LOCK BAR	LOCK BAR	LOCK BAR	WELDED LOCK- ING COLLAR

FIGURE 3-1



Reactor Internal Arrangement



Pressure Vessel - Core Support Barrel Snubber Assembly  
3-12

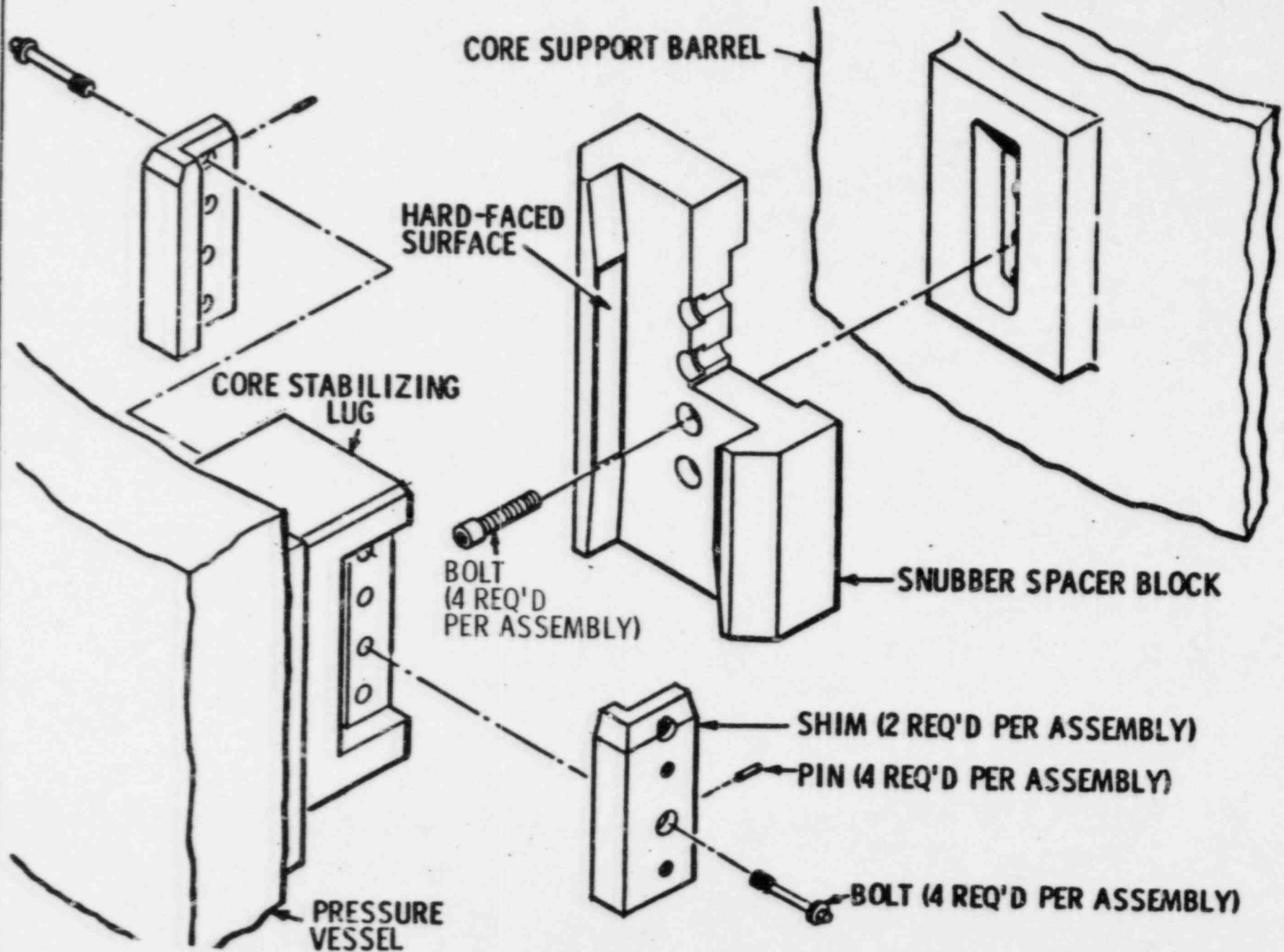
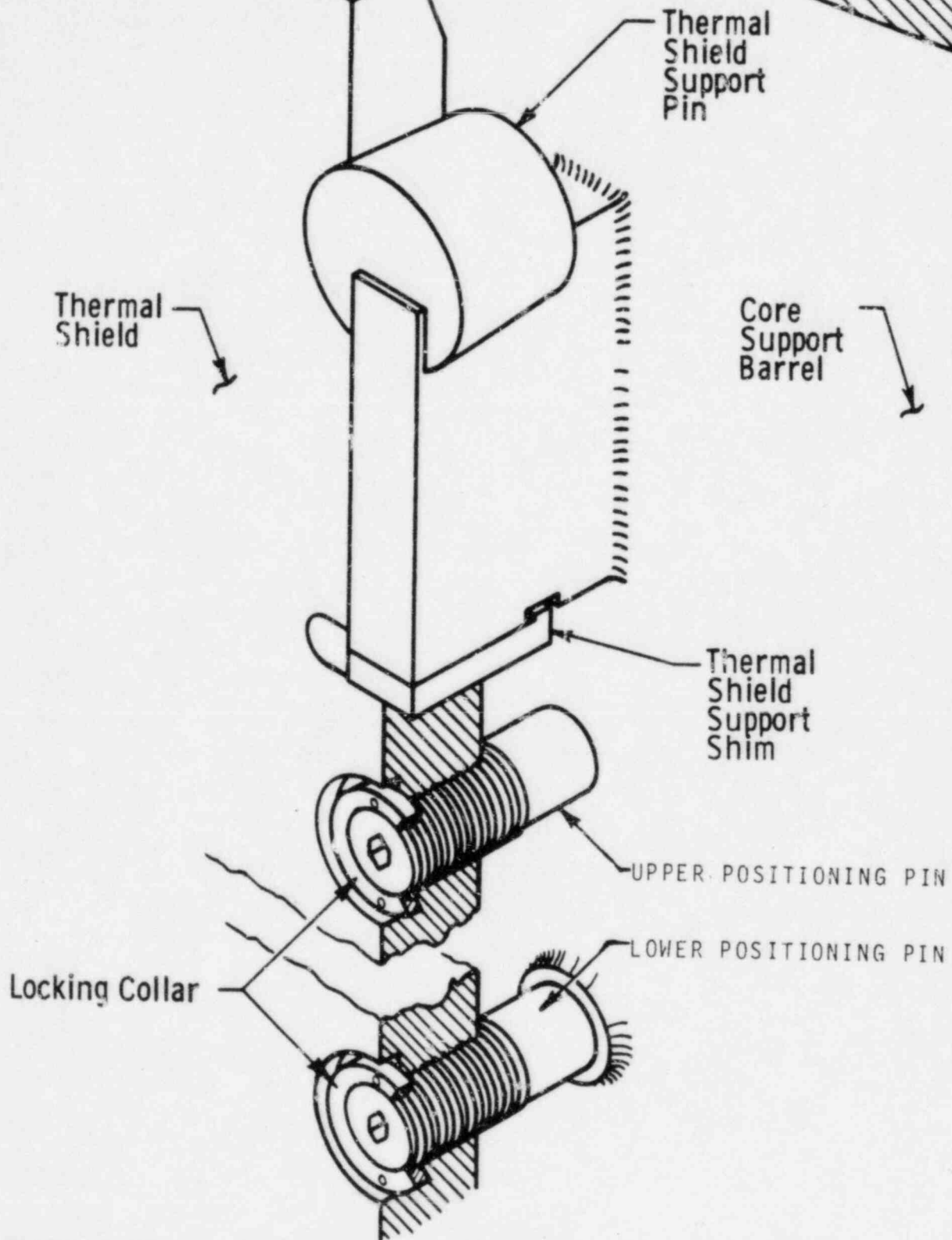


FIGURE 3-2

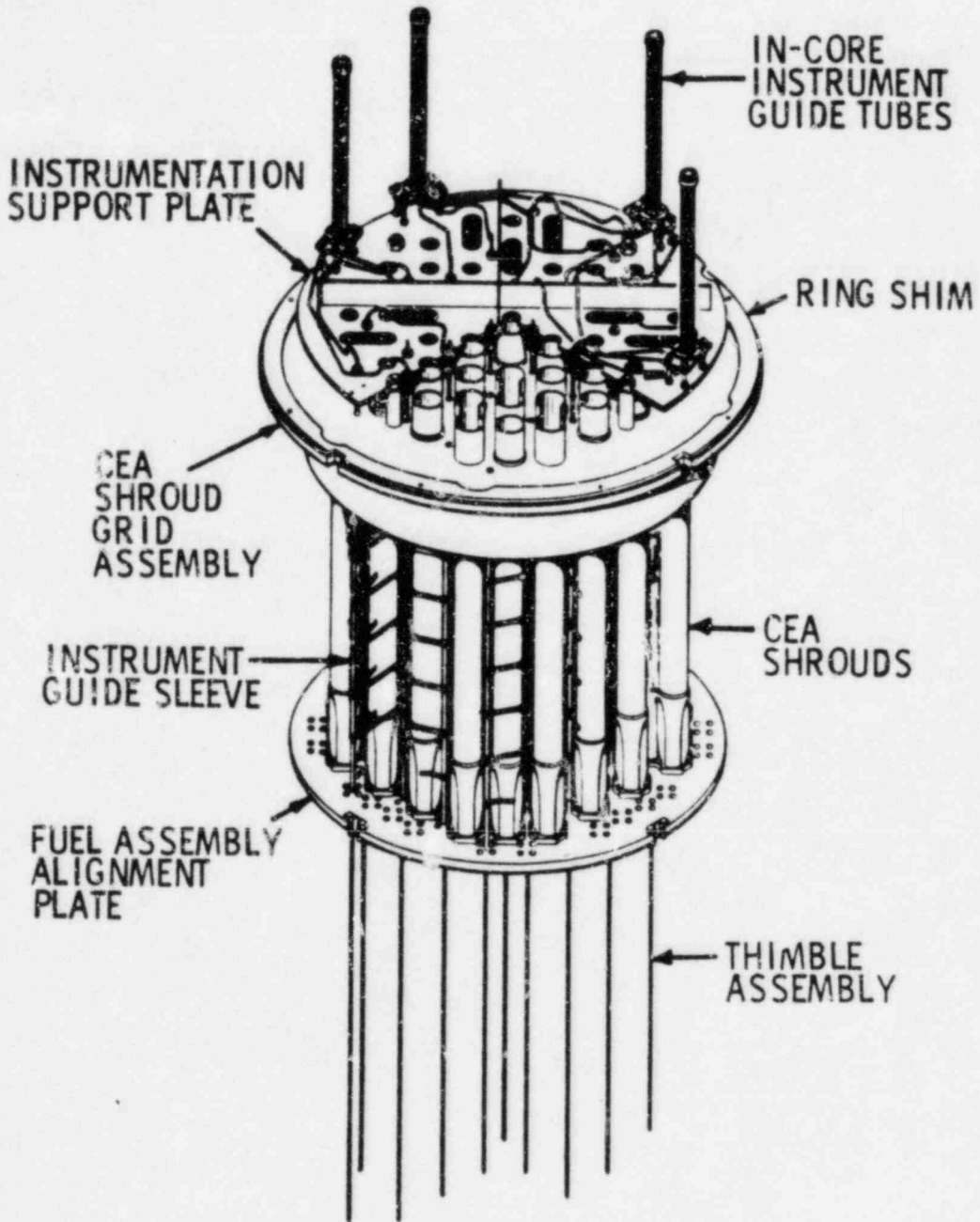


FIGURE 3-3



Thermal Shield Connection

FIGURE 3-4



#### 4.0 Thermal Shield Operating Experience

In assessing the need to do a detailed inspection of the Fort Calhoun thermal shield support system, the experience at Maine Yankee, St. Lucie Unit 1 and Millstone Unit 2 were reviewed to determine what knowledge had been gained through the evaluations conducted of their individual events. This section provides a background review of the nature of the degradation experienced at each of the affected plants and of the corrective action taken. Finally, an overall assessment of the lessons learned is provided.

##### 4.1 Maine Yankee

During the September - October 1982 outage, the Maine Yankee reactor internals were removed from the reactor vessel and inspected as part of the required ten year Inservice Inspection. The inspection disclosed that the condition of the reactor internals was normal with the following exceptions. Two of the nine upper thermal shield positioning pins were dislodged along with the two lock-bars while a third upper positioning pin was loose in the thermal shield hole in which it was installed. Of the two positioning pins dislodged, one was found outside the flow skirt in the bottom of the reactor vessel and the second was found wedged between the core support barrel and the thermal shield. The extensive wear on the pins plus the far lower radiation level of the pin retrieved from the flow skirt elevation indicated that the degradation had occurred during the first few years of plant operation.

The inspection did not reveal any evidence of wear, looseness or excessive motion at any of the thermal shield support lugs or the in place positioning pins. The inspection of the reactor vessel snubbers and core support barrel snubber lugs showed no wear which would be the result of unanticipated motion of the core support barrel. A review of the inspection results and evaluations conducted from start-up testing in 1972 up to the 1982 Inservice Inspection showed that the reactor vessel internals had responded as expected.

Based on the inspection data, analyses, and evaluation of the design and historical records, Maine Yankee reinstalled the reactor vessel internals and continued plant operation with the three positioning pins retrieved but not replaced.

Although the plant operated throughout the next fuel cycle without any indication of further thermal shield support system degradation, Maine Yankee management decided to remove the core support barrel during the next refueling outage to thoroughly inspect the thermal shield and replace the three missing positioning pins.

The thermal shield support system inspection showed the structure to be undamaged and in, or close to, the original condition.

In addition to the visual inspection and as part of the repair process of replacing the three missing positioning pins, Maine Yankee also undertook to assess whether or not the remaining positioning pins were in contact with the core support barrel. Results indicated that the upper positioning pins appeared to be in contact with the core support barrel while 11 of the 17 lower positioning pins showed evidence of a small gap. Of the lower pins showing evidence of a gap, eight were retightened to fix the thermal shield to the core support barrel in two orthogonal directions. After completing these repairs, the plant was returned to power operation. Specific details of the Maine Yankee experience can be found in References 4.1 and 4.2.

#### 4.2 St. Lucie Unit 1

During the post cycle five refueling outage in March, 1983, difficulties were encountered during core reload when a fuel assembly would not seat properly on the core support plate. Subsequent inspection determined there was debris of unknown origin on the plate. A decision was made to unload the fuel and remove the core support barrel to further investigate the source of debris.

A visual examination of the core support barrel/thermal shield assembly disclosed that the thermal shield support system was severely damaged. A number of thermal shield support pins were fractured and/or missing and damage to the core support barrel was visible. The fractured pieces from the thermal shield supports were found between the flow skirt and the reactor vessel. Two positioning pins had become dislodged; one was found between the flow skirt and the reactor vessel and the other in the reactor vessel lower head. A positioning pin lock bar was retrieved from the core support plate. An evaluation of the thermal shield support system concluded that refurbishment was impractical. Therefore, a decision was made to remove the thermal shield. Analyses were performed to evaluate operation of the plant without a thermal shield for its remaining design life. The analyses indicated that replacement of the thermal shield was not necessary.

The reactor internals interfaces with the reactor vessel were examined and were not found to exhibit evidence of excessive vibration of the reactor core support barrel and upper guide structure. A visual examination of a selected number of fuel assemblies did not disclose detrimental effects attributable to the degraded thermal shield support system. From these inspections it was concluded that the damage was confined to the core support barrel and thermal shield.

Upon removal of the thermal shield from the core support barrel, a nondestructive examination of the core support barrel was conducted. Damage of varying degrees was in evidence at eight of the nine lug locations. Four lugs were separated from the core support barrel and through wall cracks were confirmed adjacent to some damaged lug areas.

A repair process for the core support barrel was formulated. Underwater machining of the core support barrel in the damaged areas was used to reduce stress concentrations. Through-wall cracks were arrested by crack arrestor holes; non-through-wall cracks were removed by machining, and lug tear out areas were patched as necessary. The crack arrestor holes were sealed by inserting expandable plugs. After completing these repairs, the plant was returned to power operation. Specific details of the St. Lucie Unit 1 experience can be found in Reference 4.3.

#### 4.3 Millstone Unit 2

During the post cycle five refueling outage which commenced in May, 1983, the 10-year in-service inspection was performed for the reactor vessel and its internals. The thermal shield and its support system were of particular interest since St. Lucie Unit 1 had identified damage to its thermal shield and support system in March, 1983.

As with St. Lucie Unit 1, visual examination of the core support barrel/thermal shield assembly disclosed the thermal shield support system to be damaged. A few thermal shield support pins were damaged and/or missing and damage to the thermal shield was visible. Pieces from the thermal shield were found in the reactor vessel and two positioning pins which had become dislodged were found in the reactor vessel.

Although the damage incurred was not as severe as that experienced at St. Lucie Unit 1, an evaluation of the thermal shield support system concluded that refurbishment was impractical and a decision was made to remove the thermal shield. Again, analyses confirmed that operation of the plant for the remainder of its design life without the thermal shield was acceptable.



The reactor internals interfaces within the reactor vessel were examined and were found not to exhibit evidence of excessive vibration of the reactor core support barrel and upper guide structure. A visual examination of a selected number of fuel assemblies did not disclose detrimental effects attributable to the degraded thermal shield support system. From these inspections it was concluded that the damage was confined to the core support barrel and thermal shield.

Upon removal of the thermal shield from the core support barrel, a nondestructive examination of the core support barrel was conducted. Damage was in evidence at two of the nine lug locations. Throughwall cracks were confirmed adjacent to two damaged lug locations.

A repair process for the core support barrel was formulated. Underwater machining of the core support barrel in the damaged areas was used to reduce stress concentrations. Through-wall cracks were relieved by crack arrestor holes; non-through-wall cracks were removed by machining. Because of the limited amount of through wall cracks and smaller cracks arrestor holes, no plugging of these holes was undertaken as had been done for St. Lucie Unit 1. After completing these repairs, the plant was returned to power operation. The specific details of the Millstone Unit 2 experience can be found in Reference 4.4.

#### 4.4 POSTULATED SEQUENCE OF EVENTS LEADING TO DEGRADATION

This section presents a postulated sequence of events which could explain the thermal shield support system problems experienced by Maine Yankee, St. Lucie Unit 1 and Millstone Unit 2. The sequence of events is based on judgement and the examinations and analyses performed.

In case of St. Lucie Unit 1 and Millstone Unit 2, it appears certain that the damage to the thermal shield was caused by large amplitude self-excited vibration. The vibration was made possible by degradation of the thermal shield support system which was preceded by loss of preload on positioning pins. The reasons for the loss of preload have not been specifically identified, but several factors have been examined and found to be capable of contributing. It is believed that a combination of detrimental factors is the most reasonable explanation for the loss of preload.

Degradation of the support system probably began when a sufficient number of pins had lost preload to permit relative motion and impacting between the pins and the stellite pads on the core barrel. This causes wear in the threads holding the pins and on the pin-to-core support barrel interface. Thread wear would allow the pins to move axially, causing a loss of restraint of radial motion of the shield. With the loss of restraint the shield is calculated to begin to uncouple from the core barrel, especially at the elevation of the lower pins. This hypothesis is supported by analysis of St. Lucie Unit 1 IVM data which indicates significant changes in power spectral density peak frequencies and in cross core coherence early in 1980. The resultant increased response to hydraulic loads would increase the relative motion between the shield and support lugs, causing wear between the lugs and the shield.



With sufficient wear on the lugs, the thermal shield reaches an unstable dynamic condition. Dynamic stability analyses on the effect of self-excited loads show a tendency for the thermal shield to become unstable with sufficient reduction in the effective stiffness of the lugs. The resulting large amplitude motions cause high stresses in the thermal shield, causing failure in a relatively short period of time. Again, based on St. Lucie Unit 1 data, increases in the magnitude and frequency of LPM alarms and changes in frequency peaks associated with thermal shield motion from the IVM system support this sequence of events.

On the basis of the available evidence, which is summarized graphically in Figure 4-1 for St. Lucie Unit 1, it appears that the postulated sequence of events took place chronologically as follows: first pin(s) were loose prior to early 1978; lug wear becoming detectable by April, 1982; and lug wear increasing through September, 1982.

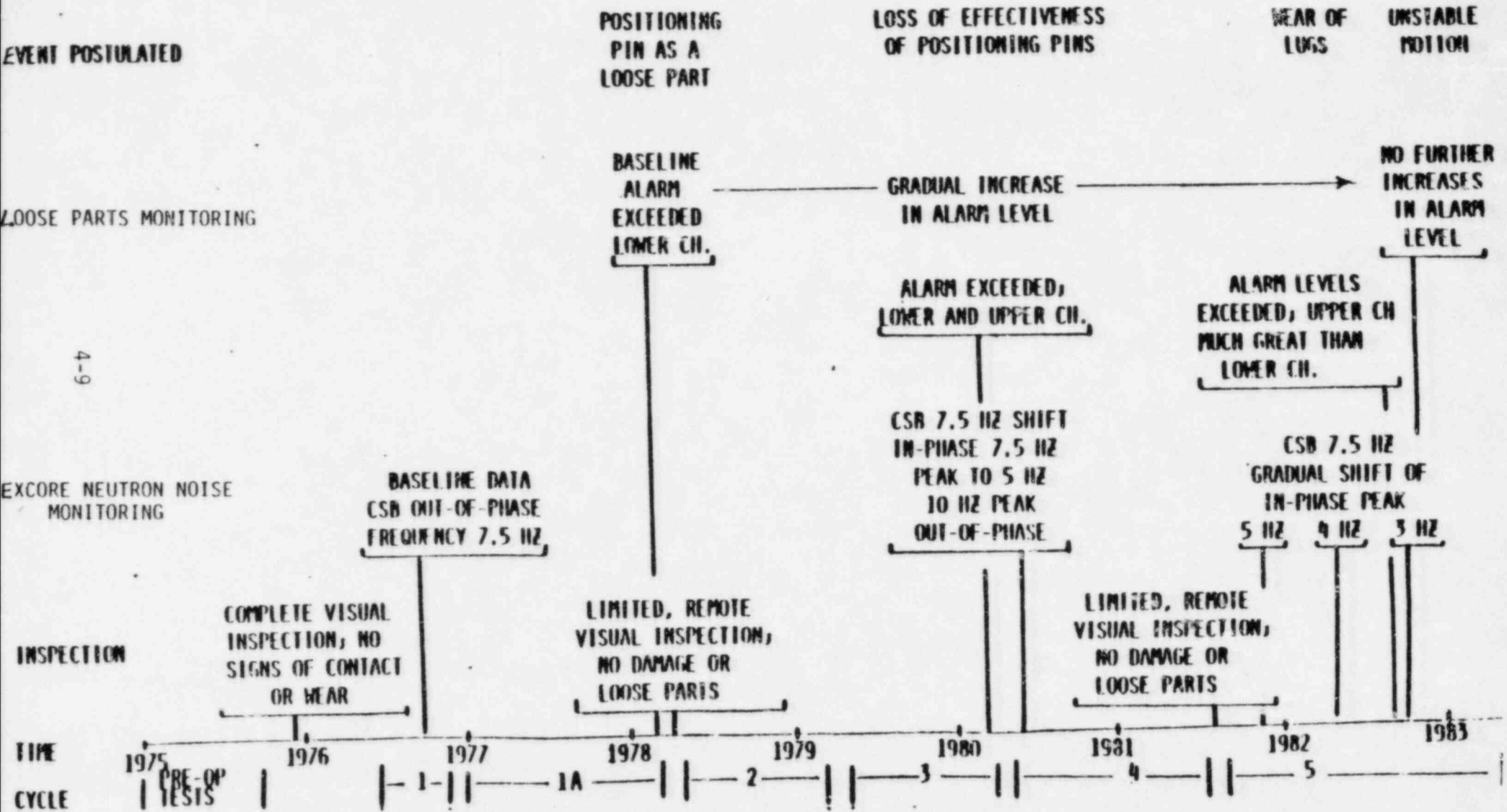
Initial impacts, detected by the lower reactor vessel accelerometers, were indicative of loss (loose pin in the bottom of the reactor vessel) of the first pin(s) in 1978. Analysis of neutron noise signals through this period did not indicate any anomalies. Loss of effectiveness of positioning pins by May, 1980 was evidenced in both the LPM and neutron noise signals. The upper vessel accelerometers indicated impacts for the first time and had g levels exceeding the lower vessel accelerometers. Significant changes in the neutron noise spectra corresponding to reductions in the shell mode frequency were identified. In addition, there was evidence of a thermal shield beam bending mode in the neutron noise data. In 1982, upper vessel accelerometers showed as much as a fivefold increase in g level. A continuing reduction in the shell mode frequency was identified in the neutron noise data. By September, 1982 there were no further increases in LPM g levels.

During this period of time the neutron noise signals continued to show a reduction in the shell mode frequency indicating that an increased number of support lugs were becoming ineffective.

The available evidence indicates that thermal shield support system degradation is a lengthy process, and that the process is detectable by means of loose parts monitoring and excore neutron noise monitoring systems.

CHRONOLOGICAL SEQUENCE OF EVENTS - ST. LUCIE 1

FIGURE 4-1



4-9

## REFERENCES

- 4.1 CEN-232(M), Thermal Shield Support System Dislodged Positioning Pin Evaluation for Maine Yankee, December 1982. J. H. Garrity to R. A. Clark, Thermal Shield Positioning Pin Report MH-83-33/JHG-83-38, February 28, 1983.
- 4.2 G. D. Whittier to J. R. Miller, 1984 Refueling Outage Thermal Shield Repair Report, MN-84-151/GDW-84-216, September 14, 1984.
- 4.3 CEN-272(F)-P, Final Report on the St. Lucie Unit 1 Post Cycle 5 Plant Recovery Program, February 1984.
- 4.4 W. G. Council to J. R. Miller, Millstone Nuclear Power Station, Unit No. 2 Thermal Shield Damage Recovery Program Final Report, December 12, 1983.

5.0 FT. CALHOUN THERMAL SHIELD SUPPORT SYSTEM STRUCTURAL CHARACTERISTICS

5.1 Dynamic Characteristics

To evaluate both the dynamic characteristics, i.e., frequencies and mode shapes, and the thermal shield positioning pin preloads, a detailed finite element model of the coupled CSB - thermal shield structure was developed.

The CSB and thermal shield form a system that is coupled both structurally and hydrodynamically. Structural coupling comes from the support lugs and positioning pins which both support and locate the thermal shield relative to the core barrel. Hydrodynamic coupling is important due to the relatively narrow fluid annuli between the vessel to shield and shield to barrel. Structural coupling must be properly considered in calculating the positioning pin preloads. Structural and hydrodynamic coupling must be properly considered in calculating the dynamic response.

A detailed three dimensional finite element model of the CSB - thermal shield system was developed (Figure 5-1). The model includes detailed representations of both the support lugs and the upper and lower positioning pins. Details of the CSB such as the outlet nozzles and changes in wall thickness are represented in the model.

5.1.1 Natural Frequencies and Mode Shapes

Experience at the St. Lucie Unit 1 demonstrated that degradation in the thermal shield supports were manifested as frequency peak shifts in the spectra of the excore detector noise signals. Therefore, analytical predictions of changes in frequency and modes with assumed changes in the thermal

shield support system are used to interpret the data acquired from the excore neutron detector signal monitoring program (Section 6).

The natural frequencies of the coupled CSB - thermal shield structure were calculated by three-dimensional finite element analysis using the SAP4 code. In-water frequencies and modes were calculated for nominal support conditions using the model as shown in Figure 5-1. The model was modified to obtain in-water frequencies and modes for the support condition of all positioning pins removed. The frequencies for both these cases are shown in Table 5-1. The mode shapes are shown in Figures 5-2 to 5-10. The mode shapes are plotted for three elevations: top positioning pins, middle of the thermal shield and bottom positioning pins.

#### 5.1.2 Thermal Shield Positioning Pin Preload

Another parameter in demonstrating the acceptability of the CSB - thermal shield support arrangement is the net load existing at each positioning pin during operating conditions. Factors which tend to increase the operating load are the initial mechanical preload and the thermal expansion effects due to operating temperature differences between the CSB and the thermal shield. Factors which tend to reduce the load include the difference in pressure on the CSB and thermal shield due to fluctuating and steady state hydraulic loads, deformation of the CSB during assembly as the weight of the thermal shield is transferred to the lugs from the jacks, and radiation induced stress relaxation. Analyses of the St. Lucie Unit 1 thermal shield arrangement have shown the effects of fluctuating hydraulic loads to be negligible.

The initial mechanical preload due to the specified installation torque of 250 ft-lbs. was calculated using the equation in Table 5-2. The preload was computed to be 10,300

lbs. The deflection at each pin location resulting from the application of the preload was obtained from a static analysis using the SAP4 code with a three dimensional finite element model of the coupled thermal shield and CSB. The analysis consisted of application of equal and opposite loads of 10,300 lbs. on each shell at each positioning pin location. In one case, all the upper pins were removed and the loads were applied at the lower pins. A similar case was examined with all the lower pins removed and the loads applied at the upper pins.

Pressure differences across the CSB and thermal shield due to steady state hydraulic loads reduce the preload in the positioning pins. The relative deflections due to steady state hydraulic loads were calculated by applying the normal operating pressure distribution to the finite element model. The pressure distribution for the CSB is shown in Figure 5-11. The uniform pressure difference on the thermal shield was calculated to be 1.73 psi acting radially outward.

Another factor that reduces pin reload is the transfer of the weight of the thermal shield from jacks to the support lugs during installation. When the jacks are removed, the thermal shield weight produces a moment on the support lug which tends to deflect the core barrel inward near the upper pins, thereby reducing the preload. The deflection of the CSB was calculated by applying the weight of the thermal shield to the finite element model of the lugs.

Stress relaxation of the positioning pins increases with fluence and, therefore, depends on the location of the positioning pins with respect to the active fuel. Since the lower positioning pins on Fort Calhoun are located in excess of 11 inches below the active fuel, fluence on these pins is less than the upper pins. Thermal stress levels and radiation induced stress relaxation were not quantified specifically for Fort Calhoun. Evaluation of deflections under power operation would not show a significant increase in the lower positioning pin deflection from that computed under isothermal conditions due to the small temperature difference and the stiffness of the core support barrel.



The combined relative deflections due to mechanical preload, static pressure differentials, and thermal shield weight are shown in Table 5-3 for each positioning pin location.

## 5.2 CONCLUSIONS

### 5.2.1 Natural Frequencies and Mode Shapes

A review of the frequencies in Table 5-1 indicates that the first shell mode ( $\cos 2\theta$ ) experiences the greatest reduction in frequency as a result of removing all the positioning pins. The remaining shell modes experience smaller reductions in frequency. The core support barrel beam bending mode frequency remains unchanged. A thermal shield beam bending mode appears with no pins at 9.4 HZ. This information provides the basis for evaluation of the IVM data to detect a degraded thermal shield support system.

### 5.2.2 Thermal Shield Positioning Pin Preload

Based on the relative deflections shown in Table 5-3 for each positioning pin location, when the reactor is at or near full power, thermal effects increase the preload.

When the reactor is at low or zero power, the preload depends on the initial mechanical preload. The last column in Table 5-3 provides the calculated preload at each positioning pin location under these isothermal conditions, neglecting the effect of stress relaxation. The results show larger margins at the upper pins, with eight of the lower pins having less than 2 mils deflection of preload available at isothermal operating conditions.

Since stress relaxation effects increase with time, the margins on the lower positioning pins would tend to decrease

with time. The locking collar located at the thermal shield end of the positioning pins is a positive factor in resisting relative motion between the thermal shield and positioning pin threads. The resistance to relative motion is developed by the preload between the thermal shield and the positioning pin provided by the locking collar. This preload prevents wear on the positioning pin threads from flow induced buffeting.

TABLE 5-1

Predictions of In-Water Modal Frequencies (Hertz)

	<u>Mode</u>	<u>Nominal</u>	<u>All Pins Removed</u>
1.	Beam	7	7
2.	cos 2 $\theta$	12.5	7.9
3.	cos 3 $\theta$	16.3	14.9
4.	cos 4 $\theta$	22.8	22

Note: When the core support barrel and thermal shield are uncoupled by removing the positioning pins, a thermal shield beam mode appears at 9.4 Hz.

TABLE 5-2

POSITIONING PIN MECHANICAL PRELOAD

$$T = \frac{F d_m}{2} \left( \frac{\tan \psi + \mu \sec \alpha}{1 - \mu \tan \psi \sec \alpha} \right) + \frac{F \mu_c d_c}{2}$$

(1)

where

T = TORQUE APPLIED TO POSITIONING PIN

F = PRELOAD

$d_m$  = MEAN THREAD DIAMETER

$d_c$  = MEAN COLLAR DIAMETER (EFFECTIVE DIAMETER OF RUBBING SURFACE AGAINST WHICH PIN BEARS)

$\mu$  = COEFFICIENT OF THREAD FRICTION

$\mu_c$  = COEFFICIENT OF COLLAR FRICTION

$\psi$  = HELIX ANGLE OF THREAD AT MEAN THREAD DIAMETER

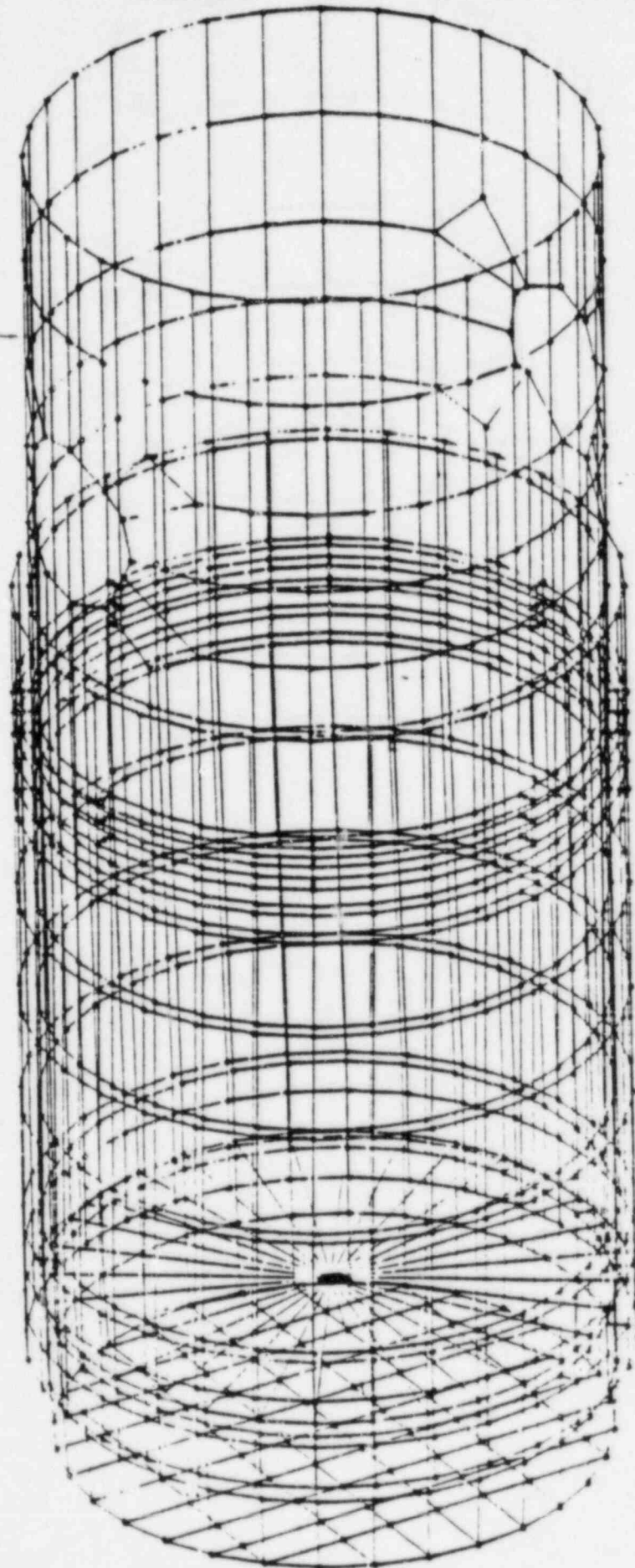
$\alpha$  = HALF THE THREAD ANGLE

(1) REFERENCE: J. E. SHIGLEY, "MECHANICAL ENGINEERING DESIGN", MCGRAW-HILL BOOK CO., 1963, P. 245.

TABLE 5-3

RELATIVE DEFLECTIONS (MILS) FOR FACTORS THAT  
INCREASE (+) AND REDUCE (-) POSITIONING PIN PRELOAD

		Mechanical Preload 10,300 lbs.	$\Delta P$ Static Due to Steady State	Thermal Shield Weight	Isothermal Operating Deflection
UPPER POSITIONING PINS	1	8.304	-1.233	-.353	6.718
	2	8.305	-2.496	-.412	5.397
	3	8.302	-1.077	-.332	6.893
	4	8.315	-1.602	-.404	6.309
	5	8.303	-2.217	-.372	5.714
	6	8.304	-0.956	-.359	6.989
	7	8.305	-2.094	-.374	5.837
	8	8.313	-1.566	-.400	6.347
LOWER POSITIONING PINS	1	2.646	+0.275	.014	2.935
	2	2.646	+0.137	.012	2.795
	3	2.644	-0.503	.020	2.161
	4	2.644	-1.156	.039	1.527
	5	2.646	-1.419	.060	1.287
	6	2.644	-1.238	.078	1.484
	7	2.644	-0.826	.081	1.899
	8	2.646	-0.375	.075	2.346
	9	2.646	-0.018	.068	2.696
	10	2.646	+0.077	.066	2.789
	11	2.644	-0.214	.068	2.498
	12	2.644	-0.829	.067	1.882
	13	2.646	-1.418	.056	1.284
	14	2.644	-1.536	.041	1.149
	15	2.644	-1.038	.027	1.633
	16	2.646	-0.242	.018	2.422



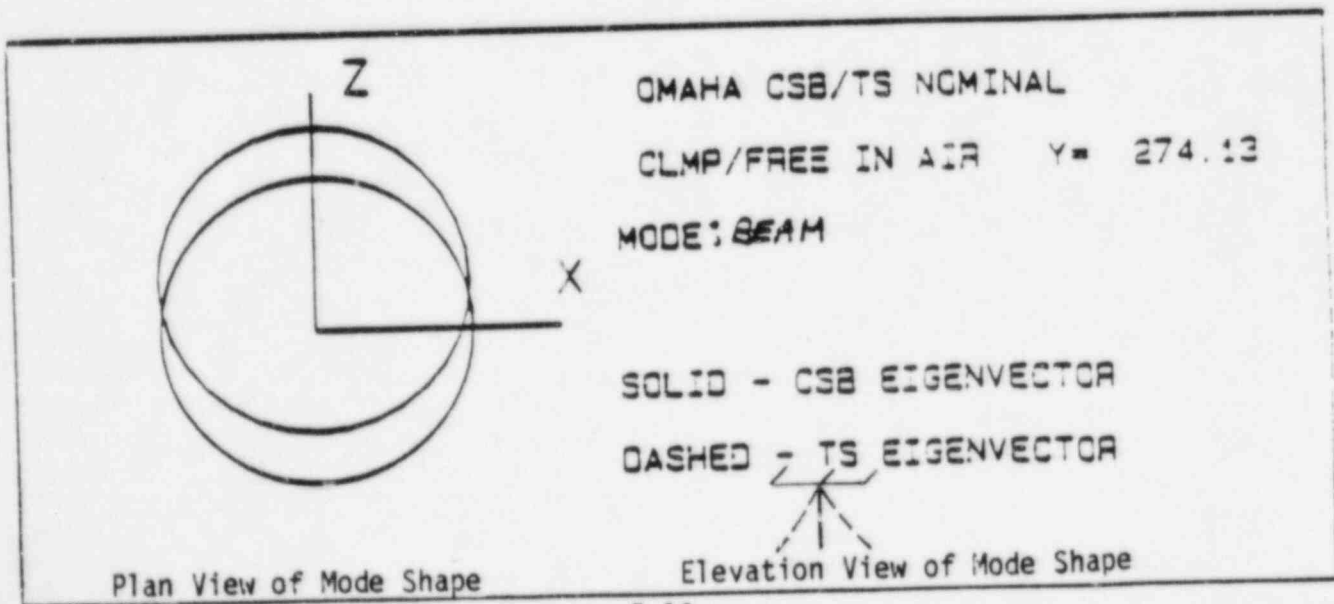
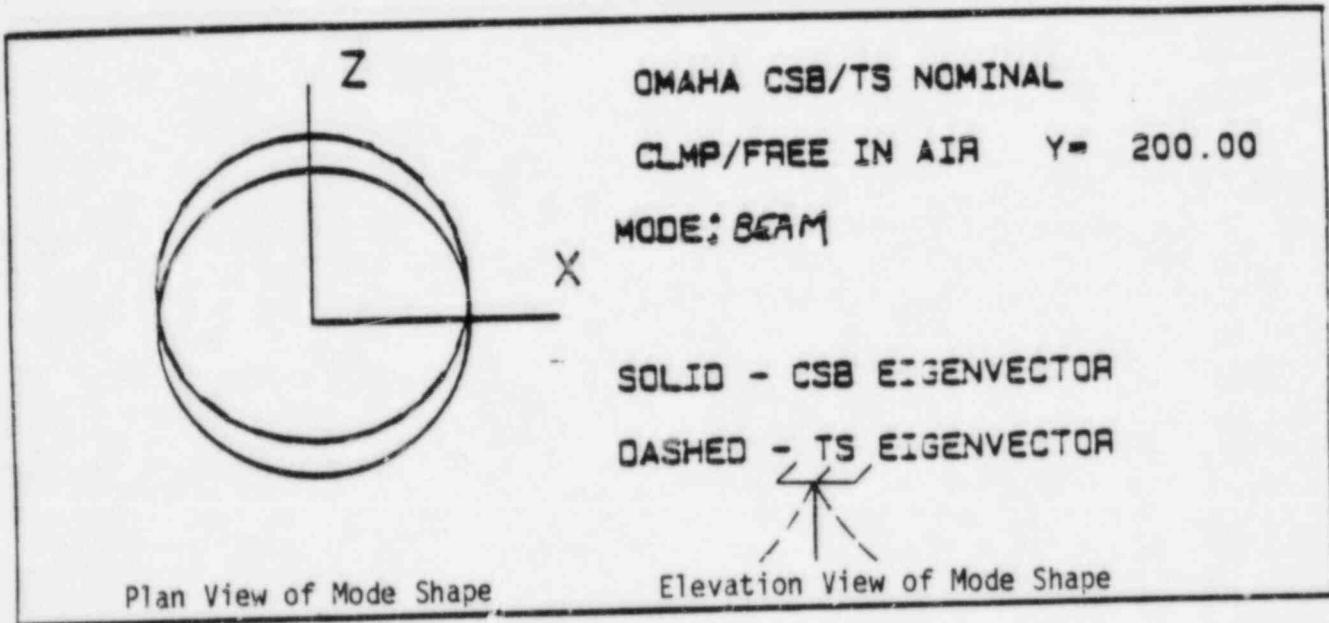
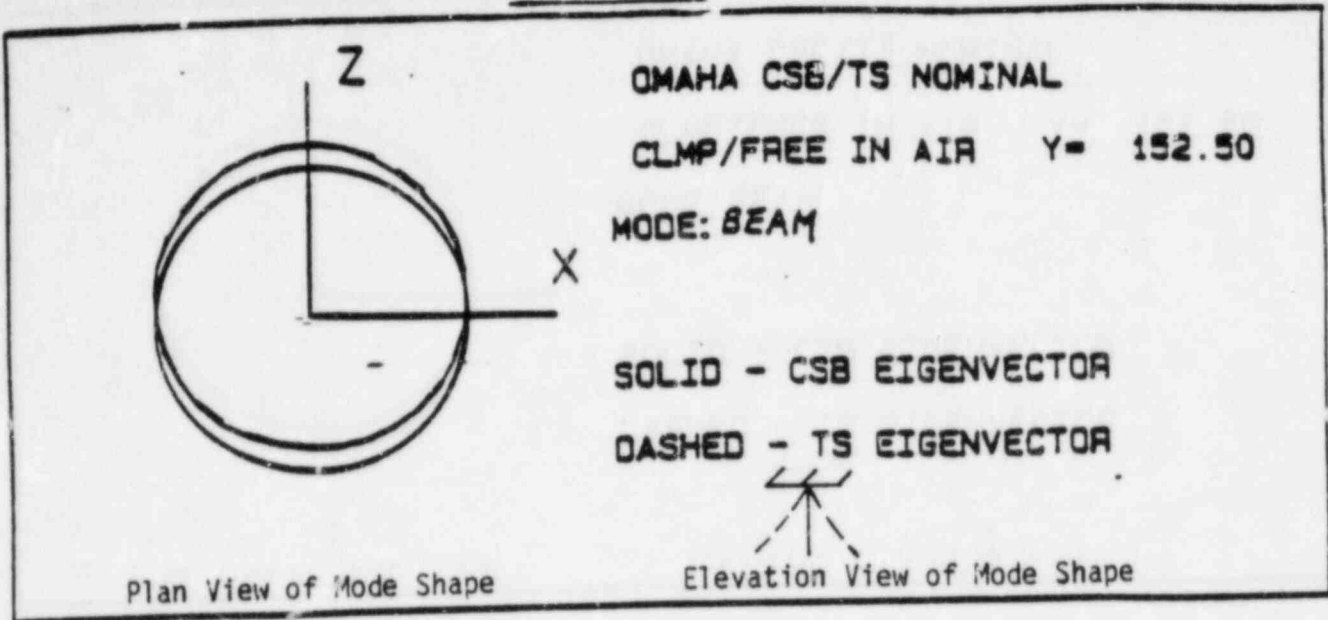
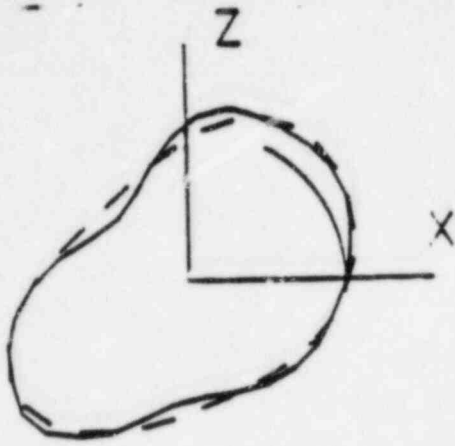


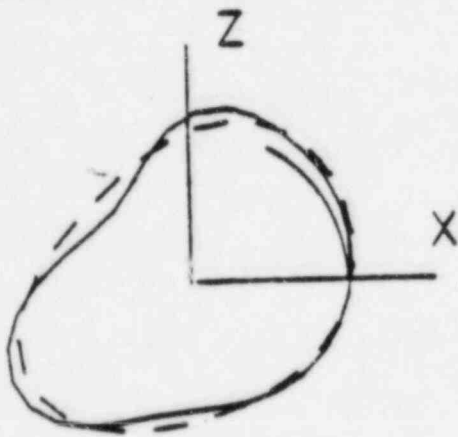


FIGURE 5-3



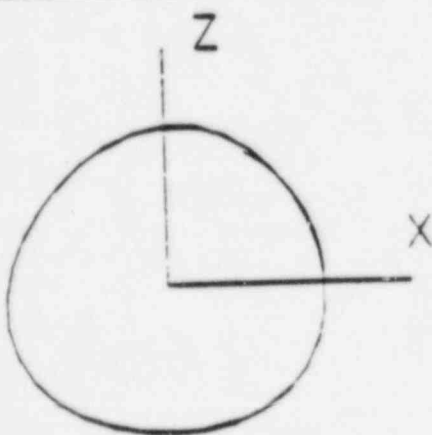
OMAHA CSB/TS NOMINAL  
CLMP/FREE IN AIR Y= 152.50  
MODE:  $\cos 2\theta$

SOLID - CSB EIGENVECTOR  
DASHED - TS EIGENVECTOR



OMAHA CSB/TS NOMINAL  
CLMP/FREE IN AIR Y= 200.00  
MODE:  $\cos 2\theta$

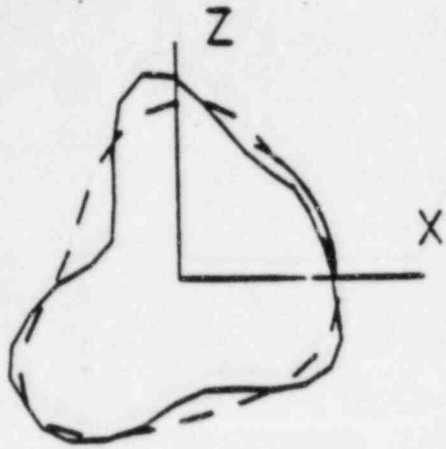
SOLID - CSB EIGENVECTOR  
DASHED - TS EIGENVECTOR



OMAHA CSB/TS NOMINAL  
CLMP/FREE IN AIR Y= 274.13  
MODE:  $\cos 2\theta$

SOLID - CSB EIGENVECTOR  
DASHED - TS EIGENVECTOR

FIGURE 5-4



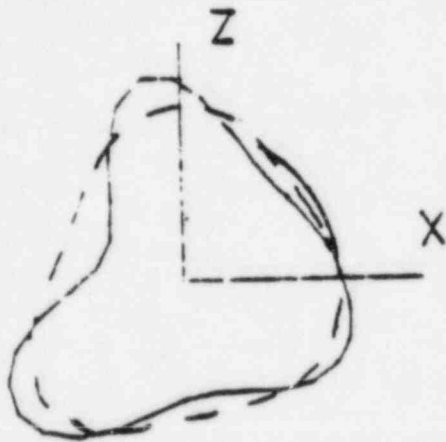
OMAHA CSB/TS NOMINAL

CLMP/FREE IN AIR Y= 152.50

MODE: COS 30

SOLID - CSB EIGENVECTOR

DASHED - TS EIGENVECTOR



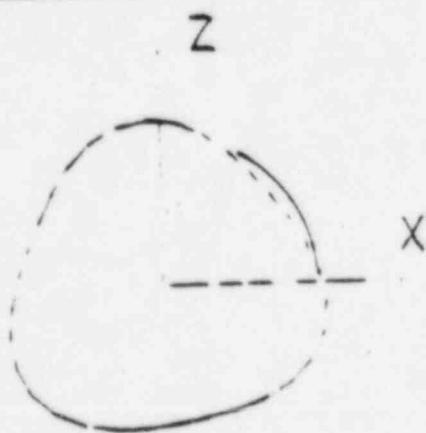
OMAHA CSB/TS NOMINAL

CLMP/FREE IN AIR Y= 200.00

MODE: COS 30

SOLID - CSB EIGENVECTOR

DASHED - TS EIGENVECTOR



OMAHA CSB/TS NOMINAL

CLMP/FREE IN AIR Y= 274.13

MODE: COS 30

SOLID - CSB EIGENVECTOR

DASHED - TS EIGENVECTOR

FIGURE 5-5

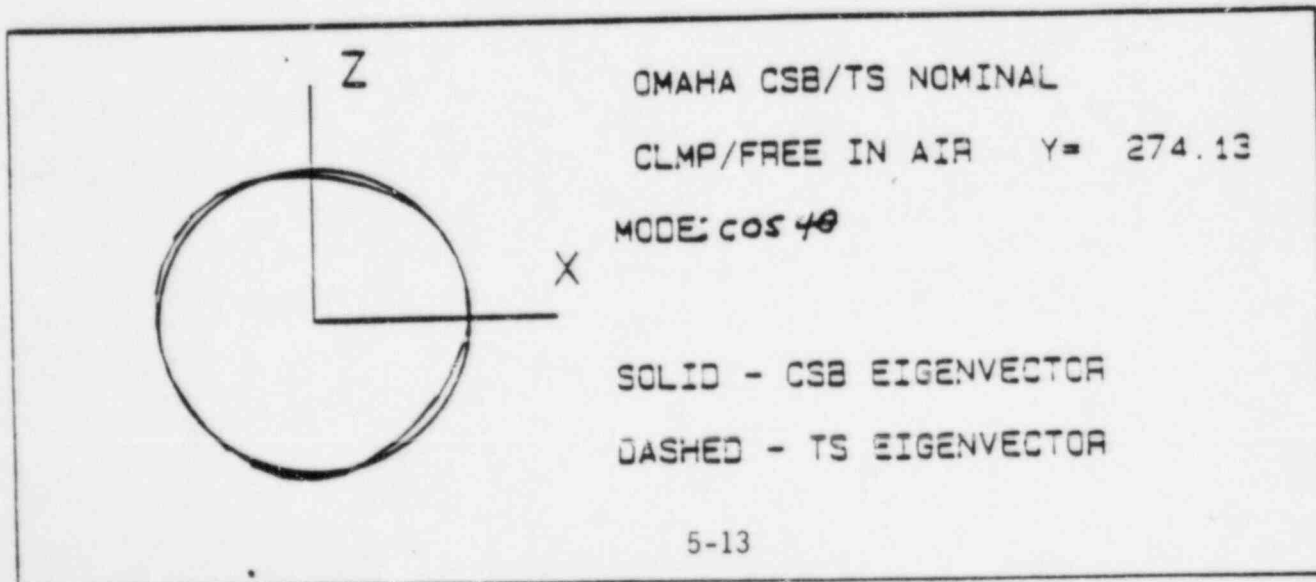
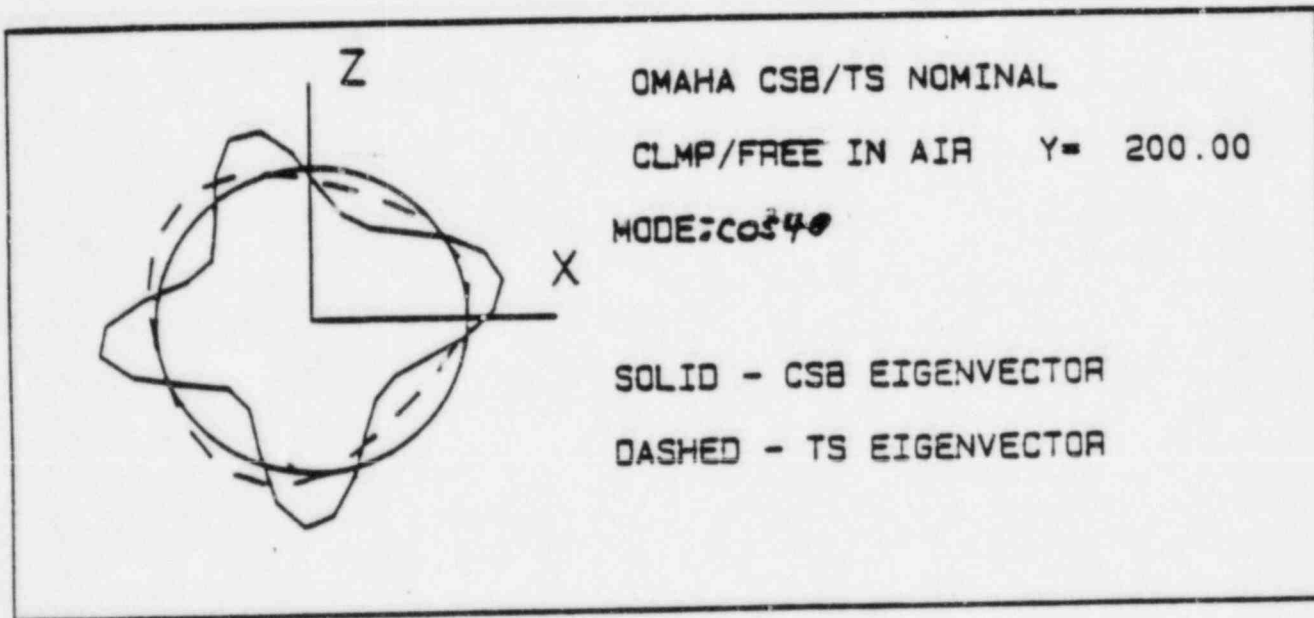
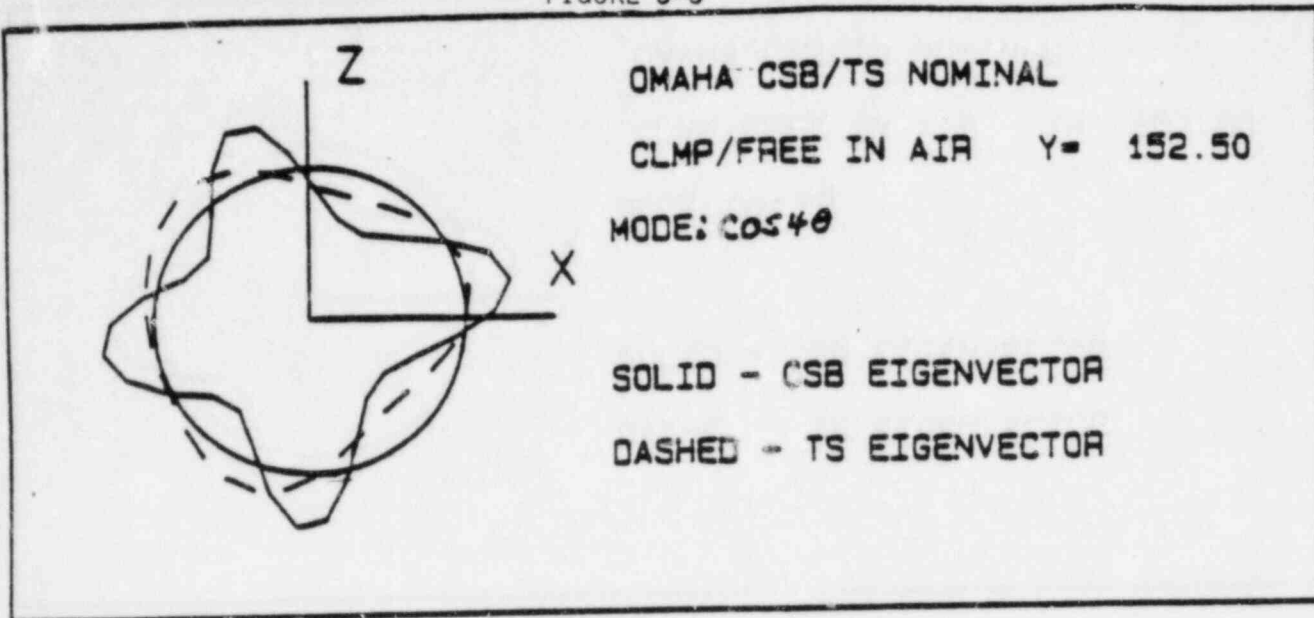
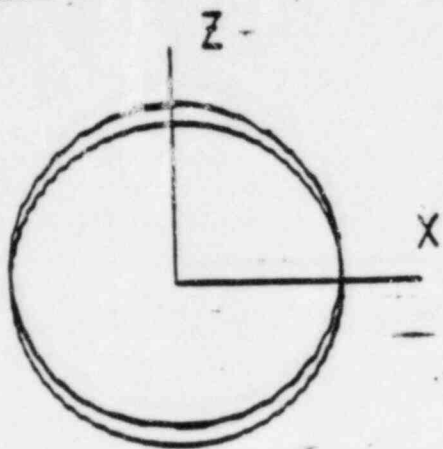
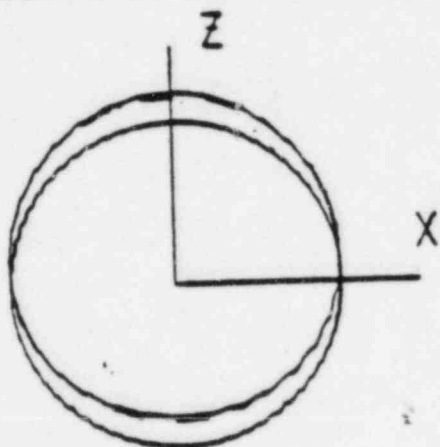


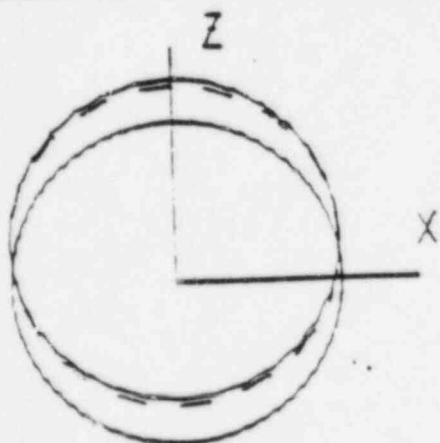
FIGURE 5-6



OMAHA CSB/TS NO PINS  
CLMP/FREE-AIR Y= 152.50  
MODE: BEAM  
— SOLID - CSB EIGENVECTOR  
- DASHED - TS EIGENVECTOR

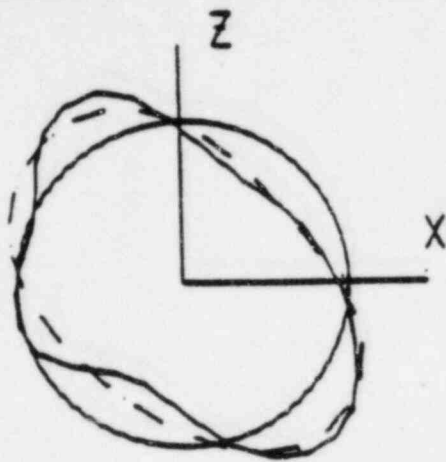


OMAHA CSB/TS NO PINS  
CLMP/FREE-AIR Y= 200.00  
MODE: BEAM  
— SOLID - CSB EIGENVECTOR  
- DASHED - TS EIGENVECTOR



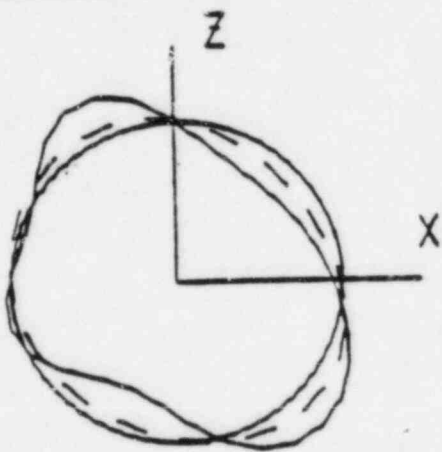
OMAHA CSB/TS NO PINS  
CLMP/FREE-AIR Y= 274.13  
MODE: BEAM  
— SOLID - CSB EIGENVECTOR  
- DASHED - TS EIGENVECTOR

FIGURE 5-7



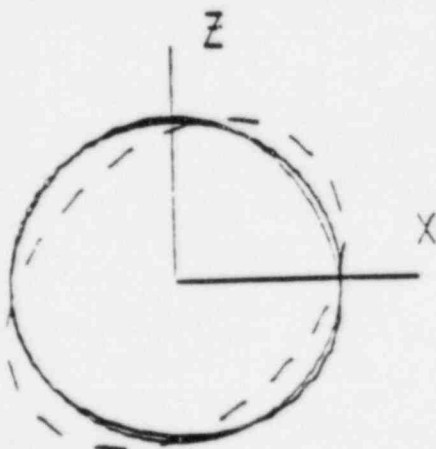
OMAHA CSB/TS NO PINS  
CLMP/FREE-AIR Y= 152.50  
MODE:  $\cos 2\theta$

SOLID - CSB EIGENVECTOR  
DASHED - TS EIGENVECTOR



OMAHA CSB/TS NO PINS  
CLMP/FREE-AIR Y= 200.00  
MODE:  $\cos 2\theta$

SOLID - CSB EIGENVECTOR  
DASHED - TS EIGENVECTOR



OMAHA CSB/TS NO PINS  
CLMP/FREE-AIR Y= 274.13  
MODE:  $\cos 2\theta$

SOLID - CSB EIGENVECTOR  
DASHED - TS EIGENVECTOR

FIGURE 5-8

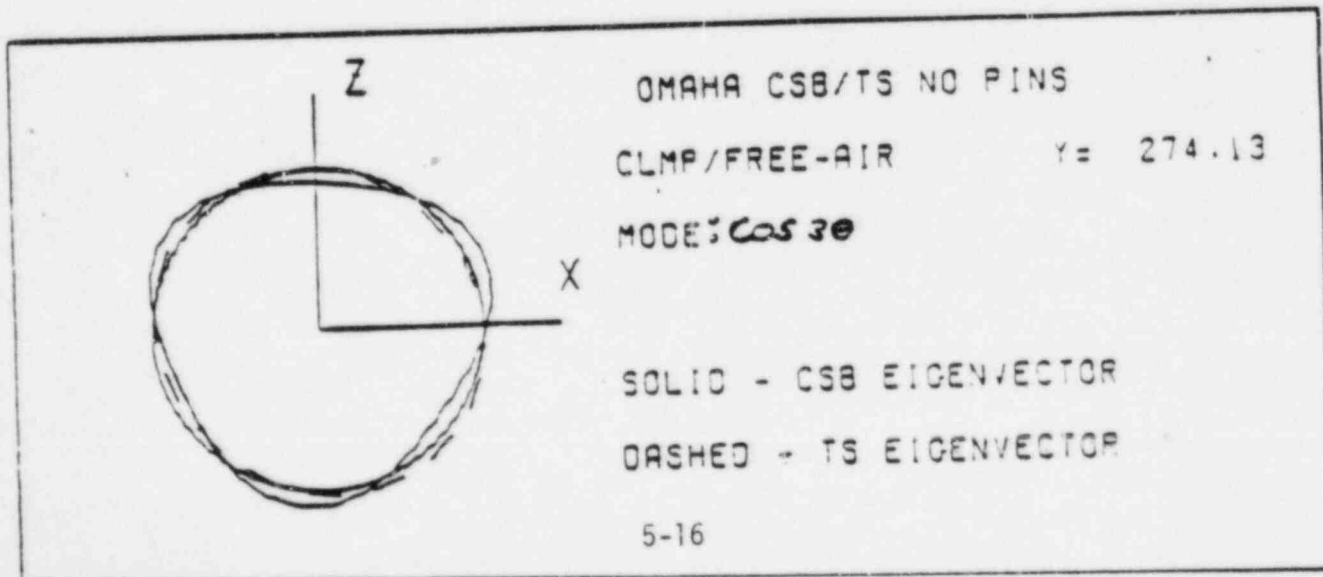
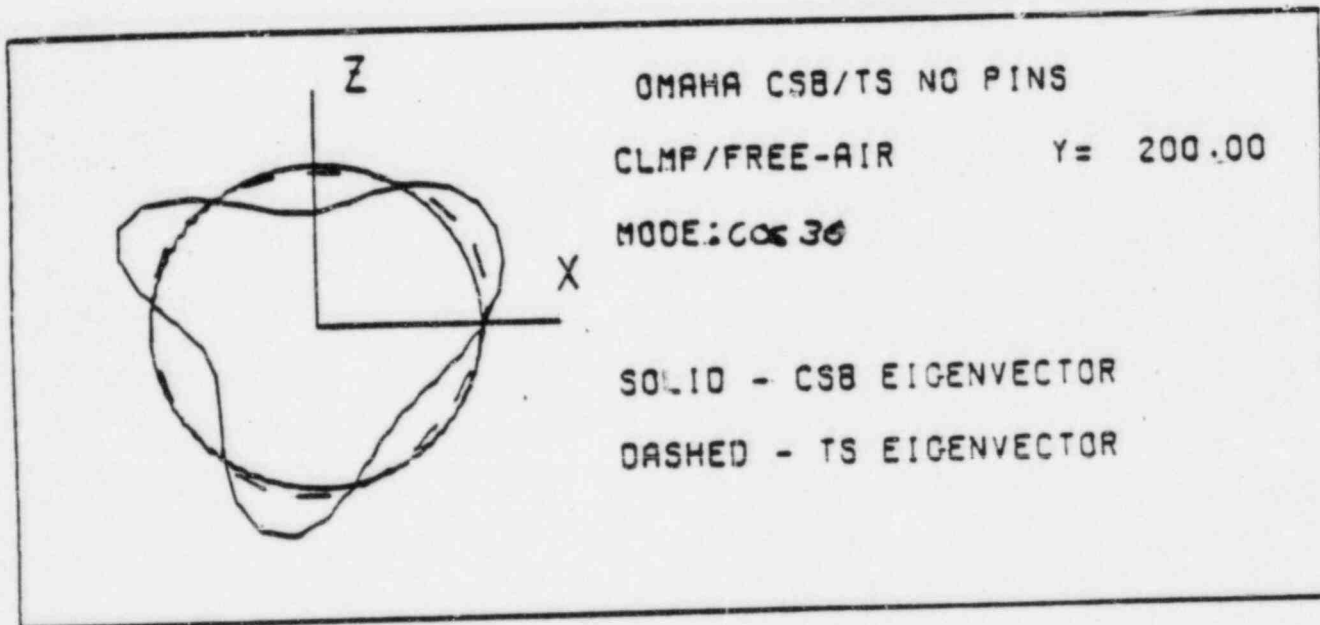
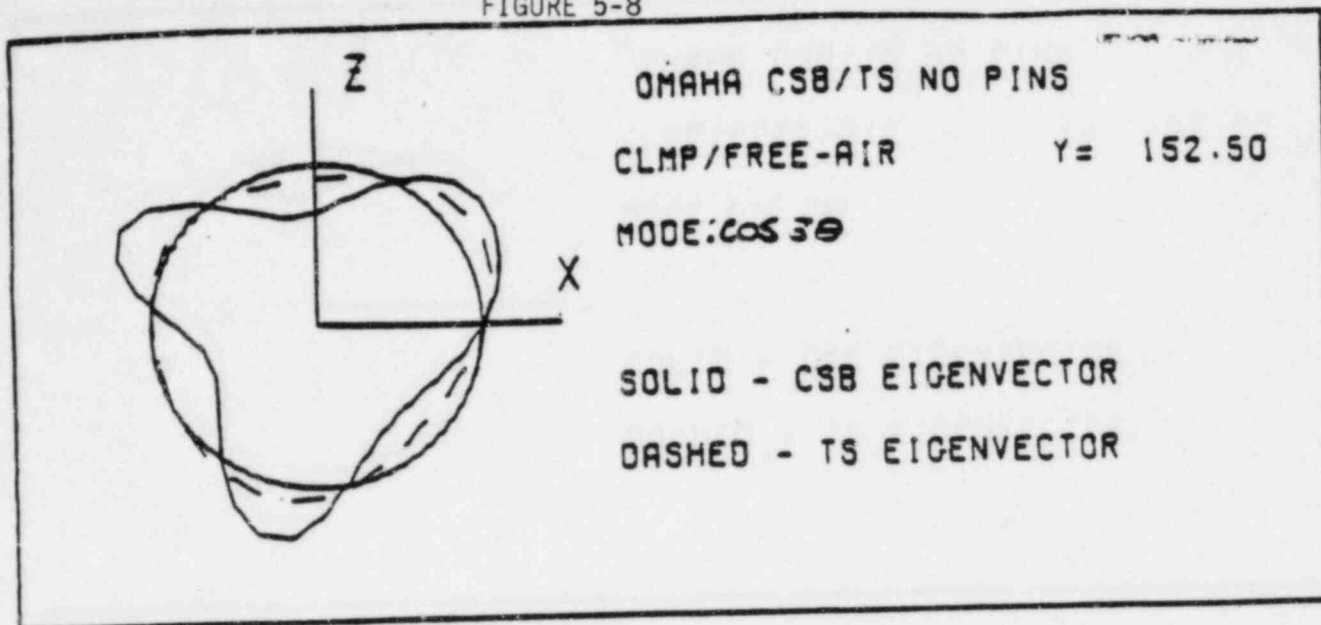


FIGURE 5-9

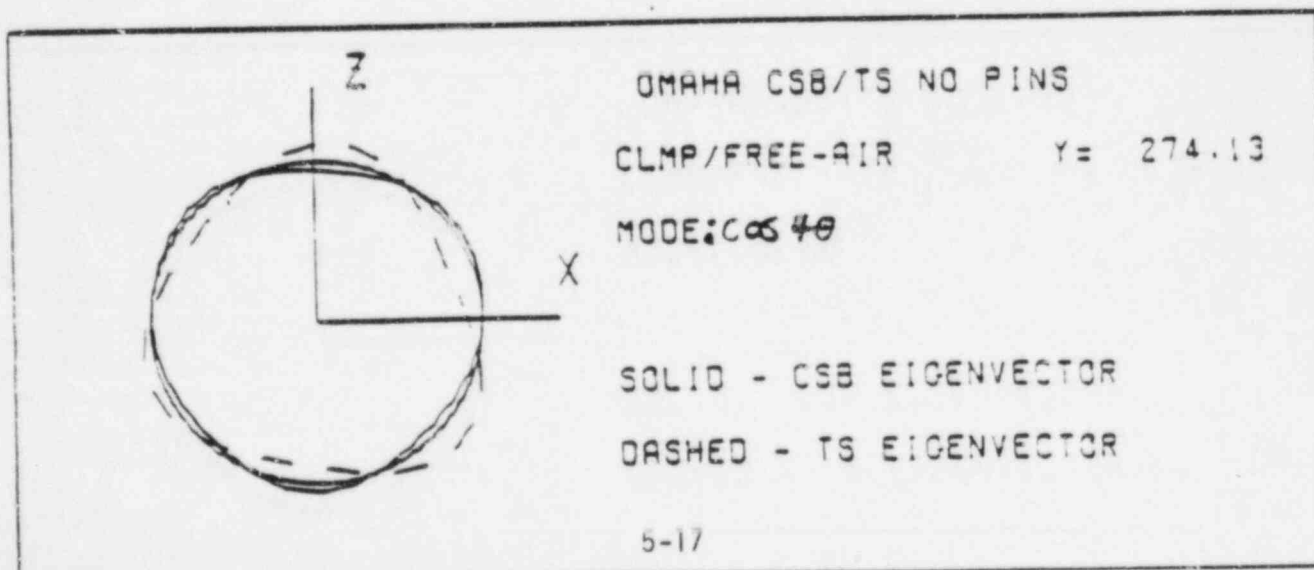
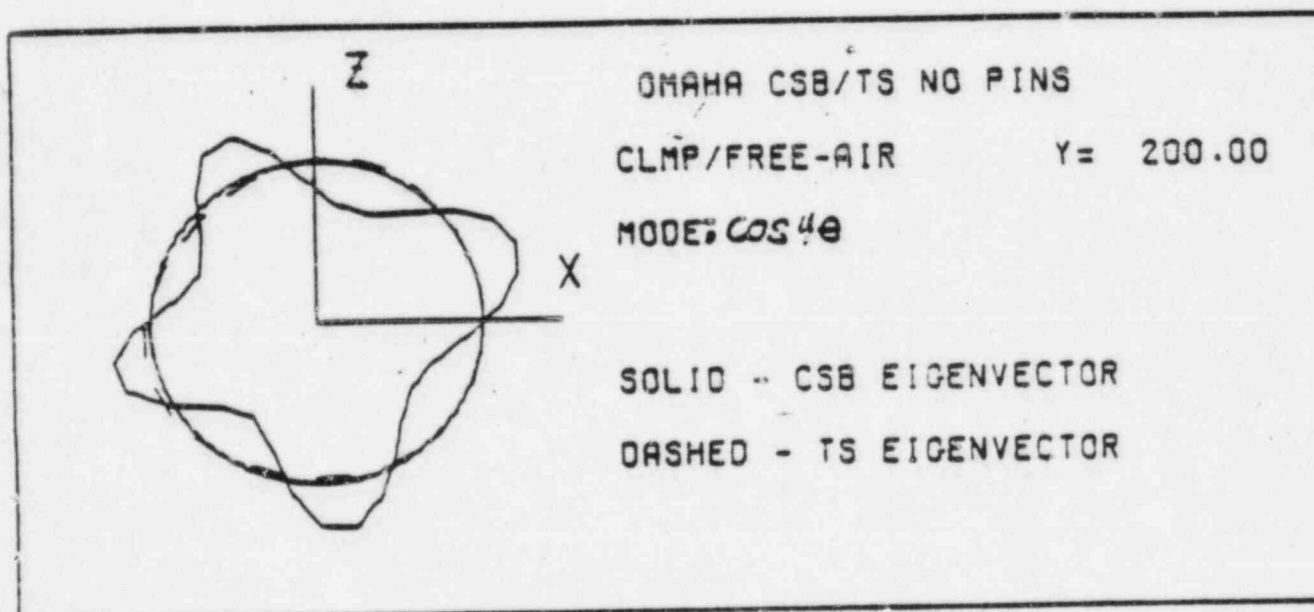
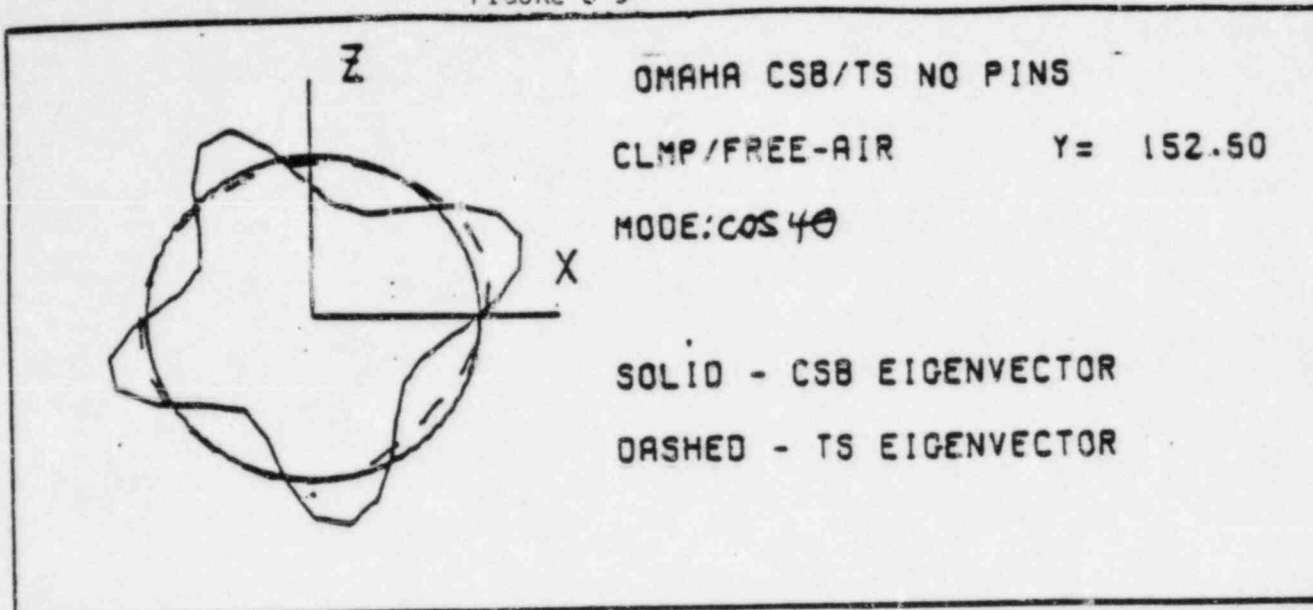
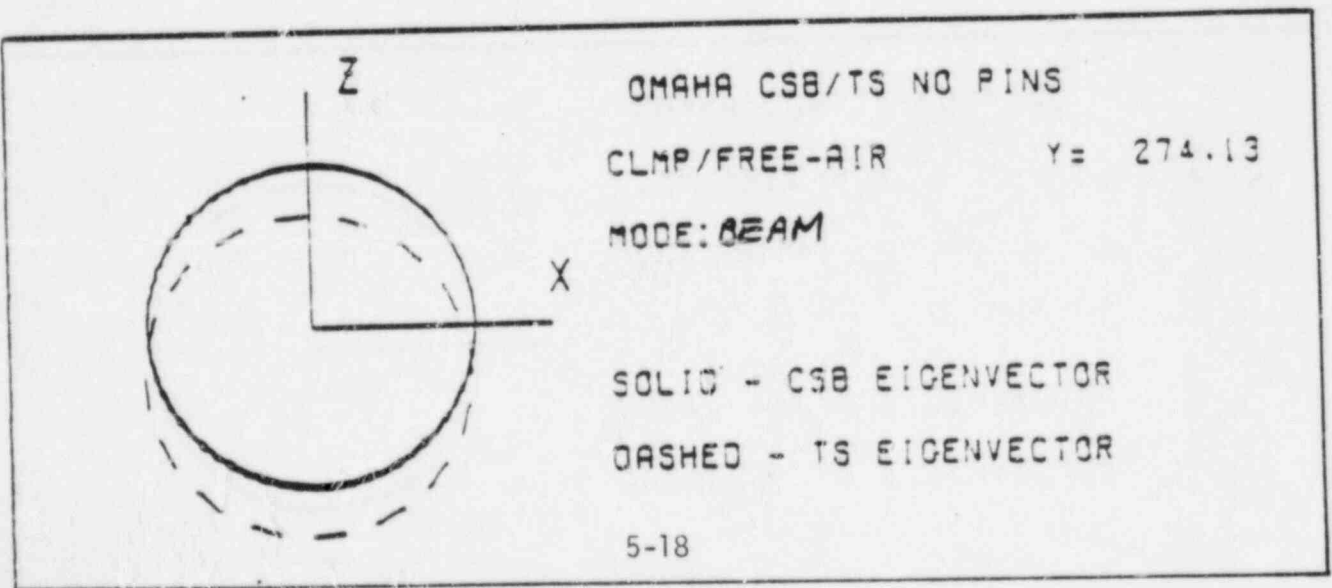
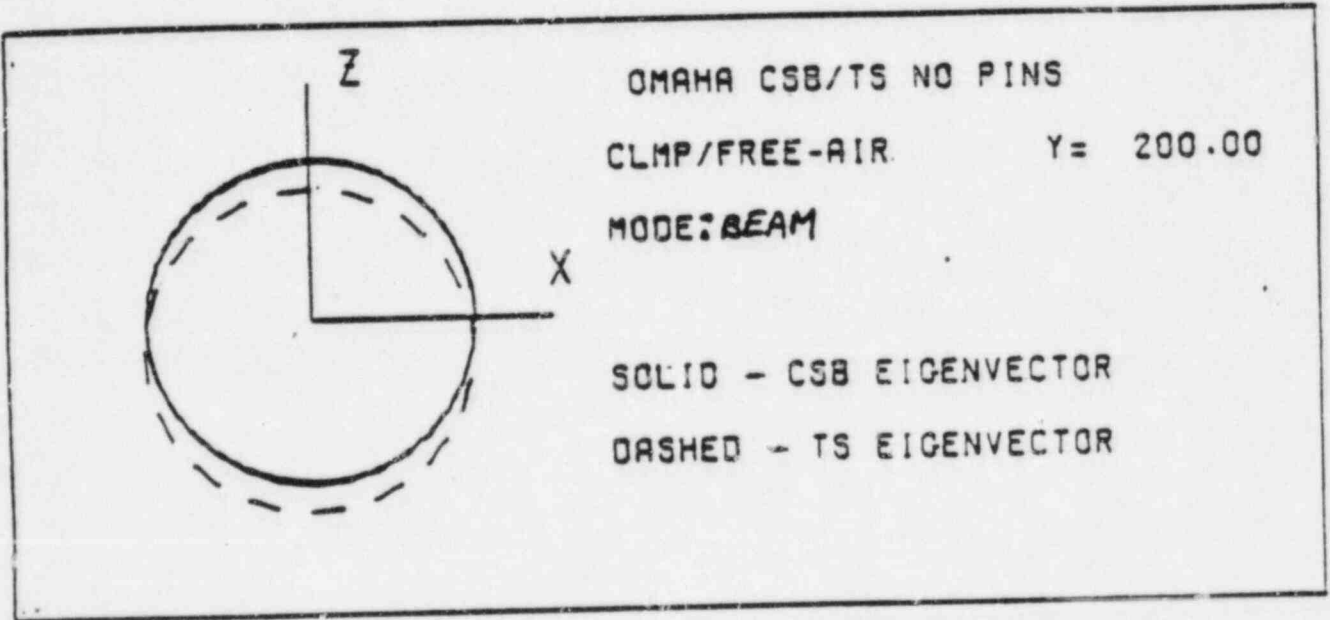
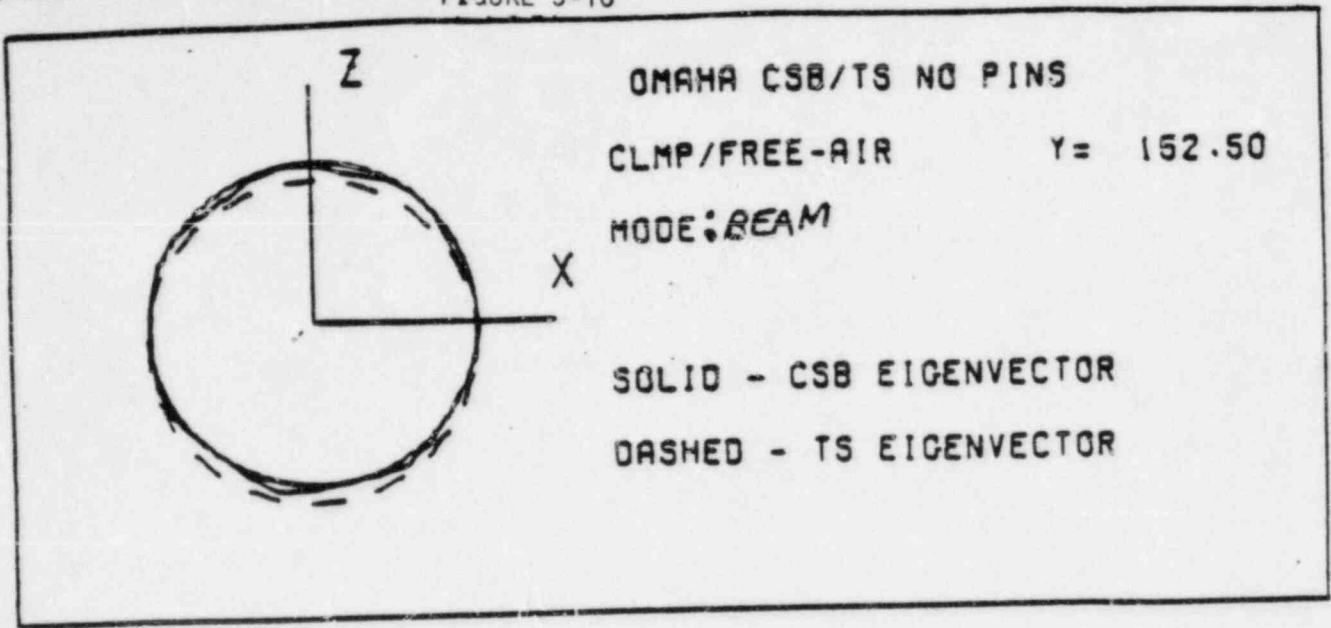
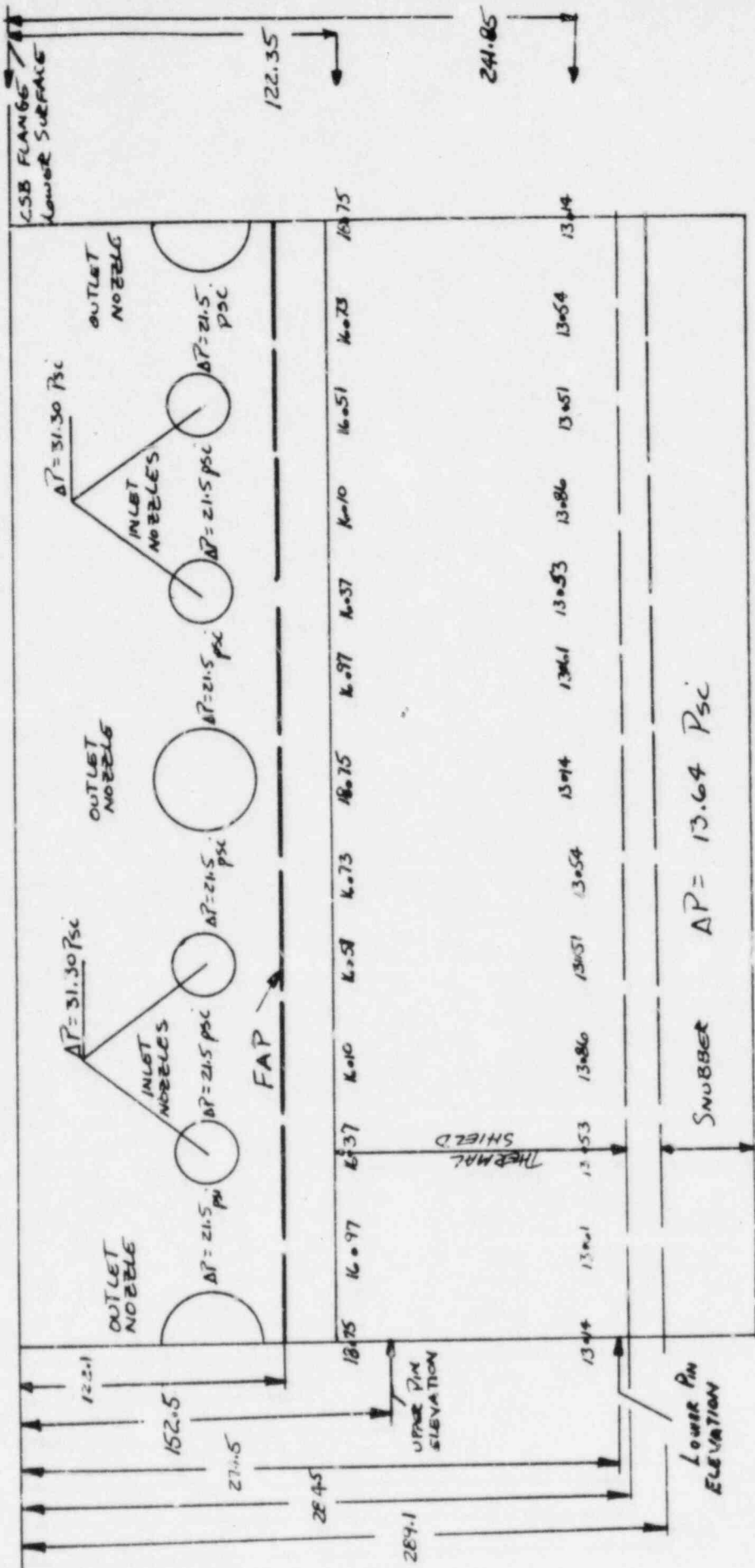




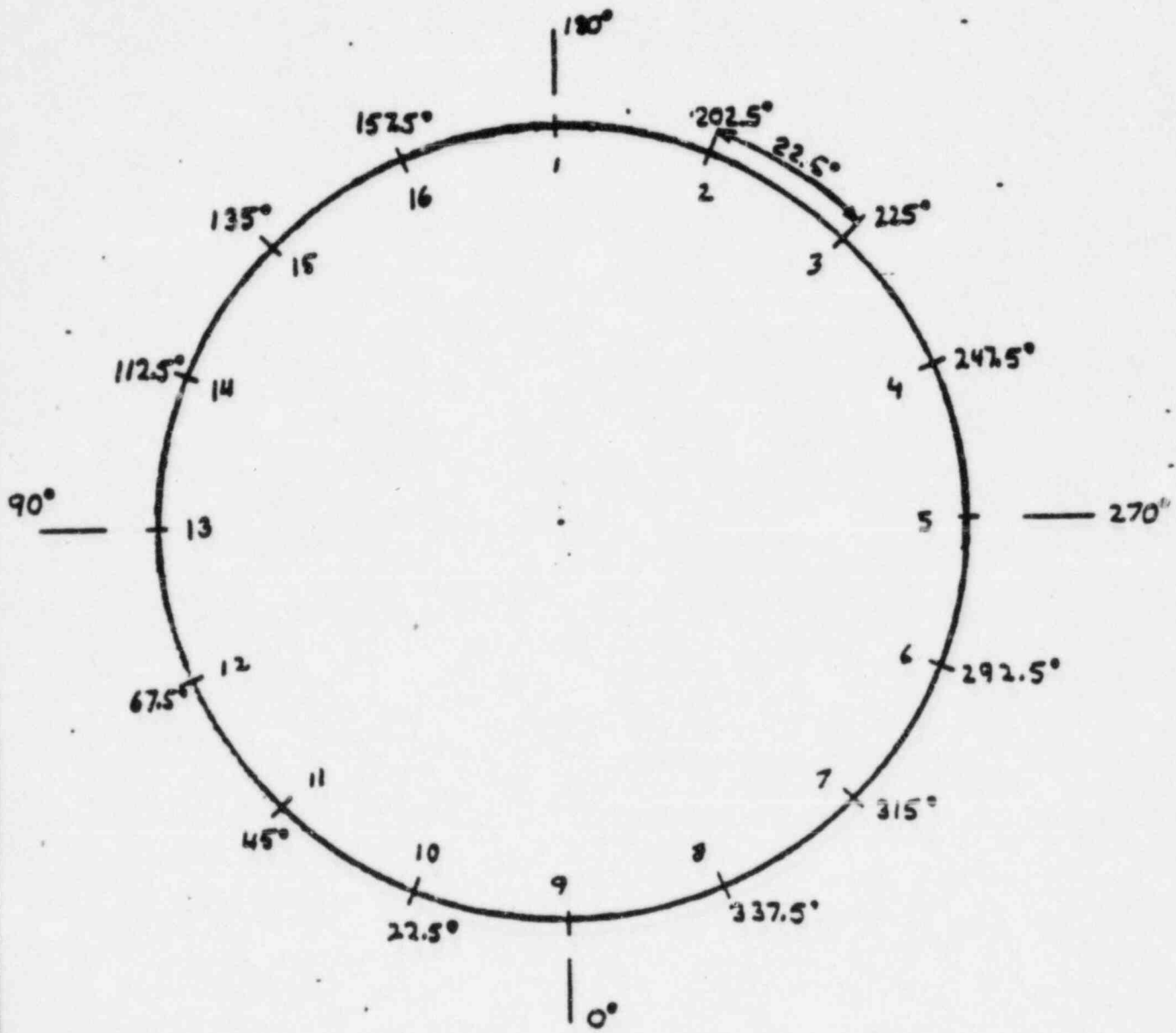
FIGURE 5-10





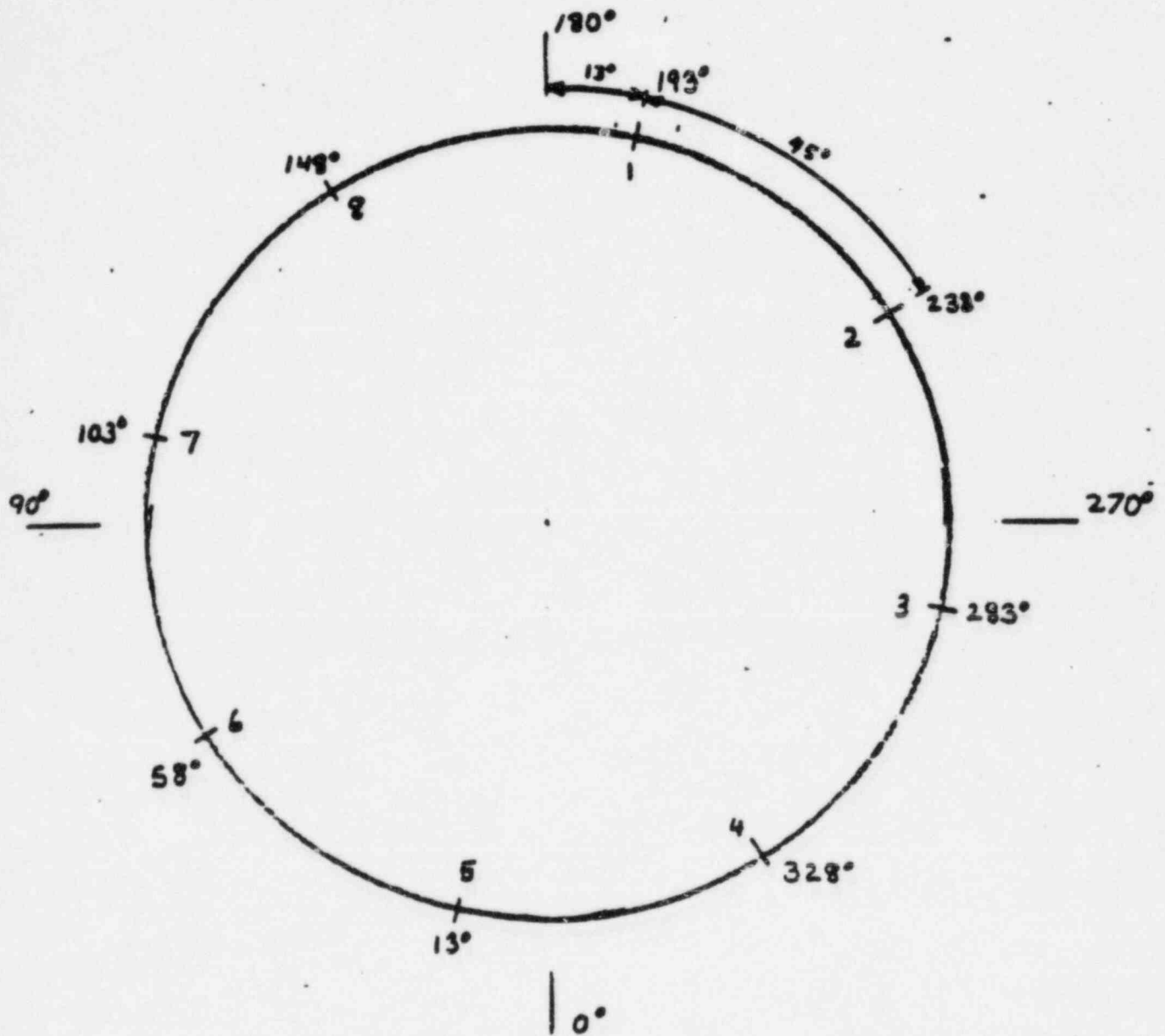
**OPERATING CONDITIONS :**  
 Power = 1500 MWt  
 T<sub>in</sub> = 545 °F  
 P = 2100 PSIA

CSB STEADY STATE PRESSURE DISTRIBUTION  
 FIGURE 5-11



LOWER POSITIONING PINS LOCATION/IDENTIFICATION  
 (REF. DWG. E-23866-164-019-06)

FIGURE 5-12



UPPER POSITIONING PINS LOCATION/IDENTIFICATION  
 (REF. DWG. E-23866-164-019-06)

FIGURE 5-13

## 6.0 REVIEW OF FORT CALHOUN OPERATIONAL DATA

### 6.1 PRECITICAL VIBRATION MONITORING PROGRAM

A comparison of the response levels of the reactor internals for Fort Calhoun, St. Lucie Unit 1, Maine Yankee and Millstone Unit 2 was performed. Response levels from both analytical predictions and Precritical Vibration Monitoring Program (PVMP) test results were compared. The comparison was concerned with dynamic response predictions and PVMP test results consisting of the following:

- 1) Dynamic Pressure Forcing Functions
- 2) CSB/TS Response Levels

#### 6.1.1 STRUCTURAL CHARACTERISTICS

The structural parameters used to describe the dynamic characteristics of the four plants having or previously having thermal shields are found in Table 3-2.

#### 6.1.2 DYNAMIC PRESSURE FORCING FUNCTIONS

The dynamic response of the CSB/TS system is due to two sources of excitation namely:

1. Random Turbulence
2. Acoustic Pump Pulsations

The random turbulence results from eddys being developed in the downcomer annulus due to the viscous fluid interacting with the CSB and Reactor Vessel (RV). An idealization of a turbulence power spectral density (PSD) is shown in Figure 6-1. Three factors contribute to the magnitude and frequency of this PSD. The magnitude is a function of kinetic head squared and distance traveled along the CSB. The frequency content is based on the physical eddy size which can be developed, i.e., a function of velocity and gap between CSB and RV. Table 6-1 gives the pertinent parameters for the plants of interest. Note that a small difference exists in the cut off frequency, but Fort Calhoun has substantially lower input forcing function as depicted by the kinetic head squared.

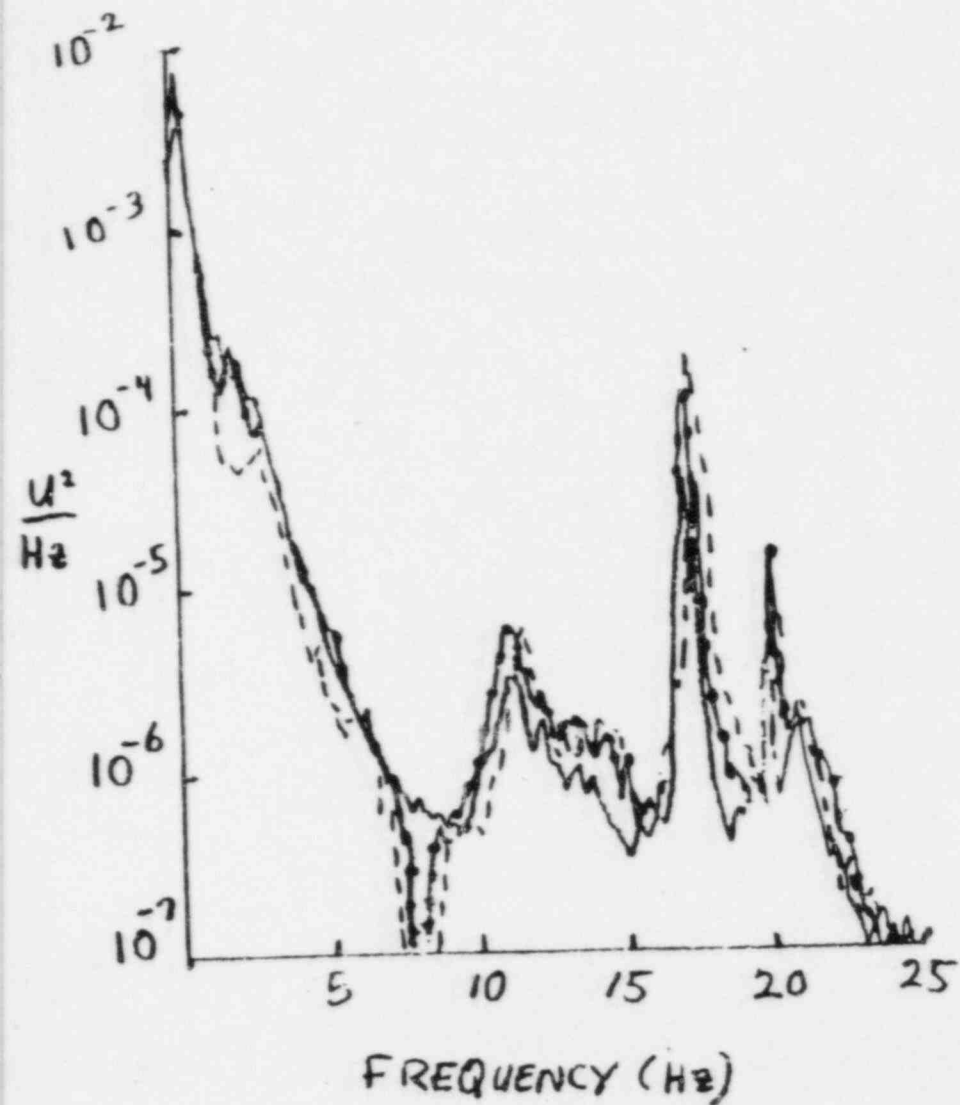
The acoustic pump pulsation loads are due to harmonic variations in fluid pressure caused by reactor coolant pumps. These pulsations propagate throughout the system as acoustic waves, independent of fluid velocity. The pulsations occur at multiples of the pump rotor speed and blade passing frequencies. The magnitude and spatial distribution of the pressure pulses are dependent on variations in the amplitude of the pump discharge pressure, phase difference between pumps, the number of pumps operating, geometry of flow path and the temperature dependent speed of sound in the liquid. A combination of mathematical analysis and empirical data are used to compute the magnitude, frequencies, and distribution of the deterministic loads caused by these pulsations.

### 6.1.3 CSB/TS RESPONSE LEVELS

A random response analysis of the CSB/TS for Fort Calhoun and Maine Yankee was performed. This analysis utilized a beam element model of the CSB/TS assembly in conjunction with measured pressure PSD's. This resulted in Root Mean Square (RMS) snubber location displacements of 3.6 mils for Maine Yankee and 0.8 mils for Fort Calhoun.

6-23

0° PHASE XPSD  $A_c \times B_c$



\_\_\_\_\_ 1985 (CYCLE 9)  
 -•-•-•- 1983 (CYCLE 8)  
 - - - - 1977 (CYCLE 3)



The random response is proportional to the kinetic head and inversely proportional to the square root of the frequency cubed. Using this in combination with the measured pressure PSD's the relative random responses of the four plants were determined, normalized to the Fort Calhoun response and presented in Table 6-2. The relative random RMS response for Fort Calhoun is less than for Maine Yankee, St. Lucie Unit 1 and Millstone Unit 2.

Pump pulsation response was also performed. This analysis used measured pump discharge pressures in conjunction with the analytical acoustic methodology. These measured pressures are given in Table 6-4. Note that Maine Yankee pressures are higher than Fort Calhoun. This analysis demonstrated a 3.5 to 1.0 ratio between Maine Yankee's maximum CSB stress with three pumps operating to Fort Calhoun's maximum CSB stress with four pumps operating. It is also noted that the majority of response occurs at the rotor frequency.

#### 6.1.4 PVMP RESULTS

A Precritical Vibration Monitoring Program (PVMP) was performed for Fort Calhoun and Maine Yankee. A full description of these programs can be found in Reference 6-1 for Fort Calhoun and Reference 6.2 for Maine Yankee. These programs consisted of analysis, measurements taken during hot functional testing and inspection of reactor internals before and after hot functional testing.

Comparison of the two PVMP reports indicates overall lower response levels for Fort Calhoun. Measured maximum random response for Fort Calhoun and Maine Yankee are 1.2 mils and 3.2 mils, respectively. Pump pulsation maximum stress both predicted and measured are given in Figure 6-2. It should be noted that the analytical predictions utilize the most severe pump phasing.

#### 6.1.5 SUMMARY AND CONCLUSIONS

As can be seen by the comparative data (Tables 6-1 through 6-3) between input forcing functions and response data the thermal shield support system for Fort Calhoun is less susceptible to degradation from flow induced vibration. This conclusion is supported by the following:

1. Random and deterministic pressure loads acting on the Fort Calhoun CSB/TS assembly are lower than corresponding values for Maine Yankee, St. Lucie Unit 1 and Millstone Unit 2.
2. CSB/TS system dynamic response to flow induced pressure loads is smaller for Fort Calhoun than that measured or predicted for Maine Yankee, St. Lucie Unit 1 and Millstone Unit 2.
3. The lower levels of dynamic response stress and displacement in Fort Calhoun, as compared to other plants, results in a higher structural integrity margin for the Fort Calhoun Thermal Shield Support System.
4. Measured values of stress and displacement are significantly lower than analytical predictions indicating the conservative nature of the analysis.

## 6.2 CORE SUPPORT BARREL AND THERMAL SHIELD VISUAL INSPECTION

### 6.2.1 INSPECTION OF THE REACTOR INTERNALS POST PRECRITICAL VIBRATION PROGRAM

The reactor internals and interfaces with the reactor vessel were inspected upon completion of the precritical vibration program in 1973. The thermal shield support system was inspected at the time and photographic documentation was obtained. The conclusion of the inspection was that there was no evidence of wear or deterioration of the thermal shield support system.

### 6.2.2 THERMAL SHIELD SUPPORT SYSTEM INSPECTION AT 10 YEAR ISI

Fort Calhoun was returned to service on April 7, 1983, following a refueling outage which included the 10-Year Inservice Inspection (ISI) of the reactor vessel and internal components. Part of this inservice inspection was a visual examination of the accessible portions of the core support barrel and thermal shield. The ISI plan included a visual inspection of all accessible sections of the core support barrel per ASME, Section XI, Table IWB-2500, Paragraph B-N-3, an inspection of points of attachment (core support barrel flange and snubbers) of the core support barrel to the reactor vessel, and an inspection of the core support barrel and thermal shield to determine the general condition after nearly 10 years of service. This inspection was performed by the District's ISI contractor, Southwest Research Institute, with assistance provided by OPPD engineers and QC technicians. As discussed in the following paragraphs, this inspection led to the conclusion that the reactor vessel and its internal components were in excellent condition.

Due to the concerns expressed by CE ADP Infobulletin 82-12, regarding the thermal shield positioning pin situation at Maine Yankee, emphasis was placed on the inspection of the accessible portions of the thermal shield

positioning pins, the locking collars and the lock welds. More than half of these positioning pins would have been examined in the course of the originally planned inspection, but it was decided to devote extra effort in this area to examine all of the pins where possible.

The core support barrel and upper guide structures were stored in a lower portion of the refueling cavity during the reactor vessel ISI. Although close clearances between the cavity structures and the core support barrel prevented a thorough inspection of all surfaces, snubbers positioning pins, etc.; sufficient inspections were performed to determine that the core support barrel and thermal shield were in excellent condition. The detailed results of the Fort Calhoun thermal shield and core support barrel visual inspections are listed below.

The heads of all upper and lower positioning pins were inspected. All pins, locking collars and lock welds were verified to be intact. No evidence of motion or cracking was noted.

Three of the six snubber assemblies on the core support barrel were visually inspected. No evidence of wear or abnormal motion between the core support barrel and the reactor vessel was noted. All six of the reactor vessel portions of the snubbers were examined with no deterioration found.

Four of the eight shield support lugs were examined with no evidence of deterioration noted. The inspection of the lugs, support pins, fillet welds, and shims showed no abnormalities.

More than 180° of the core support barrel upper to lower shell weld was examined with no indications found.

More than 180° of the core support barrel to flange weld was examined. Again, no indications were noted.

One outlet (hot leg) nozzle was examined. There were no indications of wear between this nozzle and the corresponding nozzle in the reactor vessel.

The accessible portion of the points of attachment of the core support barrel flange to the reactor vessel were examined. Again, no indications of abnormal motion were found.

The visual inspection of the reactor vessel showed no indications of abnormal motion of the core support barrel at the flange support lugs or at the outlet (hot leg) nozzles.

As a result of this visual inspection of the core support barrel and thermal shield, the District and its ISI contractor have concluded that these reactor vessel components were in excellent condition.

Video tape of the areas of the thermal shield support system inspected was provided to Combustion Engineering for an additional review. The C-E review of the tape did not produce an indication of detectable degradation of the thermal shield support system.

In summary, no evidence was found which would indicate that the types of degradation which have been experienced at Maine Yankee, St. Lucie Unit 1 and Millstone Unit 2, was occurring at Fort Calhoun.

### 6.3 Internals Vibration Monitoring (IVM)

Ft. Calhoun has had an ongoing excore neutron detector signal monitoring program. A review and summary of full power neutron noise data acquired at the Ft. Calhoun plant during the period 1974-1986 has been completed. In addition utilizing this information the current condition of the thermal shield supports were assessed.

The objectives of the data evaluations were to determine changes in the excore signals and if such changes could be associated with the structural condition of the thermal shield support system. Recent (May, 1986) excore neutron detector signal data acquired during the current fuel cycle is analyzed and compared to previous data to assess if there have been any recent indications of changes in the thermal shield support system. Natural frequencies for the coupled CSB - thermal shield structure for both nominal and degraded thermal shield support conditions have been calculated to augment the data evaluation in determining a degradation in the thermal shield support system. See Section 5 for additional details.

#### 6.3.1 Data Evaluation

The arrangement of the excore detectors is shown in Figure 6-3. The evaluation was done for cross core detector pairs  $B_S, C_S$  and  $A_C, B_C$ . These results include auto and cross power spectral densities, coherence and phase. Phase separation techniques were also used to separate the cross power spectral densities of each pair of detectors into their in - ( $0^\circ$ ) and out-of-phase ( $180^\circ$ ) components. In summarizing the available neutron data, the phase separated cross power spectral densities and coherences were used since they most clearly define the characteristics of the frequency peaks. Data from fuel cycles 3 (1977), 8 (1983), 9 (1985) and 10 (1986) were used in the evaluation summary for the following reasons:

- 1) Evaluation of St. Lucie Unit 1 neutron noise data showed that indications of thermal shield support degradation began appearing after cycle 3.
- 2) Ft. Calhoun data obtained prior to cycle 3 included the effects of the original hold down ring which was replaced in 1976. (Note holddown ring replacement was to provide additional margin on reactor internals holddown and has no relation to structural integrity of the thermal shield support system).
- 3) Cycle 3 and cycle 4 data are similar; for clarity in the comparisons presented, only cycle 3 data is used.
- 4) Cycles 8, 9 and 10 data were obtained after a 10-year Inservice Inspection (ISI) concluded that the CSB, thermal shield and the thermal shield support lugs that were examined were all in excellent condition (Reference 6-3). Since no problems were detected during the 10-year ISI, cycle 8 data, which immediately followed the ISI, could be considered new baseline data for a structurally sound thermal shield support system.
- 5) Cycles 9 and 10 data would be indicative of recent changes, if any, in the thermal shield support system.

Figures 6-4 to 6-15 present comparisons of neutron noise data obtained from 1977-1986 (fuel cycles 3, 8, 9 and 10). Figures 6-4 to 6-9 compare data from fuel cycles 3, 8 and 9. Figures 6-10 to 6-15 compare data from fuel cycles 9 and 10.

For cross core detector pair Bs x Cs, Figure 6-4 compares the 0° phase separated XPSD, Figure 6-5 compares the 180° phase



separated XPSD and Figure 6-6 compares the coherence. Figures 6-7 to 6-9 present similar comparisons for cross core detector pair Ac x Bc. For cycles 9 and 10, a similar set of comparisons are presented in Figures 6-10 to 6-15.

Table 6-4 presents a summary of analytically derived in-water modal frequencies for the coupled CSB - thermal shield structure. A review of Table 6-4 indicates loosening of positioning pins is indicated by a reduction of the first shell mode (COS 2 $\theta$ ) frequency. Therefore, evaluation of the excore neutron signals focuses on significant shifts in frequency peaks at 12.5 Hz.

Comparing the spectra in Figures 6-4 to 6-15 indicates the major peaks over the entire 0-25 Hz frequency range are consistent among the sets of data. The coherence shown in Figures 6-6 and 6-9 indicate differences below 5 Hz. Frequencies below 7 Hz are not associated with CSB - thermal shield structural characteristics (see Table 6-4). These differences as well as the shifts in amplitude of the spectra can be attributed to boron concentration as a function of core burn-up and changes in the composition of the core, i.e., C-E fuel versus EXXON fuel, between fuel cycles. Table 6-5 gives the chronology of each fuel cycle, core composition and the date the neutron noise data was acquired.

The comparisons shown in Figures 6-10 to 6-15 for cycles 9 and 10 demonstrate a consistency in frequency peaks which extends below 5 Hz. This is due primarily to the similar composition of the core between cycles 9 and 10 (see Table 6-5). The higher amplitudes in the cycle 9 versus the cycle 10 data is due to the fact that the cycle 9 data was acquired later in the fuel cycle. Resulting differences in boron concentrations produce higher amplitudes in the neutron noise spectra.

Comparing the peaks and phases of the spectra presented in Figures 6-4 to 6-15 with the analytically derived frequencies in Table 6-4 identifies the following CSB - thermal shield frequencies in the excore data:

- 1) Beam bending mode occurs at 7.5 Hz.
- 2) First shell mode (COS 20) occurs at 12 Hz.

The comparisons among cycles 3, 8, 9 and 10 indicate no frequency shifts of these two peaks. Specifically the first shell mode, the 0° - phase separated XPSD peak at 12 Hz, has remained consistent from 1977 to 1986.

Reference 6-4 analyzes neutron noise data from several plants and searches for systematic changes in the neutron noise which would indicate degradation of the thermal shield supports. Reference 6-4 evaluated Fort Calhoun neutron noise data for only cycle 4. In addition to the use of a limited amount of data, Reference 6-4 employed a finite element vibration analysis of a model which was not representative of the Ft. Calhoun CSB - thermal shield structure and therefore did not allow proper evaluation of the data.

### 6.3.2 Conclusions

Comparisons of the full power neutron noise data from 1977 - 1986 indicates no significant spectra changes have occurred in the frequency range associated with the CSB - thermal shield system. Specifically, no reduction in the first shell mode frequency has occurred. Analysis of neutron noise data acquired during the current fuel cycle has shown no shifts in frequency peaks. Therefore, based on excore neutron signal evaluations, thermal shield support system conditions have not degraded at full power conditions.

TABLE 6-1

## TURBULENCE PARAMETERS

	KINETIC HEAD			
	V (Ft/Sec.)	$\frac{(P V^2)^2}{2}$ (PSI) <sup>2</sup>	GAP (IN.)	CUT OFF FREQUENCY $f_t = \frac{V}{\lambda}$ (Hz)
OMAHA	27.5	13.3	7.8	42.1
ST. LUCIE	30.3	19.8	9.5	38.3
MILLSTONE	29.9	19.8	9.5	38.3
M.Y.	30.1	19.1	9.5	37.9

TABLE 6-2

RELATIVE RANDOM R.M.S. RESPONSE

	OMAHA	M.Y.	NE/ST. LUCIE
RMS DISPLACEMENT	1.0	1.20	1.3

TABLE 6-3

## INLET PRESSURES

	OMAHA	MAINE YANKEE
PUMP FREQUENCY (20 Hz)	.063 psi	.09 psi
PUMP HARMONIC (40 Hz)	.021 psi	.11 psi
BLADE PASSING FREQ. (100 Hz)	.096 psi	.35 psi
BLADE HARMONIC (200 Hz)	.12 psi	.18 psi

TABLE 6-4

PREDICTIONS OF IN-WATER MODAL FREQUENCIES (HERTZ)

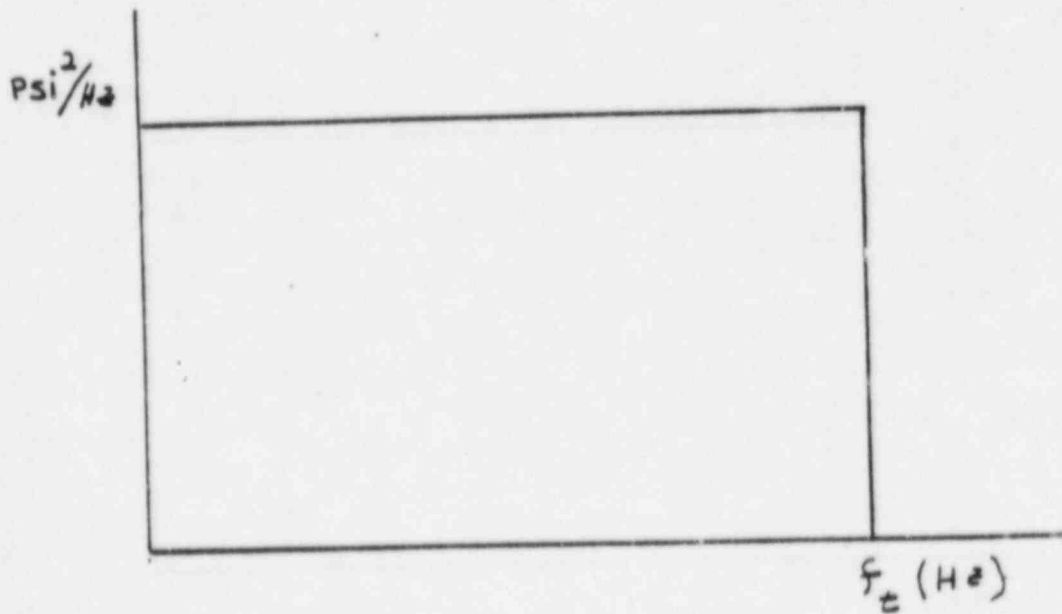
	Mode	Cross-Core Phase	Nominal	All Pins Removed
1.	Beam	180°	7.0	7.0
2.	cos 2θ	0°	12.5	7.9
3.	cos 3θ	180°	16.3	14.9
4.	cos 4θ	0°	22.8	22.0

TABLE 6-5

OPPD FUEL CYCLE CHRONOLOGY

Cycle No.	BOC	EOC	CORE COMPOSITION		NEUTRON NOISE DATA ACQUISITION
			<u>CE</u>	<u>EXXON</u>	
1	8/13/73	2/8/75	100%	0%	
2	5/4/75	10/1/76	100%	0%	
3	12/10/76	9/30/77	100%	0%	5/16/77
4	11/29/77	10/14/78	100%	0%	
5	12/15/78	1/18/80	100%	0%	
6	6/8/80	9/6/81	70%	30%	
7	12/21/81	12/3/82	33%	67%	
8	4/2/83	3/4/84	22%	78%	10/83
9	7/8/84	9/28/85	3%	97%	5/22/85
10	1/9/86		9%	91%	5/28/86

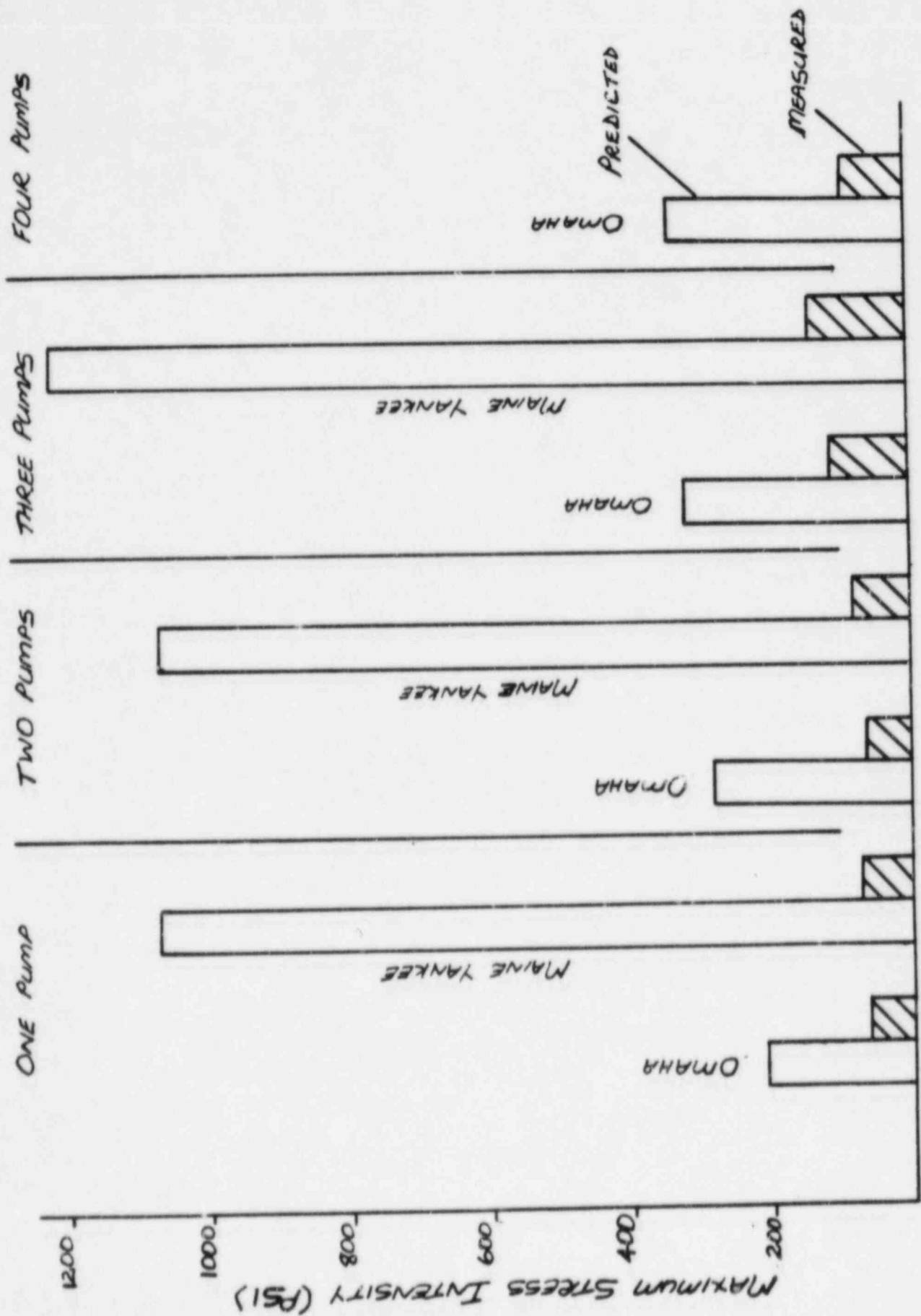




IDEALIZED RANDOM PSD

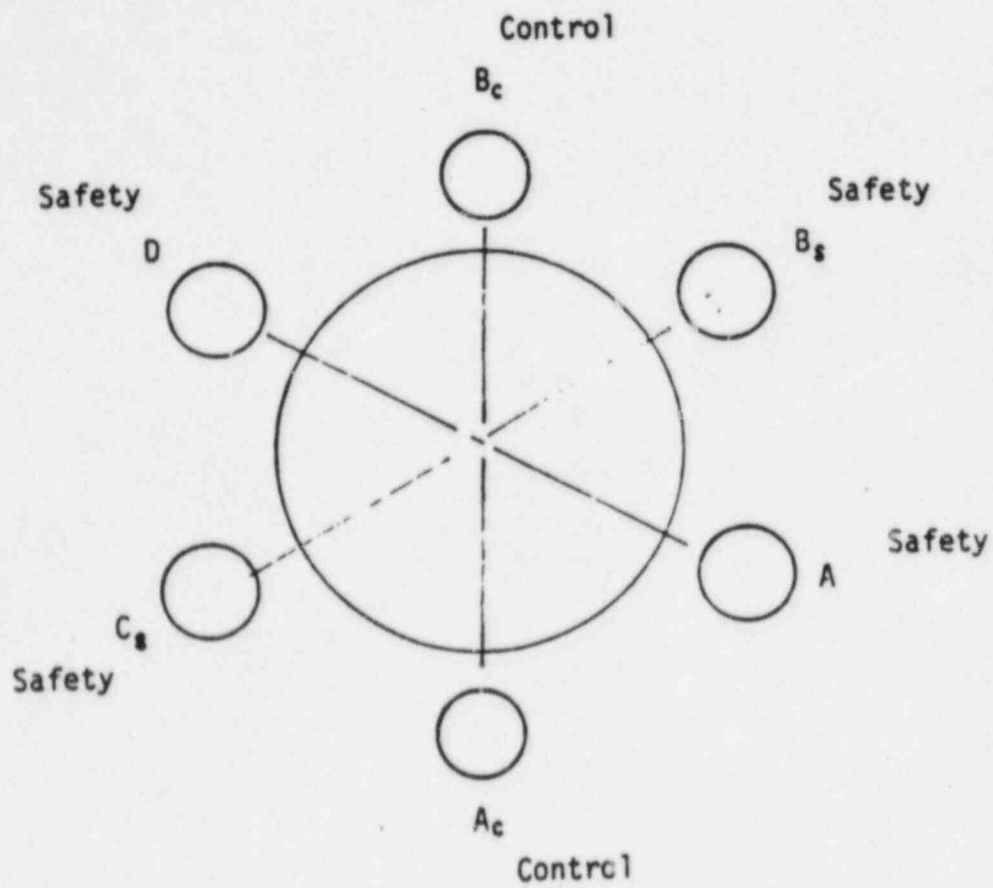
FIGURE 6-1

6-17



PREDICTED & MEASURED STRESS IN OMAHA & MAINE YANKEE (REL. 1)

FIGURE 6-2



FT. CALHOUN EXCORE DETECTOR LOCATIONS

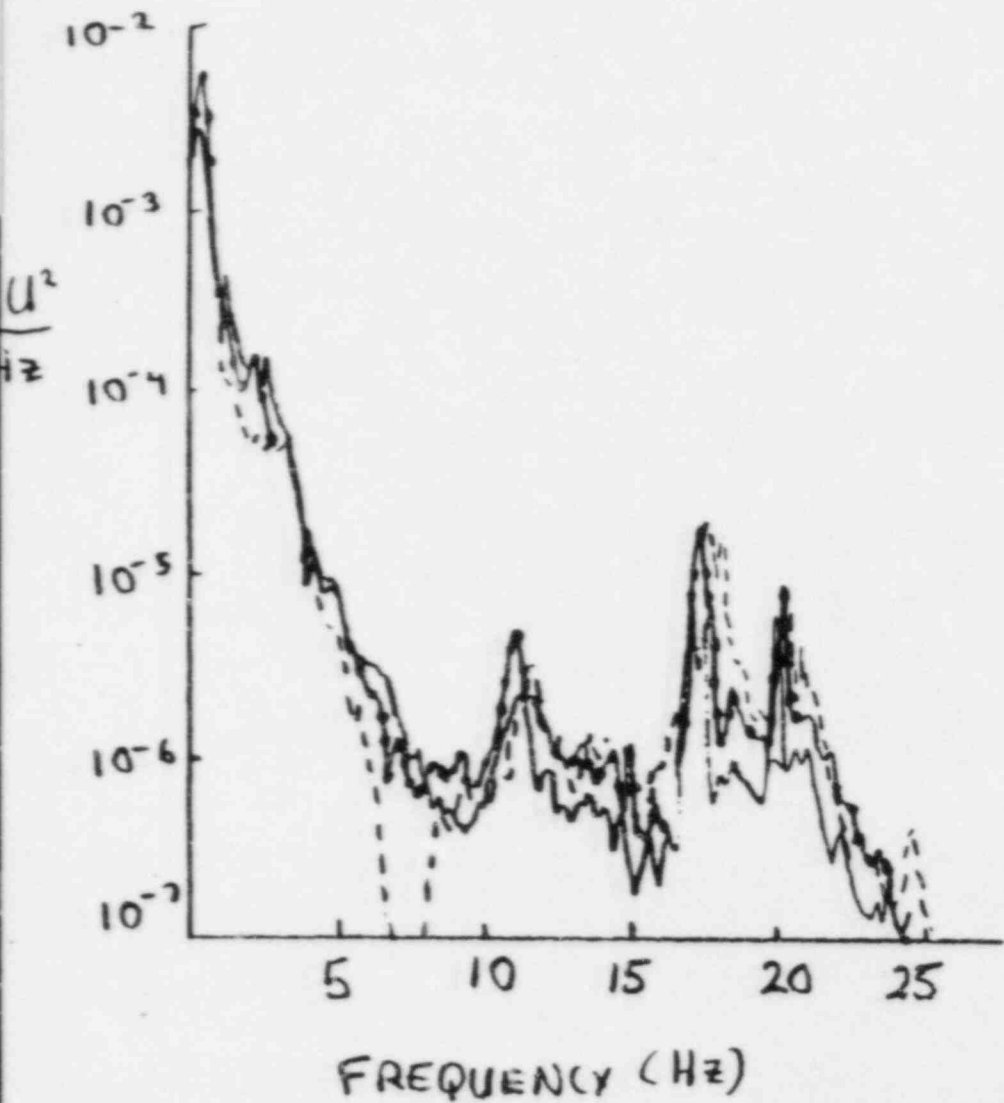
FIGURE 6-3

FIGURE 6-4

6-20

0°-PHASE XPSD

$B_s \times C_s$



— 1985 (CYCLE 9)  
—••• 1983 (CYCLE 8)  
- - - 1977 (CYCLE 3)

FIGURE 6-5

180°- PHASE XPSD

$B_5 \times C_5$

6-21

- 1985 (CYCLE 9)
- 1983 (CYCLE 8)
- - - 1977 (CYCLE 3)

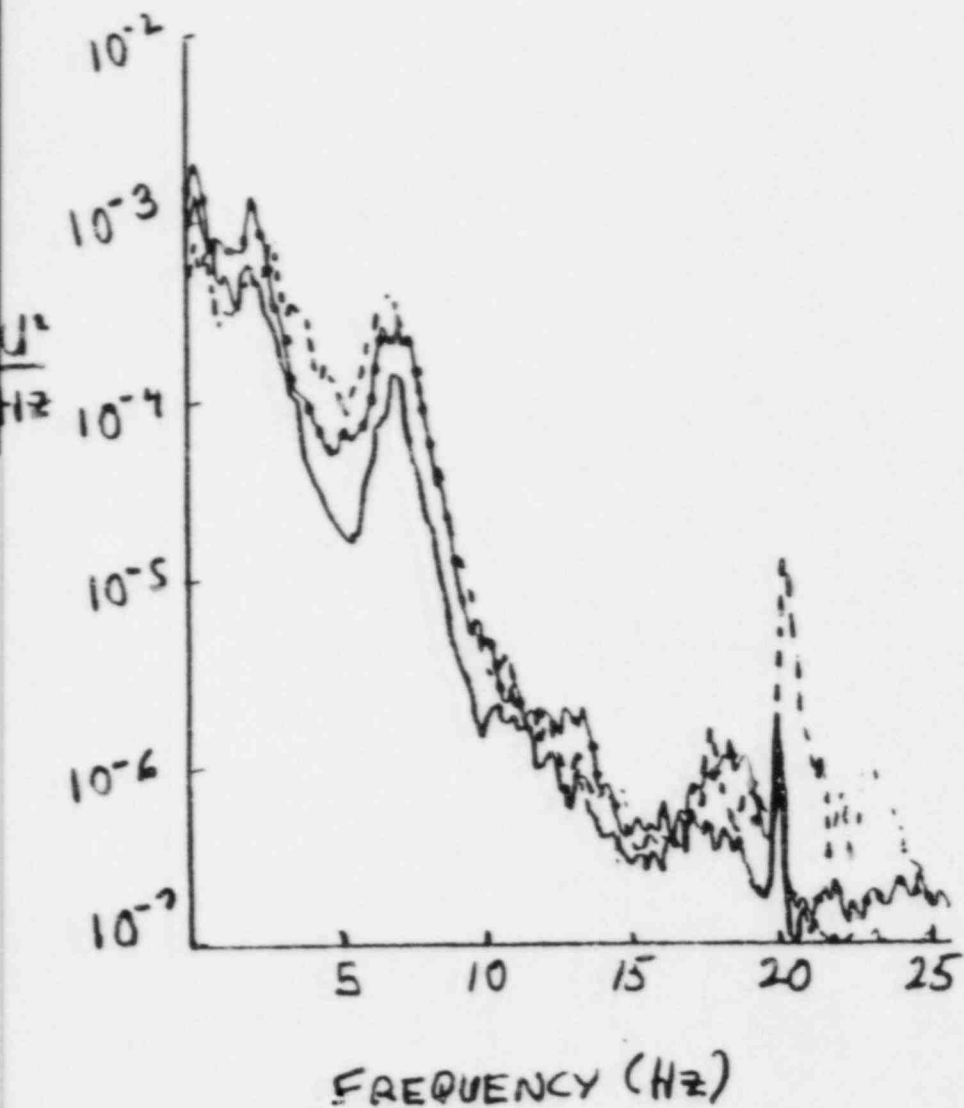
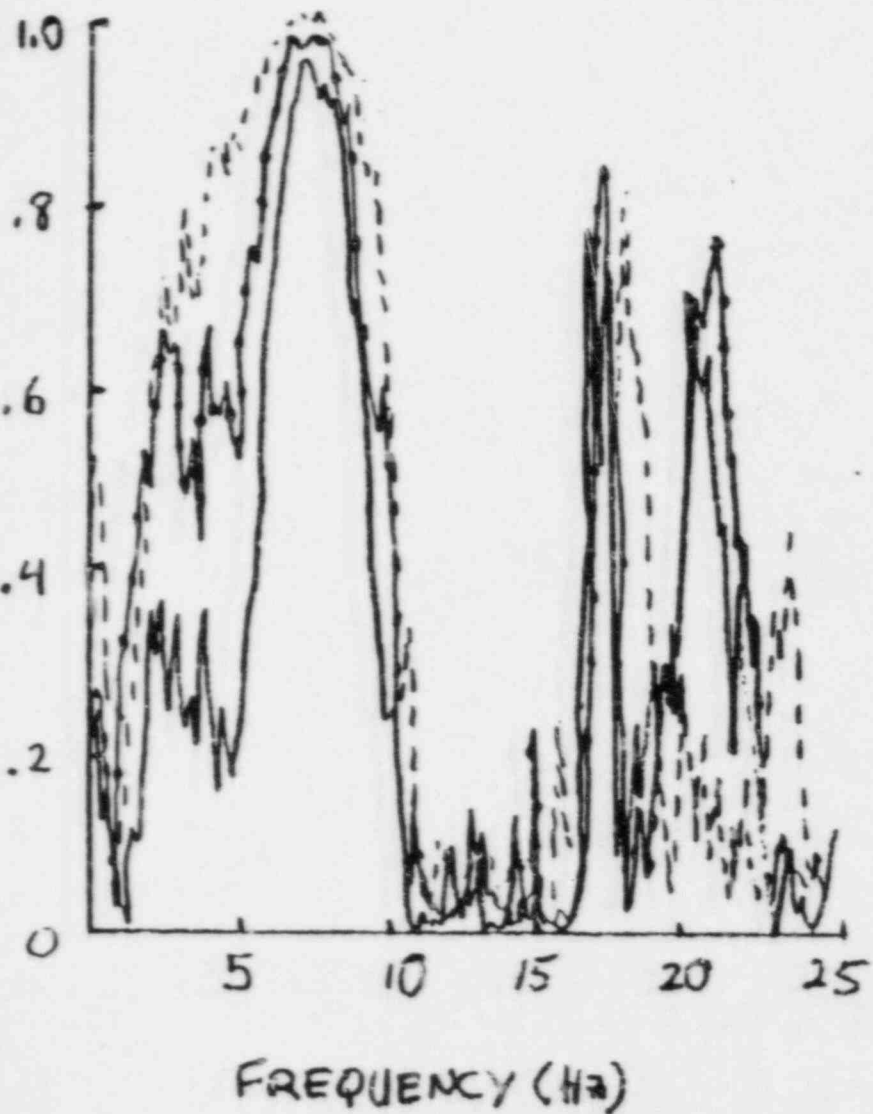


FIGURE 6-6

6-22

COHERENCE  $B_5 \times C_5$



- 1985 (CYCLE 9)
- 1983 (CYCLE 8)
- - - 1977 (CYCLE 3)

FIGURE 6-8

6-24

180°-PHASE XPSD  $A_c \times B_c$

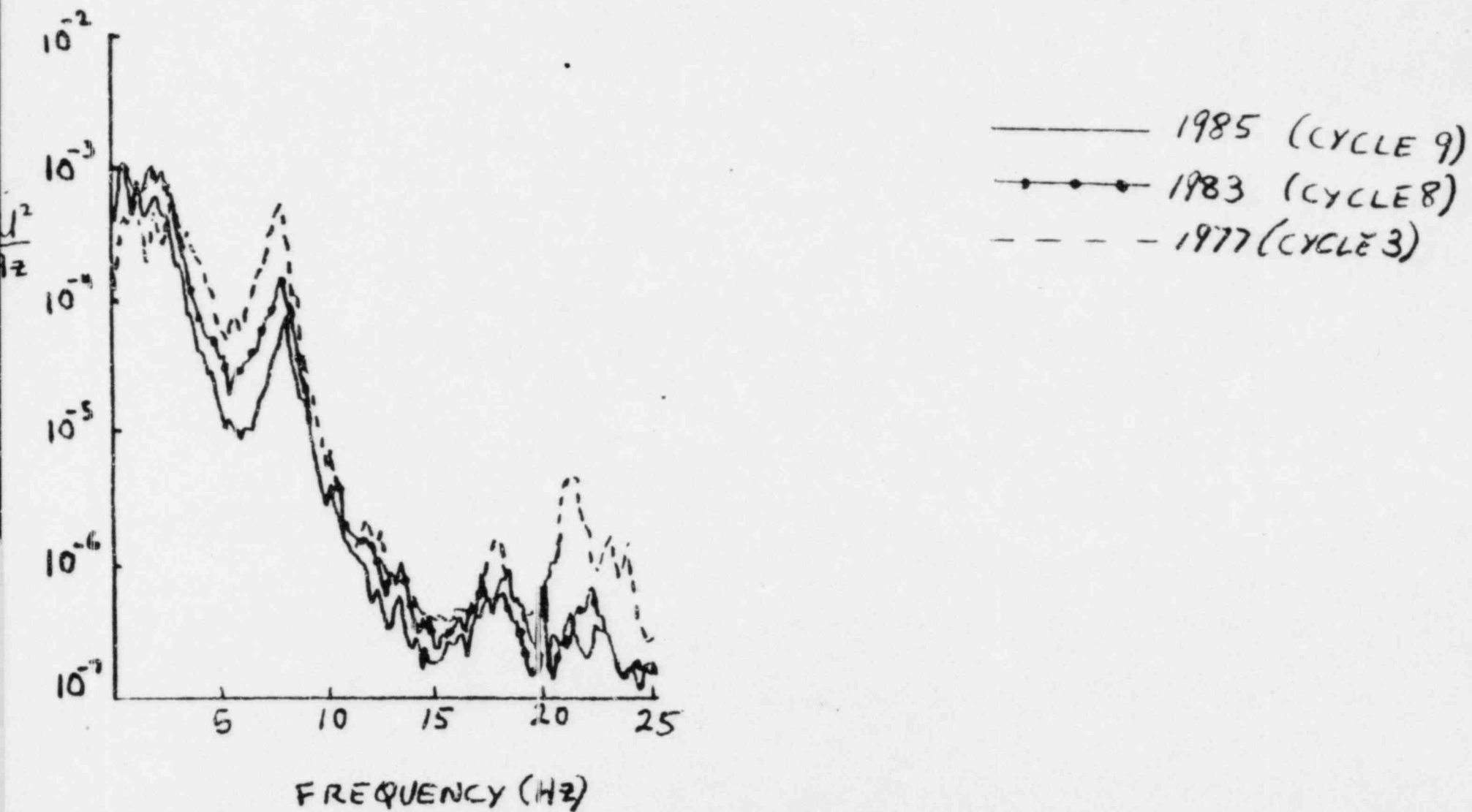




FIGURE 6-9

6-25

COHERENCE  $A_c \times B_c$

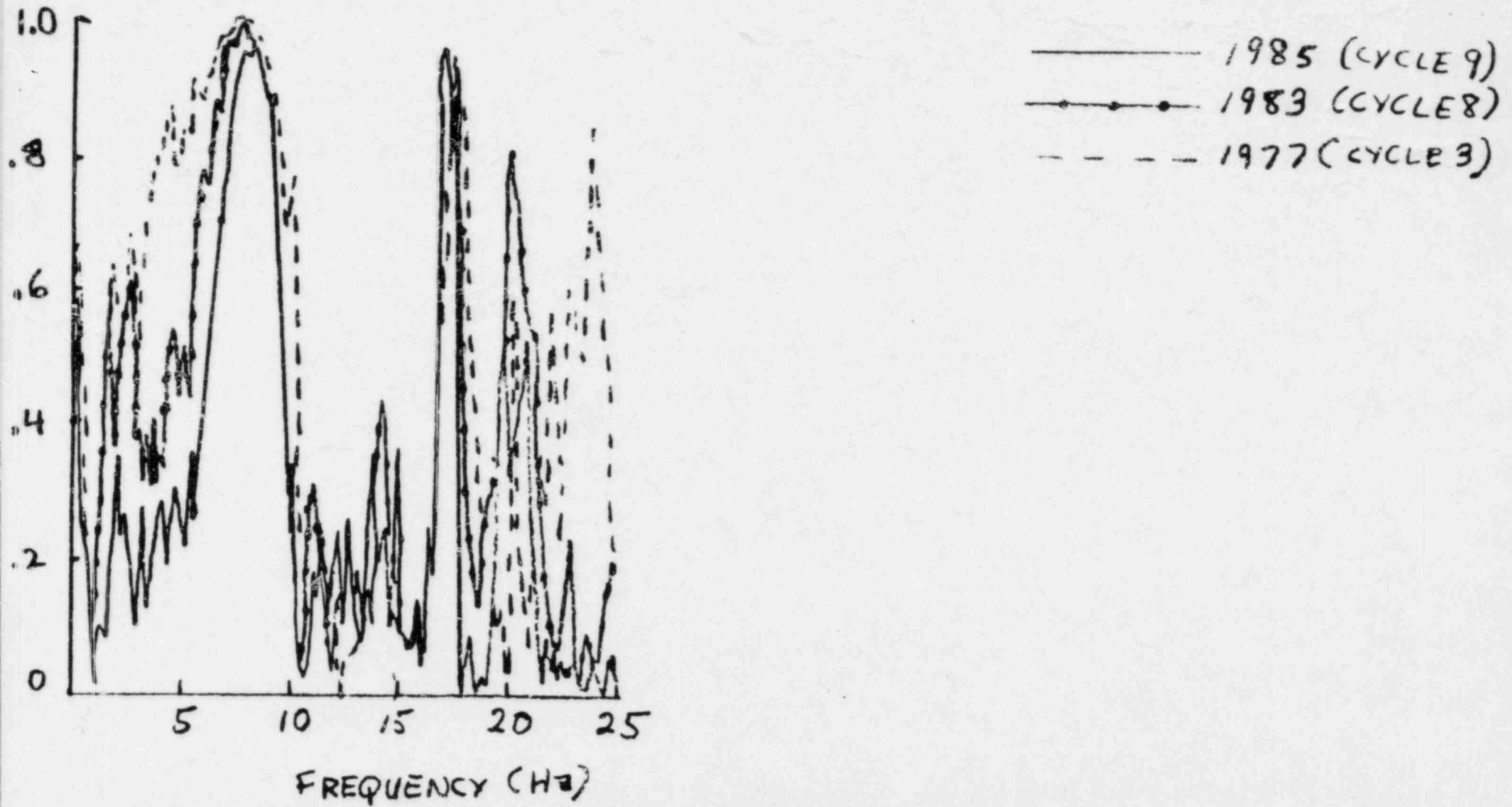


FIGURE 6-10

6-26

0°- PHASE x PSD

$B_s \times C_s$

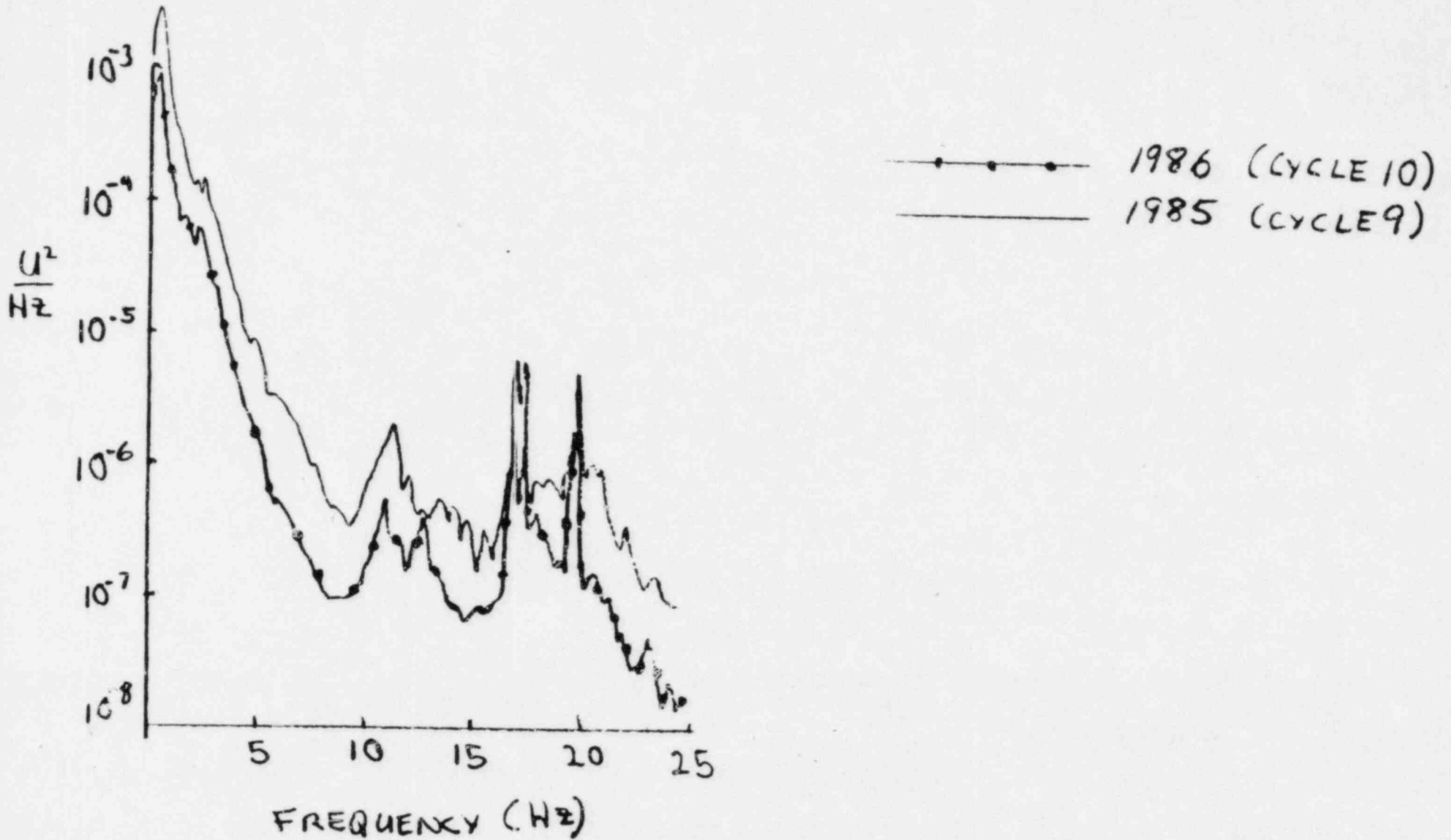
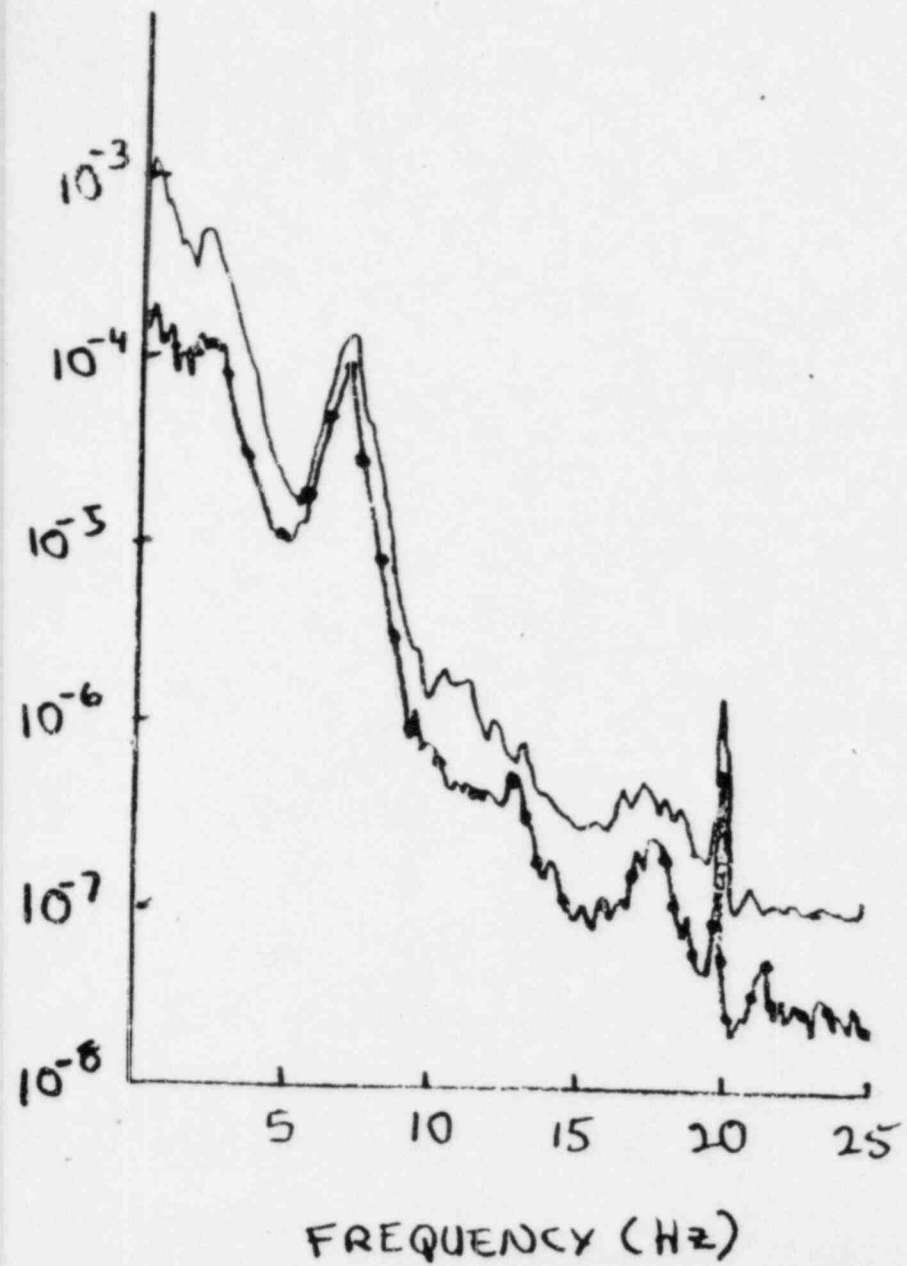


FIGURE 6-11

180°-PHASE XPSD

$B_5 \times C_5$

6-27

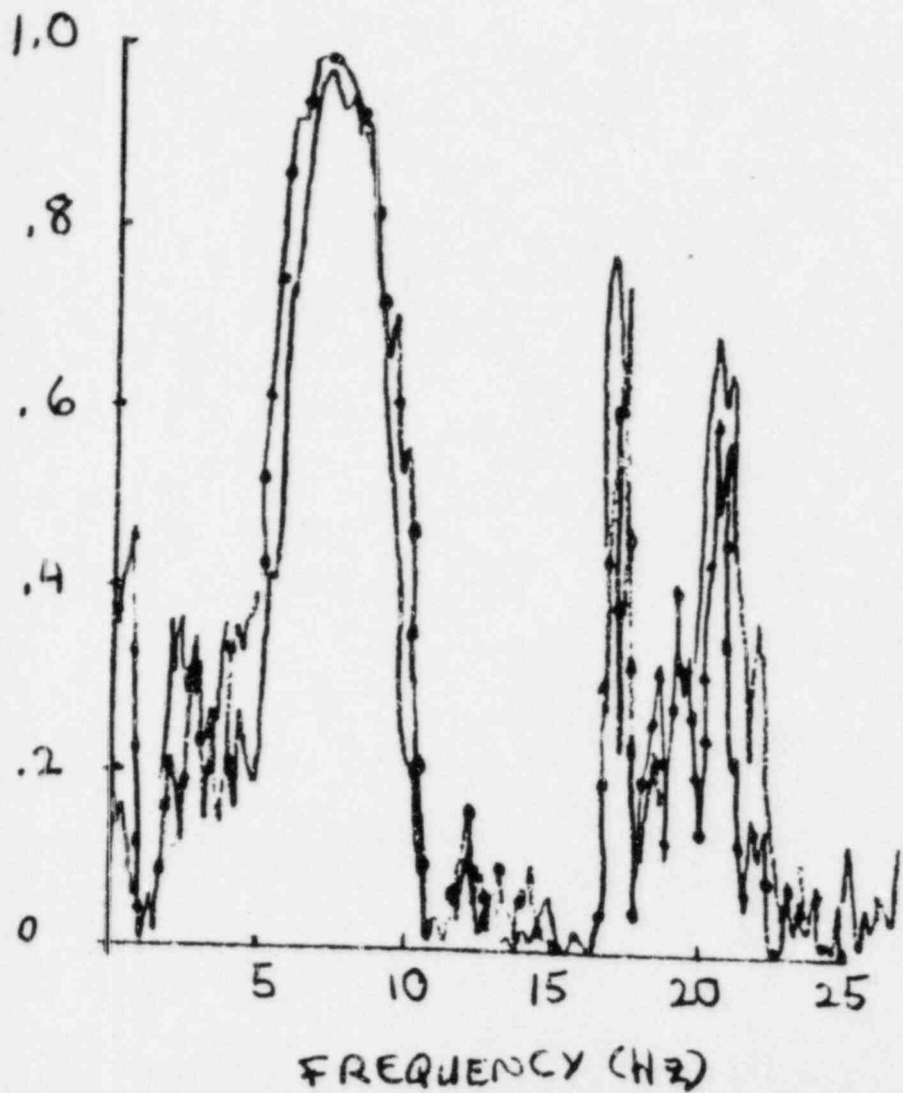


—●— 1986 (CYCLE 10)  
—●— 1985 (CYCLE 9)

FIGURE 6-12

COHERENCE

$B_5 \times C_5$



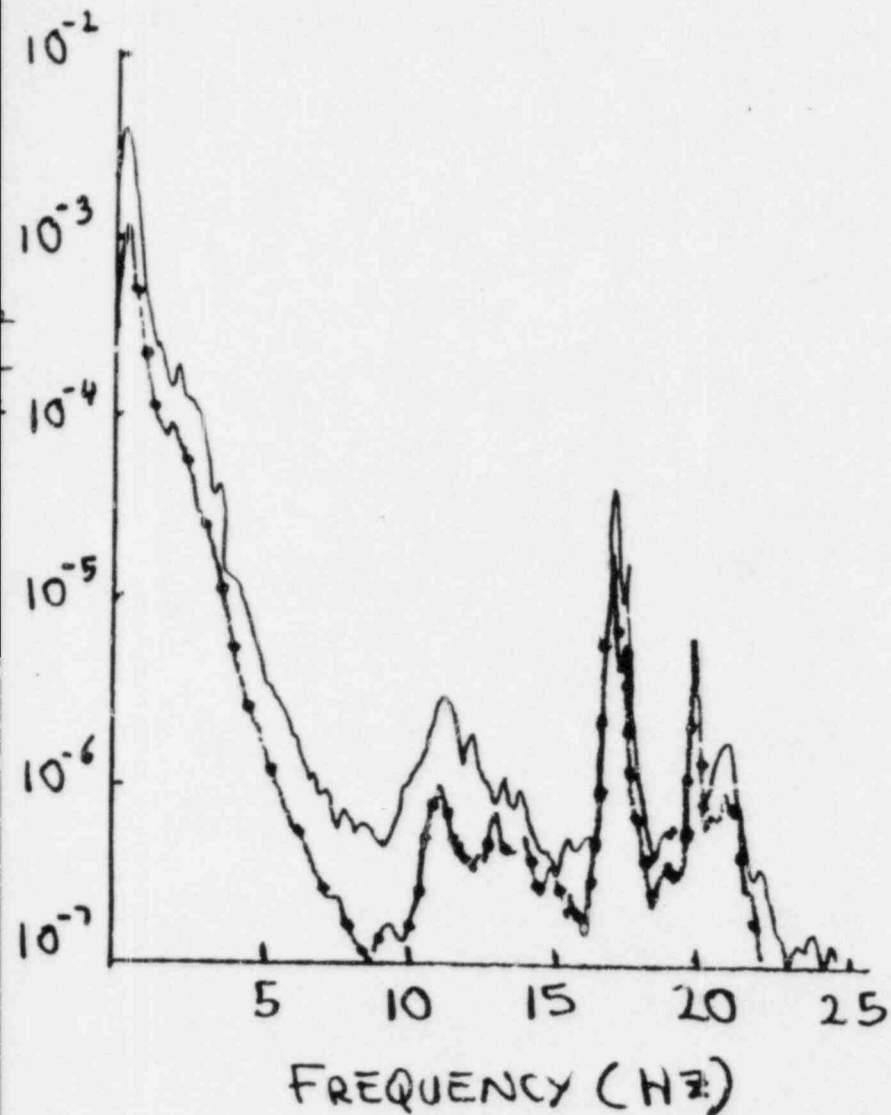
—●— 1986 (CYCLE 10)  
— 1985 (CYCLE 9)

FIGURE 6-13

0°-PHASE XPSD

$A_c \times B_c$

6-29



◆ 1986 (CYCLE 10)  
— 1985 (CYCLE 9)

6-30

180°-PHASE XPSD  $A_c \times B_c$

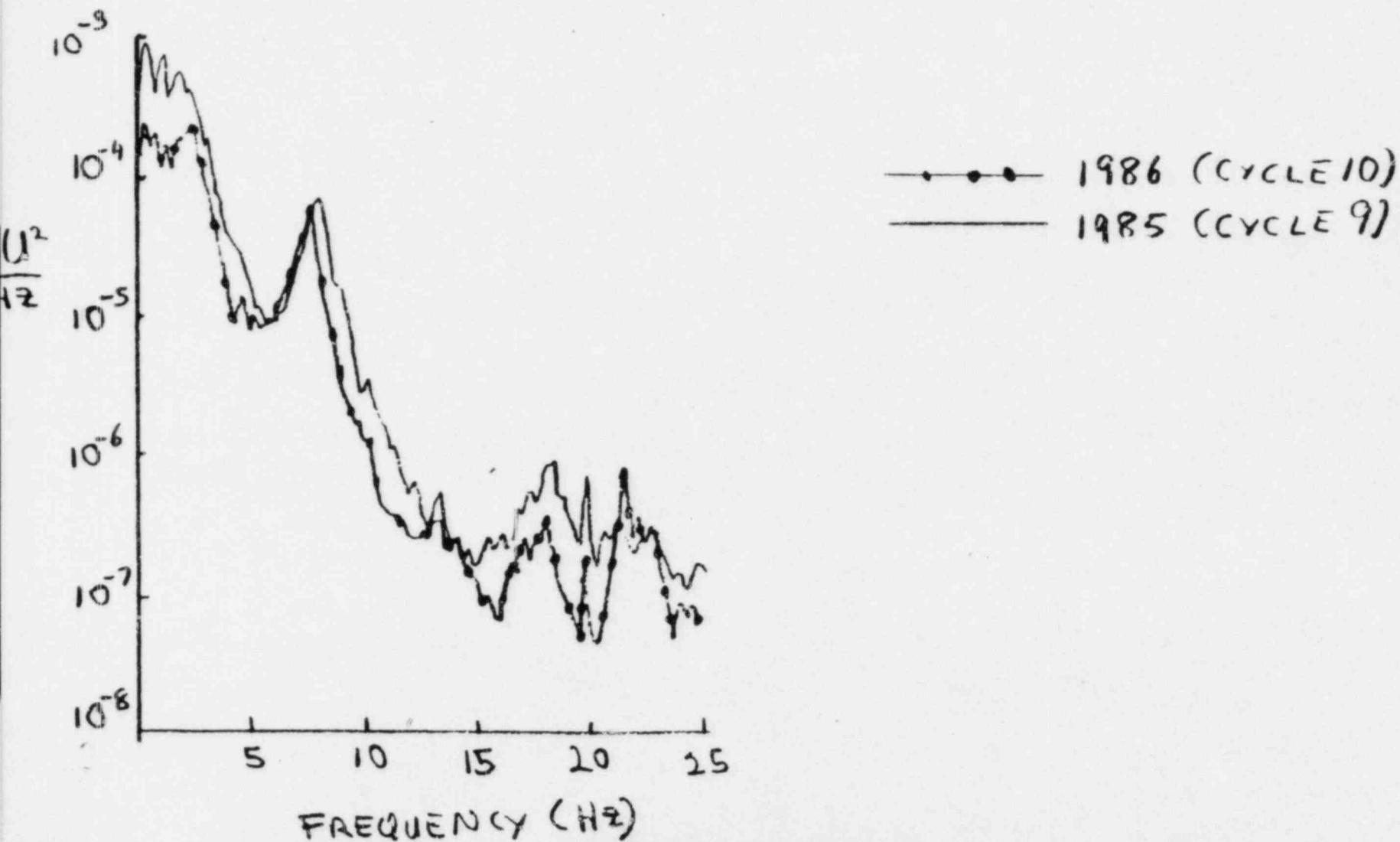
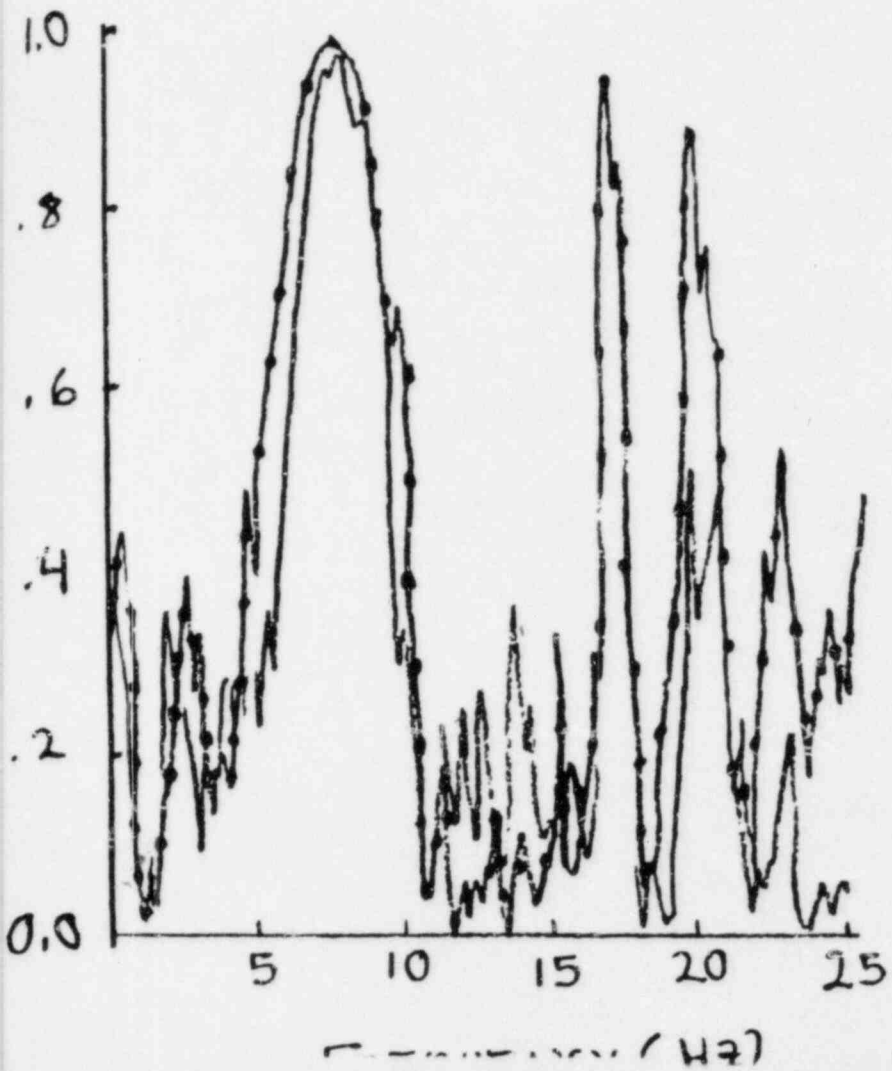


FIGURE 6-15

6-31

COHERENCE

$A_c \times B_c$



—●— 1986 (CYCLE 10)  
— 1985 (CYCLE 9)



## REFERENCES

- 6-1 "Omaha Precritical Vibration Monitoring Program", CEN-7(0).
- 6-2 "Maine Yankee Precritical Vibration Monitoring Program", CENPD-83, 1973.
- 6-3 NRC Docket No. 50-285, "Thermal Shield Concerns - Fort Calhoun Station, Unit No. 1", R. A. Clark, June 1, 1983.
- 6-4 ORNL/NRC/LTR-85/24, "Feasibility of Detecting PWR Thermal Shield Support Degradation Using Ex-Core Neutron Noise", F. J. Sweeney and D. N. Fry, July, 1985.

## 7.0 SAFETY EVALUATION

### 7.1 Potential Failure Modes

Experience has shown that if degradation of the thermal shield support system occurs, the process leading to severe damage takes a substantial period of time. After a long period of degradation when the support system is no longer effective, cracks and possibly through holes may develop in the core support barrel (CSB). Under these conditions, a leakage path may develop in the CSB while the thermal shield is still in a near normal position.

If it is postulated that the support system fails completely, the thermal shield would fall an axial distance of less than 2 inches, where it would be captured by the CSB snubbers. There are three possible failure modes, or configurations for the thermal shield:

- MODE 1: The thermal shield comes to rest in an upright, concentric position.
- MODE 2: The thermal shield assumes an upright, but eccentric position.
- MODE 3: The thermal shield drops to the snubbers in a fully eccentric, and tilted position.

#### 7.1.1 Effect on Core Bypass and System Flow Rates

For Mode 1, there is no thermal hydraulic effect if no through wall damage occurs to the CSB. If through wall damage does occur, core bypass flow will increase with a resulting impact on core overpower margin.

For Mode 2, the thermal hydraulic impact is expected to be similar to Mode 1.

Mode 3 represents the worst case situation, since the tilted thermal shield increases the hydraulic resistance in the downcomer, thereby increasing the core bypass flow through any resulting CSB through wall damage area, and impacting on system flow rate and core inlet flow distribution.

An evaluation was performed to determine the hydraulic effects of a postulated Mode 3 failure. The evaluation was performed as a function of CSB through wall damage area. The maximum CSB through wall damage per support lug was defined as being equal to the cross-sectional area of a lug, approximately 20 in<sup>2</sup>. A conservative maximum damage area, therefore, of 160 in<sup>2</sup> is projected based on all eight thermal shield support lugs detaching from the CSB, and each lug producing the maximum through wall damage area. This approach for estimating CSB through wall damage area is conservative, because a detached or partially detached support lug may not produce a through hole (or cracks) in the CSB, as evidenced by St. Lucie Unit 1 which experienced a through wall hole at only one of nine lug locations. The maximum observed through area in the CSB was on the order of 15 in<sup>2</sup>.

Figure 7.1.1 shows the effect of the CSB damage area on core bypass flow rate ratio. The bypass flow ratio is at the normal operating design value of 4.5% with no CSB through wall damage and increases as the postulated damage area increases. Figure 7.1.1 was developed for a Mode 3 failure with the inherent larger hydraulic resistance in the downcomer. But the figure may also be used to provide a conservative estimate of the bypass flow rate ratio for failure Modes 1 and 2, as well as for the pre-failure period in which some CSB through wall damage may have occurred.

Figure 7.1.2 shows the effect of increased hydraulic resistance of the eccentric, tilted thermal shield and CSB damage area on vessel (and primary system) flow rate. The vessel flow rate decreases by 2.2% of design flow rate due to the increased hydraulic resistance, with no CSB through wall damage. If CSB through wall damage area is incurred as a result of the thermal shield drop, vessel flow rate tends to increase as shown in the figure.

The combined effects of CSB through wall damage on core bypass flow rate ratio and vessel flow rate are shown in Figure 7.1.3 with core flow rate expressed as a function of CSB through wall damage area. The resulting impact of the reduced core flow rate on available overpower margin is discussed in Section 7.2.

### 7.1.2 Impact on Core Inlet Flow Distribution

Thermal shield failure Modes 1 and 2 will have no effect on core inlet flow distribution, because of the minimal changes to downcomer hydraulic resistance and relatively uniform azimuthal variation in downcomer annulus flow area. Failure Mode 3, however, will affect the core inlet flow distribution because of the large azimuthal variation in hydraulic resistance in the downcomer region.

To estimate the effect of a Mode 3 failure on the core inlet flow distribution, scaled flow model data for the Ft. Calhoun reactor, with intact thermal shield, were used as the starting point. Examination of the azimuthal variation of velocity exiting from the downcomer region shows local flow rates ranging from -18% to +29% above the average downcomer flow rate. Review of the core inlet flow distribution showed that the inlet flows to the peripheral fuel assemblies are generally below average, with the lowest fuel assembly inlet flow rate being -12 percent relative to average. Even though there is a systematic azimuthal variation in the flow rate exiting from the downcomer region in the flow model, examination of the measured core inlet flow distribution does not show a matching azimuthal variation. The reduction in azimuthal flow variation as the flow proceeds to the core inlet plane is due to the effects of the flow skirt, lower support structure bottom plate, and core support plate.

However, it was assumed that there is a direct link between the lowest flow rates at the downcomer exit and core inlet planes in order to assess the impact for a Mode 3 failure. To calculate the azimuthal flow variation at the downcomer exit, an analytical model of the downcomer region was set up. The

model consists of a network of parallel closed flow channels, with 12 channels used to represent each thermal shield annulus (the inner and outer annuli). The model starts at a station just upstream of the thermal shield and ends just downstream of the thermal shield. The pressure drop between these two stations are assumed equal for all flow channels.

The azimuthal variation of local flow rate exiting from the downcomer region was predicted with this model to range from -31 to +26% about the average flow rate. This range of variation is compared to the measured range of -18 to +29% for the intact thermal shield. The lowest local flow rate value at the downcomer exit almost doubled, or -18% to -31%. Therefore, for conservatism, it is estimated that the Mode 3 failure will produce reductions in the fuel assembly inlet flow rates of approximately twice that observed in the flow model test, or about -24% relative to the average inlet flow rate. This means that the thermal shield in a fully eccentric, tilted position will result in a flow decrease to the peripheral fuel assemblies of 12 percent beyond that observed for an intact thermal shield. For additional conservatism, it was assumed that the limiting fuel assembly from a thermal margin viewpoint will experience a flow reduction of 12% during a postulated Model 3 failure.

The addition of core bypass leakage through any CSB through wall damage area, even if distributed in an azimuthally non-uniform manner, is not expected to worsen the impact on core inlet flow distribution. This conclusion is based on:

1. The CSB through wall damage will occur near the top of the downcomer in the support lug region, thereby giving a long flow path for the flow variation (due to localized core bypass flow) to diminish.
2. Total CSB through wall damage area, if it does occur, is expected to be limited to about 10 to 20 in<sup>2</sup>. The resulting increase in bypass flow rate is 1 to 2%. Even if this bypass flow occurs at one azimuthal position, the effect will be redistributed by the intervening flow

plates. Flow model tests were run at C-E with the flow rate to one inlet nozzle set at 7% below the average for the other three inlet nozzles. Examination of the core inlet flow distribution data indicated that the inlet nozzle flow deficit had been overcome by the time the coolant reached the core inlet plane, where the distribution had become more uniform.

## 7.2 Consequence of Thermal Shield Failure

Failure of the thermal shield can impact fuel thermal-hydraulic (T-H) performance via four mechanisms:

1. Increased core bypass flow resulting from cracking of the Core Support Barrel
2. Creation of debris that could be swept into the core
3. Tilting of the thermal shield and resultant reduction in primary loop flow and skewing of the core inlet flow distribution
4. Jetting through core shroud seams

The consequences of these mechanisms pertaining to fuel T-H Performance are discussed in the following sections.

### 7.2.1 Increased Core Bypass Flow

As discussed in Section 7.1, failure of the thermal shield could result in the formation of cracks and possibly, holes through the core support barrel which would provide additional flowpaths for core bypass flow, and thereby reduce flow through the core. A series of T-H analyses was done with the TORC code at three different operating conditions and a range of core bypass flows to assess the impact of increased bypass flow on core DNB overpower margin. Based on these analyses, the maximum change in overpower margin resulting from a change in bypass flow is 0.8% change in overpower (OP) per 1% change in bypass flow.

Failure of the St. Lucie Unit 1 thermal shield resulted in Core Support Barrel (CSB) damage that opened an additional bypass flow area of approximately 15 in<sup>2</sup>. From Figure 7.1.1, it can be seen that this increase in bypass flow area would increase the bypass flow by 0.8%. Thus, based on experience with past CSB through wall damage, the Ft. Calhoun core bypass flow would be expected to



increase by 0.8% in the event of CSB through wall damage, thereby reducing core DNB overpower margin by  $0.8 \times 0.8 = 0.64\%$ . A plot of DNB margin reduction vs. CSB damage area based on the calculated bypass flow from Figure 7.1.1 and the 0.8% OP/1% bypass flow conversion factor is presented in Figure 7.2.1.

### 7.2.2 Creation of Debris

Degradation of the Ft. Calhoun thermal shield support system could generate debris that would be swept toward the core by the coolant flow during reactor operation. However, to reach the core inlet, the debris must follow a tortuous path. The flowpath within the downcomer of the reactor vessel is schematically presented in Figure 7.2.2. At the bottom of the annulus between the Core Support Barrel (CSB) and the reactor vessel (the thermal shield resides in this annulus) the debris must make a  $90^\circ$  turn and pass through the 2.25 in. diameter flow holes in the flowskirt (see Figure 3-1). The debris with dimensions greater than 2.25 in. will strike the flowskirt and settle at the bottom of the downcomer between the flow skirt and the reactor vessel.

If the debris does manage to pass through the flowskirt, it must make another  $90^\circ$  turn and move upward. Given the axial velocity distribution within the lower plenum (maximum velocity ~9 FPS) it is estimated that only debris smaller in size than a 2" cube could be carried upward by the flow.

Even if the debris of smaller size successfully passed through the Lower Support Structure and the 2.187" diameter Core Support Plate (CSP) flowholes, the Lower End Fitting (LEF) flow plate would filter out all but very small debris.

The fuel assembly LEF plate has 124 flowholes of 0.484" diameter. If the debris were smaller than the LEF flow hole it could pass into the core, but would probably be trapped by the inconel spacer grid at the bottom of the fuel assembly. This could reduce the inlet flow to a small number of fuel rods.



DNB tests with a flow blockage at the inlet to several adjacent subchannels showed that the blockage did not significantly affect the DNB performance of the fuel rods. The tests were conducted by C-E with a 21 rod, one guide tube, 5x5 test section at the Columbia University Heat Transfer Facility. The test section had a 48" heated length with a non-uniform radial power distribution and a uniform axial power distribution. The inlet to 11 of the 34 subchannels in the test section was completely blocked, reducing the inlet flow area by 36%. Two series of tests were run on the test section, one series with the inlet blockage in place and a second series with a blockage removed. Comparison of the measured Critical Heat Flux (CHF) to cause DNB for the blocked test series with those of the unblocked series showed that there was little effect on the bundle heat transfer capability due to the inlet blockage. Thus, because of the open lattice of the rods, flow was able to redistribute quickly enough downstream of the blockage to preclude premature DNB.

Thus, all but very small debris generated by thermal shield degradation would be filtered out by the structures between the CSB/vessel annulus and the core inlet. Any debris trapped just upstream of the core inlet by the LEF flow plate could block flow to a small number of fuel rods. However, CHF tests have shown that flow redistributes quickly downstream of such a blockage, thereby precluding premature DNB.

Debris small enough to pass through the LEF flow plate would probably be trapped by the spacer grids and could lead to failure of the fuel cladding due to fretting. These fretting-induced fuel failures would occur gradually over time and be apparent to the reactor operator via high coolant activity levels, which are limited by the Ft. Calhoun Technical Specifications.

### 7.2.3 Tilting of the Thermal Shield

As discussed in Section 7.1, a tilted thermal shield could reduce core average flow by up to 2.2%. Furthermore, a tilted thermal shield could affect the

distribution of flow at the core inlet, reducing flow to fuel assemblies at the core periphery (i.e., adjacent to the core shroud) by as much as 12%.

The impact on DNB overpower margin due to the reduction in core flowrate can be estimated using the 0.8% change in overpower per percent reduction in core flow discussed in Section 7.2.1. Thus, a 2.2% reduction in core flow caused by a tilted thermal shield could reduce core DNB overpower margin by as much as  $2.2 \times 0.8 = 1.8\%$ .

Additional TORC analyses were performed to assess the DNB margin impact resulting from the change in inlet flow distribution caused by a tilted thermal shield. In these analyses, inlet flow to all peripheral fuel assemblies was reduced by 12%. Results from these analyses were compared with corresponding TORC results based on the unaltered design inlet flow distribution to assess the impact on DNB margin.

Cases run at nominal conditions with a typical End of Cycle (EOC) axial power distribution (-0.07 ASI) indicated a reduction in DNB margin of 0.9%, while cases run at more adverse design conditions with a bottom peak axial power distribution (+0.34 ASI) indicated a reduction in DNB margin of 1.6%.

Thus the maximum DNB overpower margin impact of a tilted thermal shield accounting for the reduced core flow and altered core inlet flow distribution can be estimated as  $1.018 \times 1.016 = 1.034$ , or a 3.4% reduction in DNB overpower margin.

#### 7.2.4 Core Shroud Jetting

Core Support Barrel (CSB) damage resulting from thermal shield failure could open flow paths from the CSB/vessel annulus to the core shroud/CSB annulus. The effect of bypass flow through the CSB lug tear out area was discussed in Section 7.2.1. The potential for these flow paths to cause jetting through gaps in the core shroud into the fuel region was also examined.

If CSB through wall damage occurs due to thermal shield degradation, experience has shown that it will occur in the vicinity of the support lugs. Figure 7.2.3 presents a sketch of a section of the Core Support Barrel and Core Shroud showing the location of the CSB lugs relative to gaps in the Core Shroud. As can be seen from the sketch, the CSB lugs are not directly in line with the core shroud gaps. A jet from the vicinity of the CSB lug would spread significantly before reaching the core shroud gap thereby reducing the jet velocity. Thus, it is expected that isolated through wall damage in the vicinity of the CSB support lugs will not cause significant jetting through the core shroud gaps into the core.

If extensive CSB through wall damage occurred, and the CSB/core shroud annulus were at a higher pressure than the core, jetting could occur through the core shroud gaps. It must be stressed that experience has shown that CSB through wall damage is relatively localized and far from being extensive enough to increase the CSB/core shroud annulus pressure and cause jetting into the core. However, if jetting through the core shroud gaps did occur, the fuel/core shroud geometry would mitigate the effect of the jet on the fuel. As Figure 7.2.4 shows, the gaps are narrow (0.01"), separated from the fuel by a comparatively large distance (0.180" = 18 x gap width), and not directly in line with fuel rods. If jetting did occur, a narrow (0.01") jet would need to travel a relatively long (18 x the initial jet width) distance, normal to the core axial flow before interacting with the fuel. Thus, it is expected that the jet would dissipate significantly before reaching the fuel rods and not give rise to flow induced vibration.

In the event that CSB damage was so extensive that jets did exist and were not dissipated before reaching the fuel, there is still no impact on reactor safety. Strong jets could give rise to flow-induced vibration and fretting failure of the outermost row of fuel rods over a period of time. This fuel failure would occur gradually and be apparent to the operator, in the form of high coolant activity levels, who could take appropriate action to meet plant Technical Specifications.

In summary, isolated through wall damage to the CSB in the vicinity of the thermal shield support lugs is not expected to cause jetting through core shroud gaps. If extensive damage to the CSB were to occur, jets could exist, but would probably dissipate significantly before interacting with the fuel. Finally, even if damage were so extensive that jets did exist and caused flow-induced vibration and fuel failure as a result of fretting, the failures would occur gradually and be apparent to the operator in the form of high coolant activity levels.

#### 7.2.5 Summary of Failure Consequences

Four potential mechanisms have been examined as potential causes of core damage in the event of thermal shield failure:

- increased core bypass flow
- debris
- tilting of the thermal shield
- core shroud jetting

It has been concluded that it is extremely unlikely that fuel failure would occur due to debris from thermal shield failure or core shroud jetting. Even if some fuel failure did occur as a result of these mechanisms, the failure would occur gradually, over a period of time, and be apparent to the reactor operator in high coolant activity levels.

Increased core bypass flow and tilting of the thermal shield could degrade core thermal margin. Based on TORC analyses, a margin loss of 0.7% is expected as a result of increased core bypass flow based on a realistic estimate of CSB damage that could occur due to thermal shield failure. Tilting of the CSB reduces DNB overpower margin by reducing average core flow and altering the core inlet flow distribution. Based on TORC analyses, these effects are estimated to result in a 3.4% ( $1.018 \times 1.016 = 1.034$ ) reduction in DNB overpower margin. Thus, the combined effects of CSB damage and tilting of

the thermal shield are estimated to reduce DNB overpower margin by 4.1% ( $1.0064 \times 1.018 \times 1.016 = 1.041$ ).

Since the available overpower margin for Anticipated Operational Occurrences is in excess of 10%, considerable margin is available to accommodate the estimated margin loss associated with postulated thermal shield failures and avoid violation of the Minimum DNBR limit. Failure of the thermal shield support system and dropping of the thermal shield will be detected by the reactor operator with appropriate monitoring and the reactor will be shut down after detection of thermal shield failure.

FIGURE 7.1.1

CORE BYPASS FLOW RATIO VS DAMAGE AREA IN CORE SUPPORT BARREL

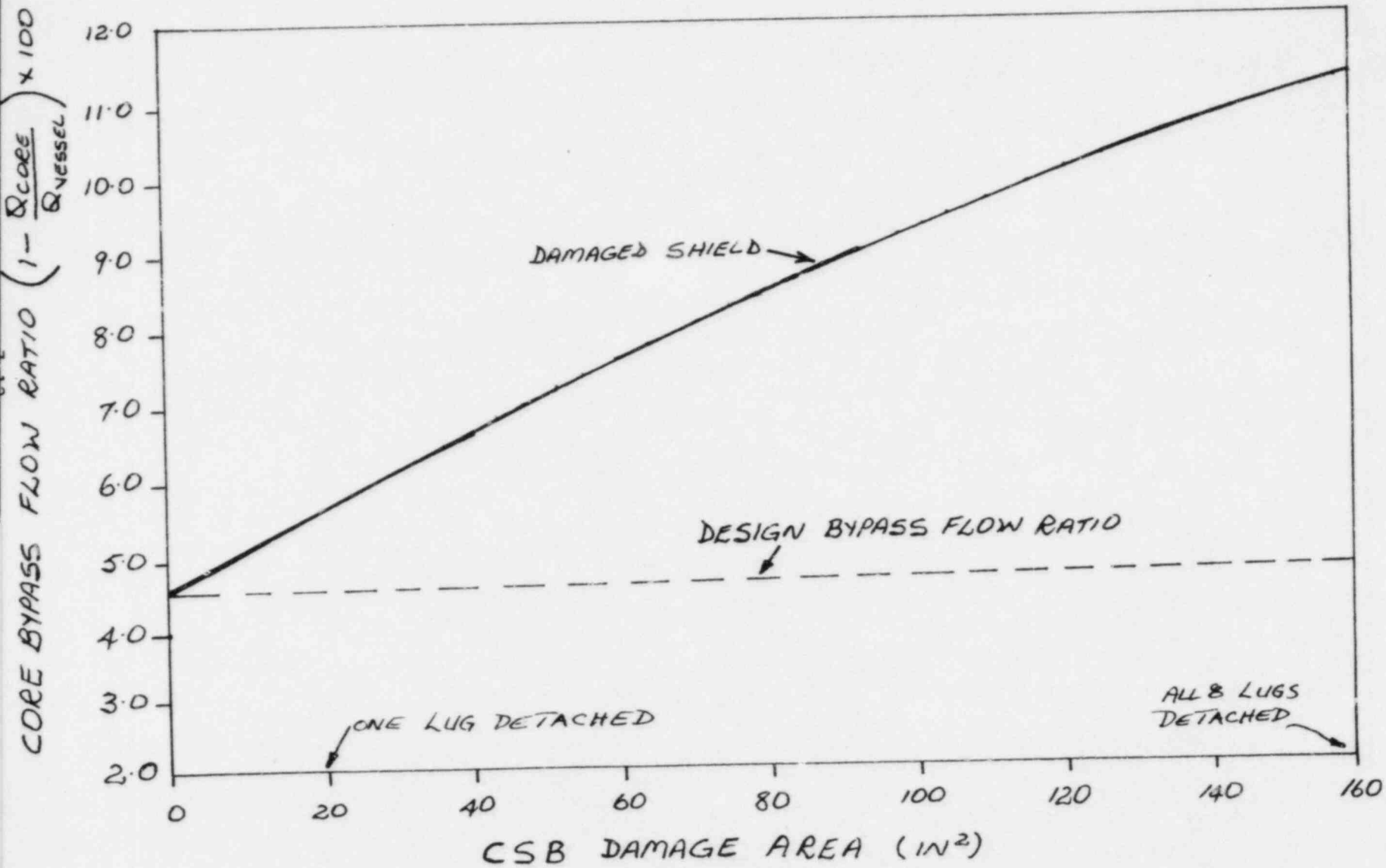


FIGURE 7.1.2

VESSEL FLOWRATE RATIO VS.  
DAMAGE AREA IN CORE SUPPORT BARREL

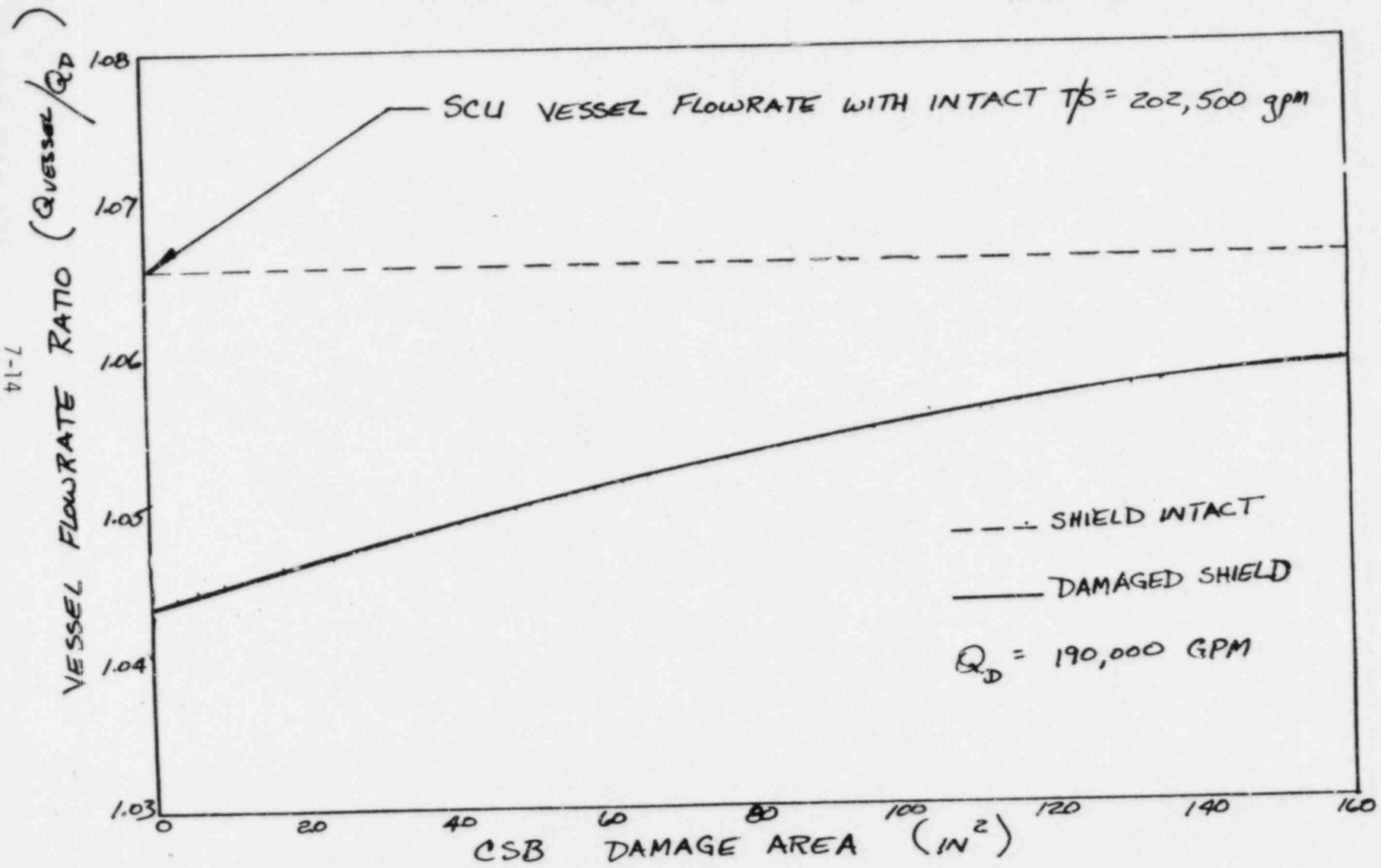




FIGURE 7.1.3  
CORE FLOWRATE RATIO VS. DAMAGE AREA IN CORE SUPPORT BARREL

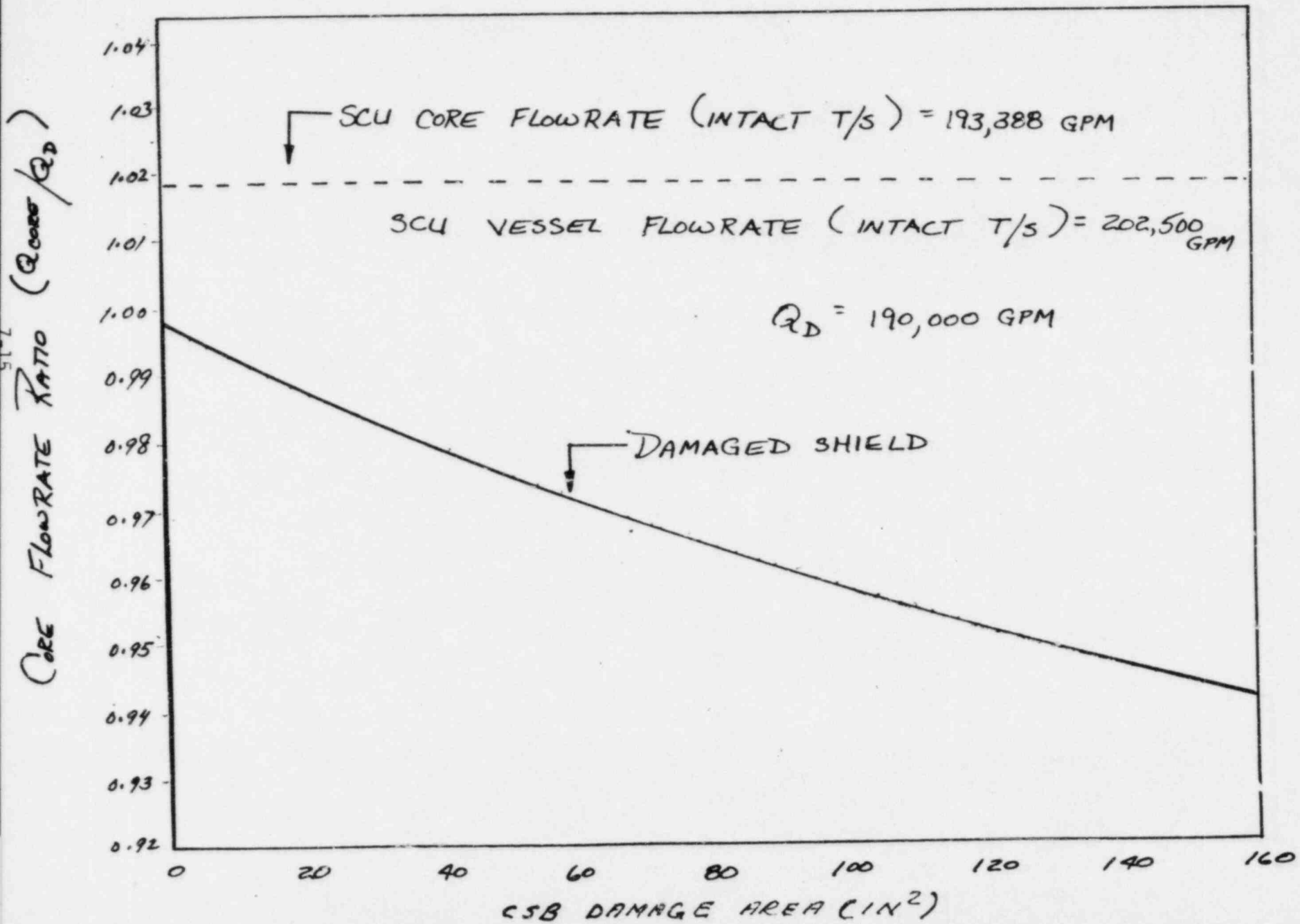
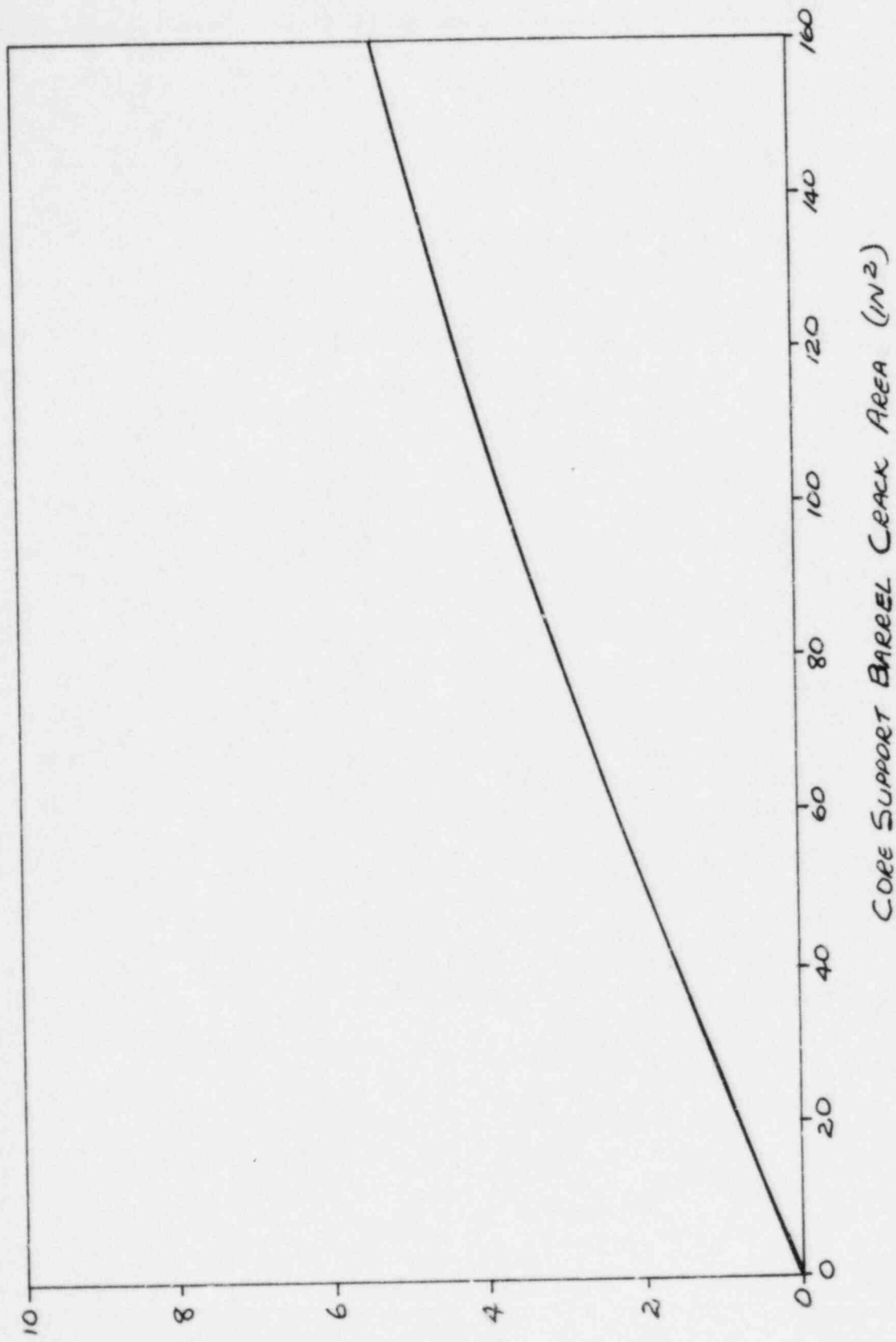


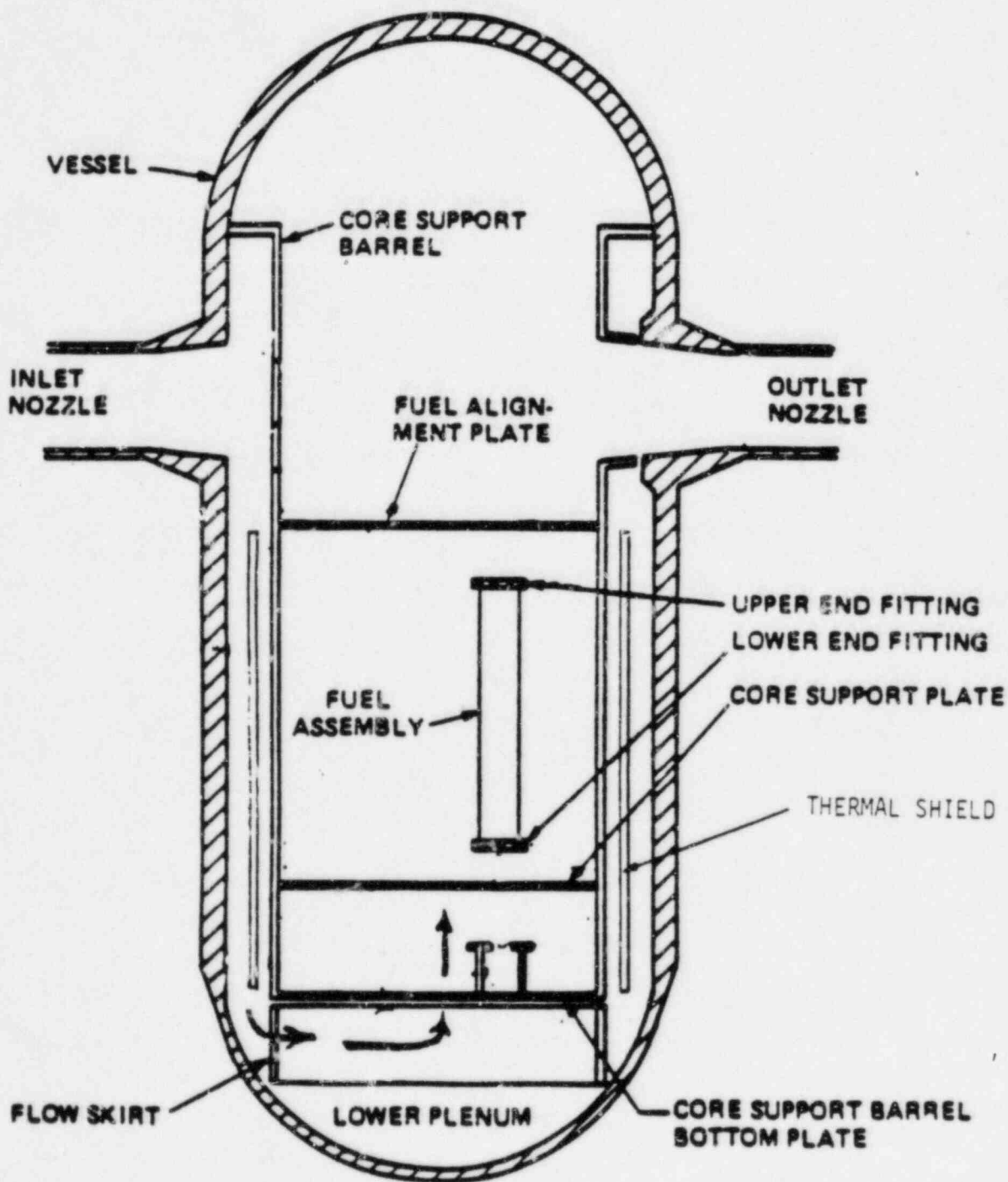


FIGURE 7.2.1: REDUCTION IN DNB MARGIN ASSOCIATED WITH CSB DAMAGE



REDUCTION IN OVERPOWER MARGIN (%)

Figure 7.2.2: Reactor Vessel Flow Paths



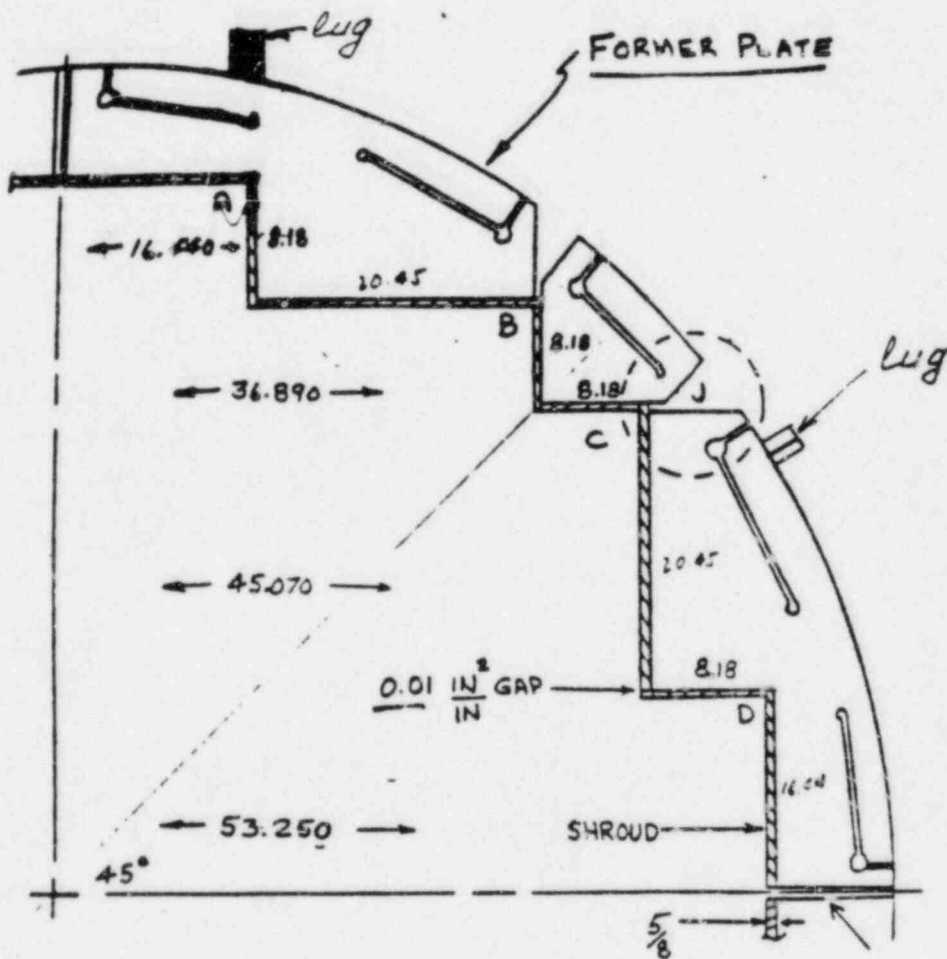


Figure 7.2-3 Location of CSB Lugs Relative to Core Shroud Gaps

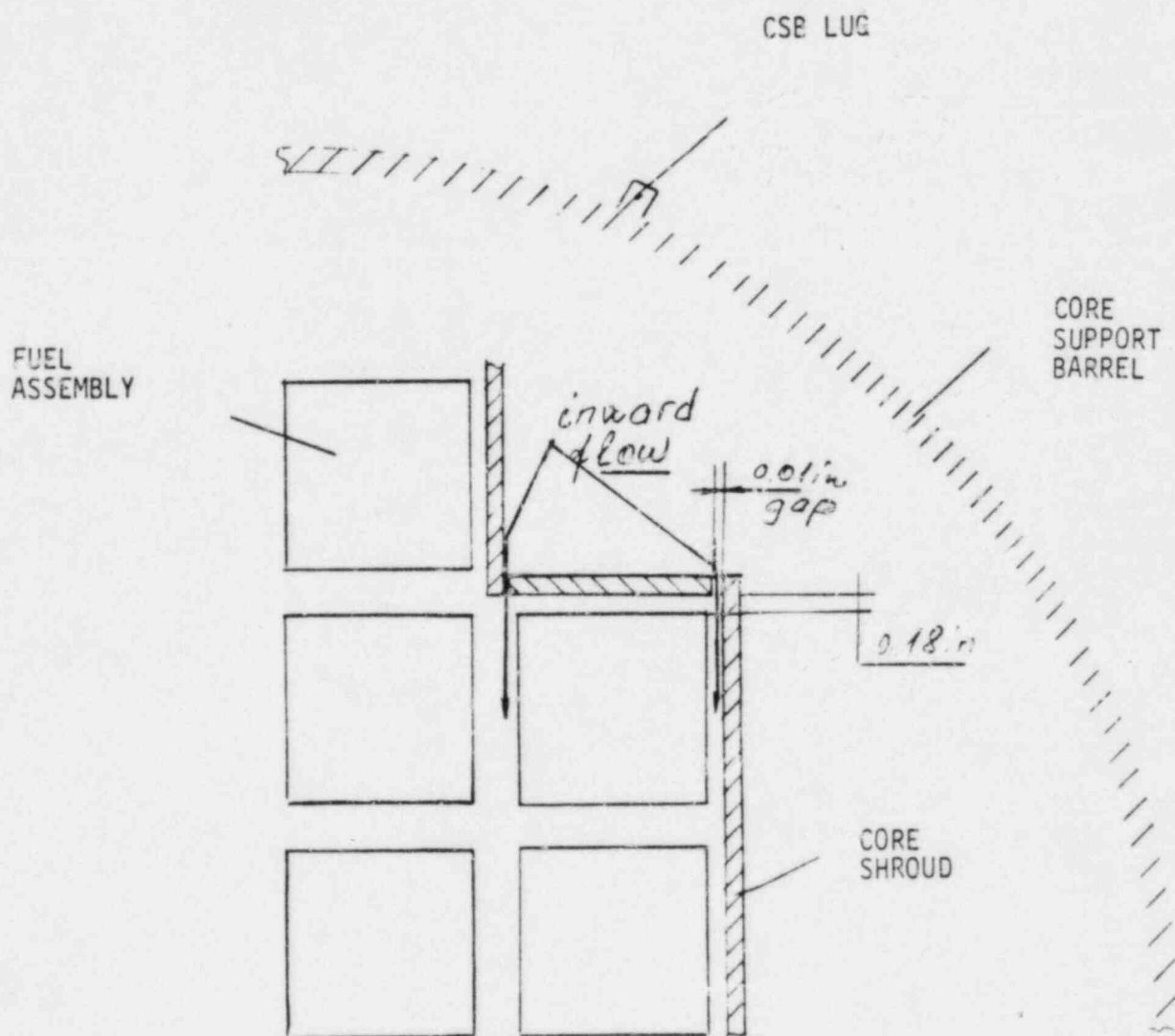


Figure 7.2.4 Location of Core Shroud Gaps Relative to Fuel Assemblies

## 8.0

FORT CALHOUN THERMAL SHIELD STABILITY ANALYSIS

A thermal shield support system stability analysis was performed for Fort Calhoun to insure that the differences in thermal shield support system from Maine Yankee, St. Lucie Unit 1 and Millstone Unit 2 did not result in a support system that has significantly different stability characteristics. The concern being that experience has shown that the degradation process occurs over a long period of time and a support system with a large decrease in stability would be more susceptible to degradation of the thermal shield support system. As was determined by analysis the Fort Calhoun thermal shield support system is essentially the same as the comparative plants and, therefore, the degradation process would take place over a similar period of time.

## 8.1

Background

Unlike forced response, where excitation is independent of the response, self-excited motion is dependent on feedback, or coupling, between the dynamic response of the structure and the magnitude of the force acting on the structure. The behavior of a system subject to self-excited forces can be examined using the equation of motion for a single degree of freedom, lumped mass system.

$$M\ddot{x} + C\dot{x} + Kx = F(\ddot{x}, \dot{x}, x) \quad (1)$$

where M, C, K are the system mass, damping and stiffness and  $F(\ddot{x}, \dot{x}, x)$  is the hydraulic force on the system which is a function of the system response. Assume that the self-excited force can be written as,

$$F(\ddot{x}, \dot{x}, x) = -m\ddot{x} + c\dot{x} + kx \quad (2)$$

Substitution of equation (2) into (1) and transposing of all terms to the left side yields,

$$(M + m) \ddot{x} + (C - c) \dot{x} + (K - k) x = 0 \quad (3)$$

Solution of equation (3) results in a system response amplitude  $x$  that can decrease or increase as a function of time depending on the sign of the damping and stiffness terms. A solution that predicts increased amplitude with time is termed unstable. This unstable motion can be classified into two categories:

- Dynamically unstable, or flutter, where the damping is negative and the oscillatory motion increases in amplitude with time.
- Statically unstable, or divergent, where the stiffness is negative and the amplitude increases exponentially with time.

A number of investigations have shown that plates in channels exposed to fluid flow are susceptible to self-excited forces that can produce unstable motions. These motions include flutter and divergent; both characterized by motions of increasing amplitude.

## 8.2 Discussion

The thermal shield supported in the fluid channel between the core support barrel and reactor vessel walls can be represented by the self-excited response system described above.

A one dimensional analysis, similar to that in Reference 8-1 was performed considering the thermal shield modeled as a flat plate in a channel which can have rigid body motion consisting of translation and rotation (Figure 8-1). The model is reasonable for the large diameter thermal shield geometry. Based on the standard assumptions of inviscid flow and small motions of the plate, the conservation of mass and momentum for the fluid was derived and solved for the self-excited force on the plate. Upon equating this force to the sum of the inertial, damping, and spring force on the plate the Routh criteria was applied to solve for the stability map of the fluid-structure system. The map is shown in Figure 8-2 for the Fort Calhoun system. The divergence limit is a function of the ratio of the equivalent spring constants of the upper and lower supports divided by the fluid stiffness. The flutter is a function of the ratio of solid to hydrodynamic mass in addition to these stiffness ratios. The stiffness value range shown on the map illustrates the stability of the thermal shield system for various degrees of support effectiveness.

### 8.3 Conclusions

Evaluation of the mass parameters has shown that flutter, in a one dimensional analysis, is not a problem for the thermal shield geometry. Divergence, however, is dependent on the stiffness of both upper and lower supports. The upper support stiffness includes positioning pins and support lugs.

The stiffnesses at the upper and lower supports were evaluated using finite element methods. The range of values was determined assuming the pins to be totally effective or totally ineffective. The entire range showed the thermal shield to be stable as long as the lugs remain effective. However, if the support lugs and positioning pins become ineffective, the stiffnesses could be reduced sufficiently to enter the unstable region.

A stability map was prepared using St. Lucie Unit 1, Millstone Unit 2 and Maine Yankee data (Figure 8-3) for comparison with the Fort Calhoun results. Divergence stability criteria is very similar for all three plants as shown by the stability boundaries in Figures 8-2 and 8-3. The range of stiffness values is also of the same magnitude in all cases. It is therefore concluded that the stability margin for the Fort Calhoun thermal shield is essentially the same as that for St. Lucie Unit 1, Millstone Unit 2 and Maine Yankee.



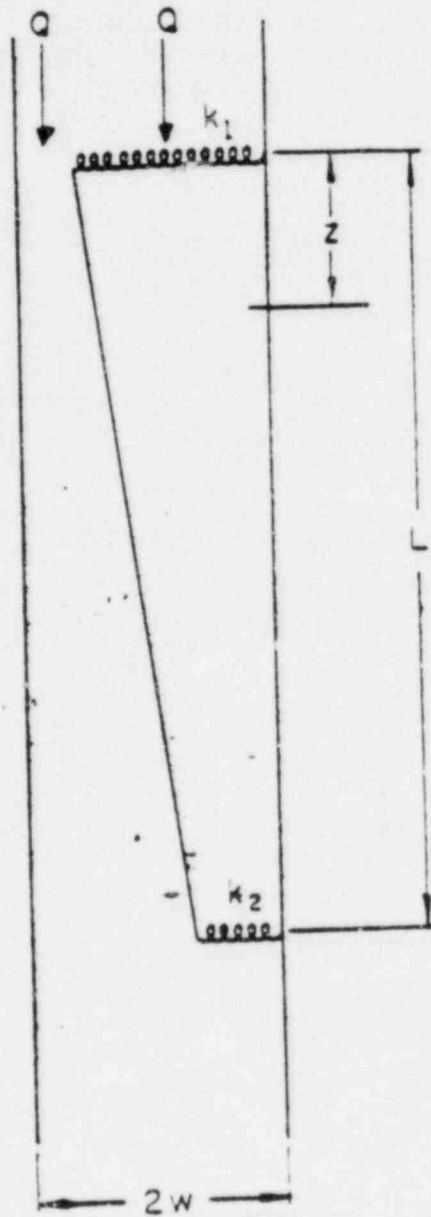
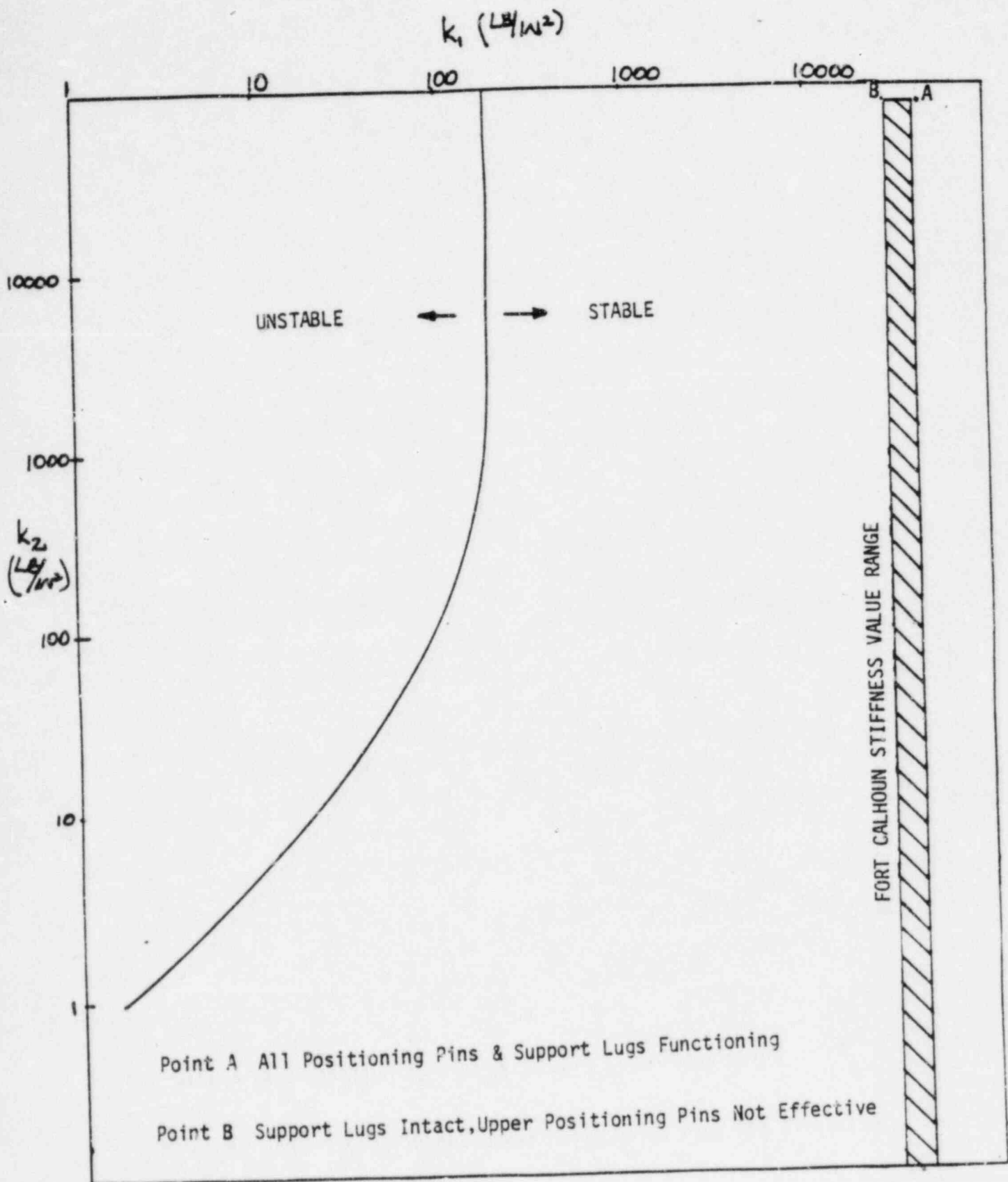


FIGURE 8-1

ILLUSTRATING STIFF ELASTICALLY  
SUPPORTED PLATE OF LENGTH  $L$  IN  
NARROW CHANNEL OF WIDTH  $2w$  WITH FLOW



Point A All Positioning Pins & Support Lugs Functioning  
 Point B Support Lugs Intact, Upper Positioning Pins Not Effective

FIGURE 8-2

FORT CALHOUN THERMAL SHIELD STABILITY DIAGRAM

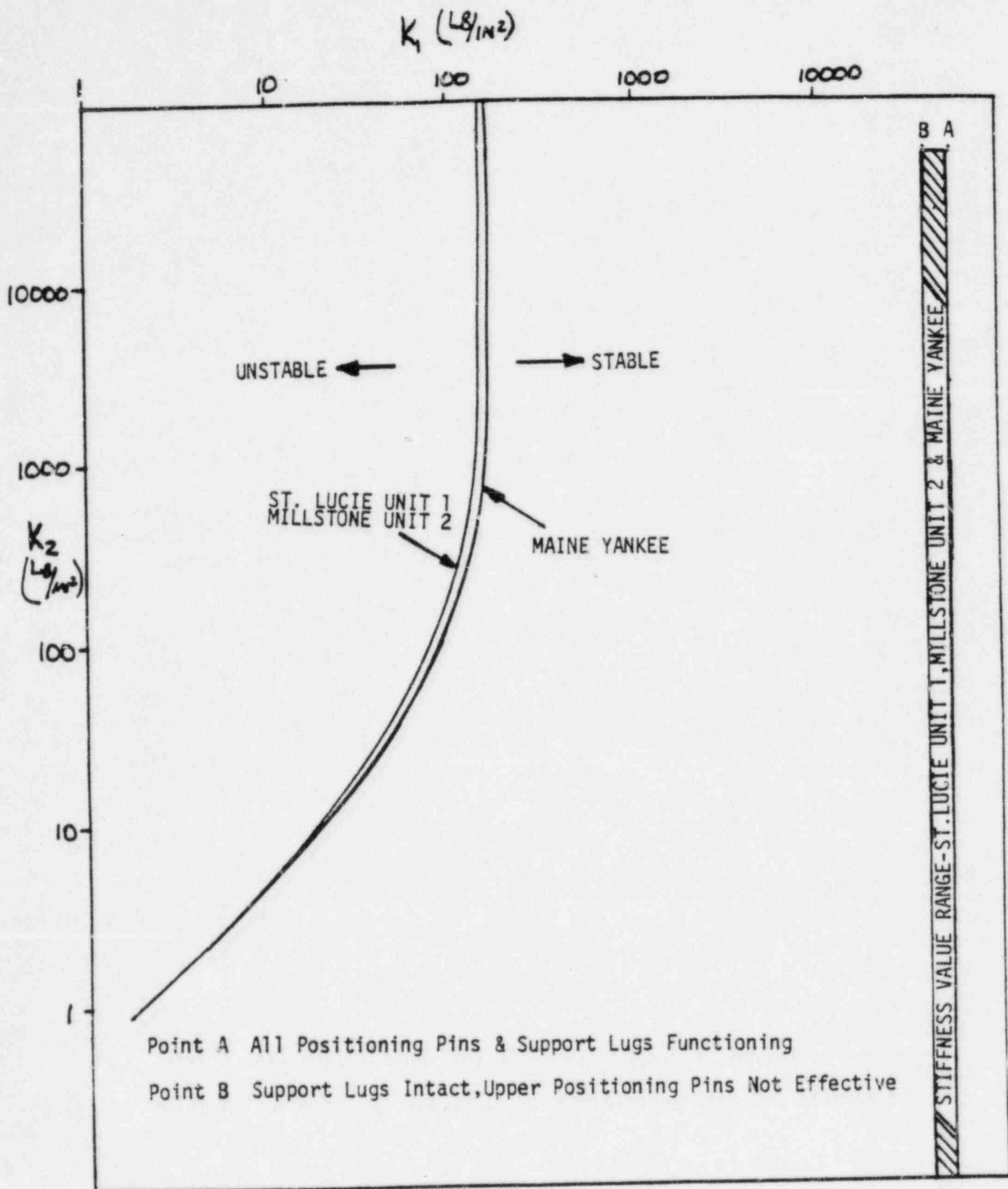


FIGURE 8-3

ST. LUCIE UNIT 1, MILLSTONE UNIT 2 & MAINE YANKEE STABILITY DIAGRAM

### References

- 8-1 "Analysis of the Dynamic Stability of Elastically Supported Plates in Narrow Channels with Applications to Thermal Shield and Core Barrel Stability", BBN Job No. 151273, W.D. Mark, July 1967.